Investigating the Impact of Tobacco Particulate Matter and selected components on Monoamine Oxidase Activity, Protein Expression, and Gene Expression in Brain SH-SY5Y Cells.

A thesis presented in partial fulfilment of the

requirements for the degree of

Doctor of Philosophy

in

Health Sciences

at Massey University, Wellington,

New Zealand

Prakshit Niraula

2023

Abstract

Smoking addiction is one of the most widely discussed topics today due to a large number of smokers and the millions of lives it claims every year. Though a large population makes effort to quit smoking, the quit attempts mostly end in relapse, indicating the complex nature of smoking addiction. Nicotine is believed to be the major component responsible for the addiction, however, nicotine replacement therapy (NRT) has not proved to be a completely satisfying approach to smoking cessation. The low efficacy of NRT, as well as much research related to smoking addiction, suggest the role of non-nicotinic components in smoking addiction. It is hypothesised that monoamine oxidase inhibitors (MAOIs) present in tobacco smoke play a role in smoking addiction by prolonging nicotine's reinforcing effect. Based on this hypothesis, Tobacco Research Group, Wellington has identified six candidate MAOIs in cigarette smoke. This PhD project aims to investigate the effect of nicotine, tobacco particulate matter (TPM) and the candidate MAOIs on MAO activity, MAO protein levels, MAO genes expression and global gene expression.

A human neuroblast SH-SY5Y cell line was exposed to different regimens, which included ethanol (control), nicotine, TPM and the cocktail of candidate MAOIs for a period of 1, 3, 5 and 7 days. A modified kynuramine assay was performed after SH-SY5Y cells were exposed to the different treatments to determine the effect of the exposure treatments on MAO activity and to identify the optimum period of exposure that would result in maximum MAO inhibition. Exposure for a period of 3 days was chosen as an optimum period of time for exposure and for expression and whole genome experiments. Similarly, a MTT assay was performed to determine if the exposure treatment had any cytotoxic effect. Change in MAO protein and MAO gene expression after exposure to the different treatments for the optimum period of time were then determined using Western blot and qPCR, respectively. Finally, the effect of exposure treatments for an optimum period of time on global gene expression was determined using RNA sequencing (RNAseq) technology.

It was observed that nicotine did not have any significant MAO inhibitory effect compared to the control in any of the treatments examined. TPM and MAOIs caused significant inhibition of total MAO activity when exposed for 1 and 3 days. However, no significant inhibition was seen in the exposure for 5 and 7 days. Change in MAO A and MAO B gene and protein expression levels after the exposure treatment for 3 days was not observed. Nevertheless, several genes were found to have differential expression after exposure to the treatments for 3 days. Many of these differentially expressed genes were linked with diseases and conditions related to smoking and addiction. The results suggest that the candidate MAO inhibitors identified by the Tobacco Research Group, Wellington could be the primary contributors of the MAO inhibitory property observed in cigarette smoke. This data could also possibly answer the major question regarding the component responsible for MAO inhibition by cigarette smoke in smokers. Further research is required to fully elucidate and understand the mechanisms behind the MAO inhibition from the MAOIs, and a better understanding of these mechanisms may provide a framework for the development of novel smoking cessation therapies.

Acknowledgements

I would like to start by expressing my deepest gratitude to my esteemed supervisors, Dr Barry Palmer, Dr Penelope Truman, and Associate Professor Rachel Page. I am grateful for their unwavering support, cooperation, and motivation that I received throughout my PhD journey. Their invaluable expertise has been instrumental in shaping the outcome of my research. Apart from the expertise of my supervisors that greatly helped me to complete my thesis, specifically I am thankful to Barry for motivating me to complete my doctoral degree despite my personal challenges and hardships, Penny for her continuous assistance and support since the first day of my arrival in New Zealand, and to Rachel for her insightful ideas, suggestions and continual support as a departmental head. I feel myself extremely fortunate to have had supervisors, who not only supported my research and doctoral study, but also cared about my overall well-being.

I am thankful to Massey University for providing me with a scholarship to continue my study and the Massey University Research Fund for funding my RNA sequencing studies. I would also like to appreciate and thank academic staff of Massey University Dr Collette Bromhead, Dr Beth Mallard, Dr Nick Kim, Prof David Rowlands, Assoc Prof Wyatt Page, and Dr Wei-Hang Chua for supporting my research in one way or other. I would also like to thank the technical staff at the School of Health Sciences, Karishma Deo and Anneke Walls. They have been super helpful in laboratory during my PhD. I am equally thankful to Jill Brakensiek for the administrative support. I am grateful to Dr Kirsty Danielson and other administrative staffs at the University of Otago, Wellington for helping me gain access to their instruments, despite the limitations posed by COVID-19 restrictions.

I would also like to express my gratitude to the members of the Tobacco Research Group, Wellington, including Associate Professor Robert Keyzers, Professor Bart Ellenbroek, Associate Professor Paul Teesdale-Spittle for their

input to my research and the overall research group's success. I would also like to acknowledge the preliminary works by Dr Ali Heydari and Paris Wilson.

I am very thankful to all my colleagues and friends at Massey University for their support and assistance throughout my study. I am particularly thankful to Dr Panchamee Dharmadasha and Dr Sudesh Raj Sharma for their help during my initial PhD days, Dr Wouter Peeters for letting me use many of his excess chemicals, and Dr Sa Weon Hong for his continuous support and motivation throughout my doctoral degree.

I would like to express my gratitude to Professor Man Su Kim, my MS degree supervisor at Inje University, South Korea. Thanks to his guidance and mentorship, I gained a good foundation in research and was inspired to continue my doctoral studies. My special appreciation to the Nepalese community in Wellington, especially Mr. Adarsha Raj Tiwari and his family for making me feel at home.

Last but not the least, I could not have accomplished my PhD journey without the support and love of my family members. I am forever indebted to my parents, Keshab Prasad Niraula and Deepa Niraula, for their tireless effort and dedication in raising me. I owe them everything for what I am today. I have no words to thank my wife, Grishma Bhattarai for her support and sacrifice throughout my PhD journey. Grishma, it would have been impossible without your support. I am blessed to have our lovely daughter Prisha in our lives during this journey. I feel so lucky to have received extreme support and love from my siblings Preeti Niraula, Preksha Niraula, and Prabesh Niraula. I would like to honour the memories of my grandmothers, Tara Shrestha and Bhagwati Shrestha, and my cousin Gitaram Niraula, who always wished to see me complete my doctoral degree, but are no longer with us to witness my accomplishment. Their love, support, and encouragement have been invaluable throughout my life.

Table of Contents

List of Figures

List of Tables

Chapter One: Introduction

1.1 Background

Tobacco smoking is one of the most common causes of preventable death in the world. Smoking has been found to cause several diseases and instigate health problems, which are discussed in further detail in Section 2.3. Globally, tobacco is associated with over 7 million deaths every year (World Health Organization, 2022). In 20th century across the world 100 million people have died from smoking and it is projected to kill about 1 billion people in the 21st century (Jha et al., 2015).

In New Zealand smoking or secondhand smoke exposure is estimated to kill about 5000 people each year (Ministry of Health NZ, 2021). Though the prevalence rate of cigarette smoking in New Zealand has shown a trend of decrease from 35.6% (adults aged 15 and over) in 1976 to 10.9% in 2020, it is still a major health problem (Edwards, Ball, Hoek, Wilson, & Waa, 2021)

It is not that most people are unaware of the insidious effects of smoking and want to keep smoking. Most tobacco smokers wish to stop smoking and make an effort to do so. However, most individual quit attempts are unsuccessful (Rigotti, 2012). A survey in New Zealand showed about 40% of people made quit attempts in the previous 12 months, while only 3-5% were able to successfully quit for a duration of more than 6 months without the support of health professionals (Borland, Partos, Yong, Cummings, & Hyland, 2012; Hughes, Keely, & Naud, 2004). Most of the quit attempts end in relapse and it requires several attempts before successfully being able to quit. The American Cancer Society suggests that 8-10 quit attempts are required before smokers will succeed in quitting, while the Australian Cancer Council determined 12-14 attempts to be required (Chaiton et al., 2016).

Nicotine replacement therapy (NRT), which provides a person with low amount of nicotine, without the other toxic components present in cigarette smoke, is a widely used treatment regimen to aid smoking cessation. It aids smoking cessation by relieving withdrawal symptoms through the supply of nicotine that a person would normally get from cigarette smoke. In a Cochrane review of NRT efficacy that included 136 different studies with a total of 64,640 participants, it was concluded that use of NRT increased the likelihood of a person being able to quit smoking by about 50-60% (Hartmann-Boyce, Chepkin, Ye, Bullen, & Lancaster, 2018). Though NRT has been reported to increase the success of quitting, it is costly, the success rate is lesser than anticipated earlier and it requires behavioural support and monitoring to be provided in conjugation (Myers Smith et al., 2022). Also, nicotine exhibits a relatively weak reinforcing effect that may be insufficient to explain the powerful addictive property of tobacco smoke (Balfour, 2008). This gives an indication of the complexity of tobacco dependence and suggests that there is a possibility of factors other than nicotine, which might have roles in tobacco addiction (Rose, 2006).

Cigarette smoke can create a nicotine spike in the human brain, activating nicotinic cholinergic receptors in the midbrain. It triggers the release of dopamine and other catecholamine neurotransmitters, which gives the smoker pleasurable sensation and activates the reward pathway associating it with smoking. A smoker continues smoking to maintain the level of dopamine that provides pleasurable feeling and avoids withdrawal symptoms (Benowitz, 2009). These neurotransmitters (including dopamine) causing the reinforcing effect of cigarette smoking are metabolised by monoamine oxidase (MAO), which is an enzyme located in catecholaminergic and other neurons (Abell & Kwan, 2000). Studies have shown that cigarette smoking, apart from stimulation of neurotransmitter release, is also able to reduce brain MAO activity (Lewis, Miller, & Lea, 2007). In imaging studies, the average reductions in brain MAO-A and –B activity were found to be 30% and 40%

respectively (Fowler et al., 1996b; Fowler, Logan, Wang, & Volkow, 2003). It has been proposed that MAO inhibition would increase the levels of neurotransmitters such as dopamine thereby prolonging the effect of nicotine and enhancing the reinforcing effect of smoking (Hogg, 2016).

1.2 Rationale of the research

Mounting evidence suggests non-nicotinic components in cigarette smoke may have some role in smoking addiction (Etter & Stapleton, 2006; Hogg, 2016; Truman, Grounds, & Brennan, 2017) and further evaluation and study of tobacco particulate matter (TPM) and its components is required. This PhD project revolves around a hypothesis that MAO inhibitors (MAOIs) present in cigarette smoke have a role in cigarette addiction.

TPM collected from cigarette smoke is equivalent to the combustion products from tobacco smoke, that a person would normally inhale when smoking a cigarette. Studies have shown cigarette smoke or TPM to inhibit both isoforms of MAO (i.e. MAO-A and MAO-B). Van der Toorn et al. (2019) performed bioluminescent MAO assay using 96-well plates to compare the MAO inhibition by cigarettes and different modified risk tobacco products. It was observed that Kentucky reference cigarette (3R4F cigarette) and Snus products could significantly inhibit both the MAO isoforms. Similarly, PET imaging studies revealed MAO-A and MAO-B levels in smokers' brain to be lower by 30% and 40% respectively compared to the brain of non-smokers and former smokers (Fowler et al., 1996a; Fowler et al., 1996b). This suggests inhibition of MAO by TPM and/or its specific component/s have a role in addiction to cigarette smoking. However, the mechanism involved or the component responsible for the MAO inhibitory effect seen is not well understood. Several MAOIs have been found so far in cigarette smoke, and harman and norharman have been reported to be the most potent MAOIs (George et al., 2008). However, these most well-known MAOIs are responsible for only a small part (about 10%) of the total MAO-A inhibitory

activity in cigarette smoke suggesting the possibility of other potent MAOIs present in cigarettes (Truman et al., 2017). As a result, a quest for the MAOIs responsible for MAO inhibitory effect shown by cigarette smoke has continued. To address this gap in the knowledge, this PhD study aims to study the impact of TPM and its specific components on different aspects of MAO such as MAO activity and protein and gene expression levels.

The Tobacco Research Group, Wellington led by Dr Penelope Truman has isolated and identified six novel candidate inhibitors from tobacco smoke which have shown promising MAO inhibitory effects (manuscripts in preparation). There obviously are other MAOIs, but these inhibitors are particularly interesting because they are present in much larger amounts compared to other inhibitors and, together, have shown higher inhibition (about 10 times) than harman and norharman in preliminary biochemical studies (SW Hong, pers. comm., manuscripts in preparation). It is therefore essential to observe the effect of these MAOIs in cell culture and compare with the inhibitory effect shown by TPM. In this PhD project, I determined and compared the effects of TPM, and a cocktail of the selected candidate inhibitors identified by the Tobacco Research Group, Wellington on MAO activity and MAO protein and gene expression. TPM has been found to be more reinforcing and demonstrate different behavioural profile associated with reward (Brennan et al., 2015; Harris et al., 2022). MAO inhibitors have also been found to increase the reinforcing effect of nicotine (Smith et al). These findings suggest MAO inhibition likely to have a role in tobacco dependency. The outcome of this research might help in better understanding tobacco dependence and be useful to help people in quitting smoking.

Several *in vitro* and *in vivo* systems are utilised for studies related to addiction. This study concentrated on *in vitro* cell culture work. There are many cell lines that are available for research like this. The human neuroblastoma SH-SY5Y cell line has the necessary characteristics, such as several biochemical and functional characteristics of neurons and has also

been used previously to study the effects of nicotine and tobacco extracts. This led to the decision to utilise SH-SY5Y cells in this PhD project.

1.3 Overall aim and objectives

The overall aim of this research was to examine the impact of nicotine, TPM and the selected MAOIs on MAO activity, protein and gene expression and global gene expression in human neuroblastoma SH-SY5Y cells. The hypothesis is that MAO activity will be reduced in cells exposed to TPM. I also aimed to determine whether the six candidate MAOIs isolated by the Tobacco Research Group, Wellington could replicate the effects of TPM on MAO activity and whether the change in activity was supported by change in MAO protein and gene expression.

The following research objectives facilitated the overall aim of this project:

1. Determination of total MAO activity in SH-SY5Y cells after the exposure to different treatments.
2. Determination of change in MAO isoenzyme protein expression levels in SH-SY5Y cells after exposure to different treatments.
3. Determination of change in MAO isoenzyme gene expression levels in SH-SY5Y cells after exposure to different treatments.
4. Study of differential gene expression in SH-SY5Y cells after exposure to different treatments.

This PhD project was focused on developing our understanding of tobacco dependence. Understanding the role of MAOIs in cigarette smoke may provide insight on development of an improved form of NRT that can better replace the addictive effect produced in the human body when a cigarette is smoked.

1.4 Structure of thesis

This thesis follows the traditional monograph format and contains eight chapters. The structure of this thesis is outlined below:

Chapter 1 provides some background information, rationale, overall aims and objectives for the PhD study and the structure of this thesis.

Chapter 2 provides information on the existing literature on the research topic. It discusses the theories, findings obtained, and methods employed in other similar research studies. It also includes the fundamentals and general concept of methods employed in this study.

Chapter 3 gives an overview of the study, details general methods employed for different experiments conducted and data analysis techniques used.

Chapters 4-7 provide information about different experiments and results of the study. Chapter 4 details about the preparatory works that are essential for major experiments. Chapter 5 addresses the first research objective (Section 1.3); Chapter 6 addresses the second and third research objective (Section 1.3), while Chapter 7 addresses the last research objective (Section 1.3).

Chapter 8 summarizes the main findings of the study and highlights the limitations. It also identifies directions for future study that would be helpful in expanding on the knowledge obtained from this thesis.

References lists all the sources cited in this thesis.

Appendix include supplementary information that supports the procedure of obtaining results and some data not included in the main text.

Chapter Two: Literature Review

2.1 Introduction

This chapter discusses the existing literature and research relating to smoking addiction and monoamine oxidase (MAO), which is an enzyme involved in oxidative deamination of neurotransmitters including dopamine. It also discusses the gaps in the existing literature, thereby providing a foundation for this PhD study. Methods employed in other similar studies are discussed to conclude the method most suitable for this PhD study. The basic principles behind the methods chosen are also discussed.

2.2 History of smoking consumption

Smoking is a practice of inhaling and exhaling the fumes of plant materials such as tobacco, marijuana and hashish. However, this practice is commonly linked with tobacco as smoked in the form of a cigarette (Henningfield, 2019). Tobacco is a plant from the *Nicotiana* genus which originated in the temperate regions of North and South America. Chewing and smoking tobacco leaves were extremely popular, which led to the widespread use of tobacco plants in America. By 1492 tobacco became available throughout the American continents and nearby islands, and in the 1500s it started becoming popular amongst Spanish, Portuguese and English sailors. The scientific name of tobacco, *Nicotiana tabacum* was taken from the name of a French ambassador Jean Nicot de Villemain, who had introduced it to the French court. The cultivation of tobacco was officially started in 1612, and a cigarette rolling machine was invented in 1880 that helped commercial cigarette use to spread widely. By the early 1900s, billions of cigarettes were marketed annually (Dani & Balfour, 2011).

In New Zealand, Europeans introduced tobacco to Māori in the late 1700s and by the 1840s, tobacco use became widespread among Māori. Strong opposition by Māori leaders to the use of tobacco started towards the end of the 1800s, which received legal recognition in The Māori Councils Act 1900 that forbade children to smoke. The distribution of free cigarettes during World War I contributed to the increased prevalence of smoking in New Zealand (Health Promotion Agency, 2020). There were 58% male and 70% female Māori smokers, while the male and female percentages of the overall general population in New Zealand (both Māori and non-Māori) was 38% and 31%, respectively, according to an early study reported in (Cook, 2013). Several measures, such as a ban on tobacco advertisements on televisions and radio in 1963, taxation on tobacco, and initiation of a tobacco control program in 1984, helped a steady decrease in smoking prevalence in New Zealand from 32% in 1984 to 9.2% in 2021 (Trainor, 2008; Ministry of Health 2021). Though the rate of smoking continues to decrease gradually, the smoking rate among Māori adults is still much higher compared to other ethnicities in New Zealand. The prevalence data of Māori, Pacific, Asian, European (and others) smokers is 22.3%, 16.4%, 3.9%, and 8.3%, respectively (Ministry of Health, 2021). A 2019 study showed the expenditure on tobacco in 2018 by Māori accounted for 26% of total New Zealand expenditure, and Māori paid $723 million in tobacco taxes (Siddhartha, 2019).

2.3 Smoking and health problems

The consumption of tobacco, particularly in the form of cigarette smoking, is an important cause of disease in the world. According to a report from the National Health Interview Survey (NHIS), the prevalence rate of smokers in 2015 was about 15% (30 million) in the USA (Jamal et al., 2016).

The list of diseases caused by smoking has been growing continuously since the first publication of the Surgeon General's report on smoking (U.S. Department of Health, Education and Welfare, Public Health Service, 1964;

U.S. Department of Health and Human Services, 2014). Some of the key health issues associated with smoking include but are not limited to stroke, blindness, congenital defects (such as orofacial clefts and periodontitis), abdominal aortic atherosclerosis, coronary heart diseases, pneumonia, chronic obstructive pulmonary diseases (COPD), rheumatoid arthritis and type 2 diabetes. Smoking has also been linked with an increased risk of cancer of the mouth, nose, throat, oesophagus, trachea, liver, lung, stomach, pancreas, kidney, cervix, bladder and acute myeloid leukaemia. It has also been linked with ectopic pregnancy, erectile dysfunction, hip fractures and loss of immune functions (U.S. Department of Health and Human Services, 2014)

2.4 Smoking and addiction

The act of smoking is often associated with addiction, which is a multifaceted condition involving powerful motivation to engage oneself in a repeated activity, that is usually manifested as compulsive use of a substance (West, 2009). The New Zealand Government has set a long-term goal of reducing the prevalence of smoking to a minimal level in order to make New Zealand an essentially smoke-free nation by 2025. The number of tobacco smokers declined to 380,000 (9.2%) in 2020/21, which is a significant decrease from a peak of 33% in 1983 (Ministry of Health, 2021). As a replacement for the nicotine from tobacco, nicotine replacement therapy (NRT) was introduced to reduce tobacco consumption and prevent nicotine withdrawal symptoms aiming for complete abstinence (Wadgave & Nagesh, 2016). Nonetheless, people who had quit smoking in the past, regardless of their use of NRTs have relapsed at an equivalent rate, and the older population (75+ years), despite having less addiction to nicotine are reluctant to quit (Alpert, Connolly, & Biener, 2013; Jordan et al., 2017). This puts the effectiveness of this widely popular smoking cessation therapy in doubt.

2.4.1 Mechanism of addiction

The mesolimbic system has been the main target for addiction research as it is one of the major substrates for reward sensations in drugs of abuse. It is comprised of the nucleus accumbens (NA) and the midbrain ventral tegmental area (VTA). Dopamine is released from dopaminergic projection neurons in the VTA to the NA in the ventral striatum that mediates reward and limbic brain regions such as the prefrontal cortex, hippocampus and amygdala that are responsible for behavioural control, memory, and mood (Ikemoto, 2007). The dopaminergic mesolimbic system gets activated by rewards, and the NA is able to learn the stimuli that produce the reward as a result of its connection with limbic brain regions (Day & Carelli, 2007). The NA plays a role in both mediating the sensation of pleasure arising from drug use and learning to associate environmental cues with drug use and the resulting psychomotor effects (Drevets et al., 2001; Sampedro-Piquero, Santín, & Castilla-Ortega, 2019).

Different drugs of abuse have slightly different effects on the brain, but in general, all produce a pleasurable spike of dopamine. With the repeated use of these substances, the sensitivity of dopamine is scaled back, leading to a reduction in a substance's ability to produce pleasurable feeling in the user with the dose that used to before. This phenomenon is termed as tolerance, and it increases the amount of the substance of abuse required to produce a pleasurable feeling (Murthy, 2017). Addiction also reduces the ability to experience other rewards, and impairment of the limbic function causes cognitive symptoms, which can hamper new adaptive learnings. As a result, dependence and desire for an addictive substance lead to intensified action on the brain and behaviour (Sampedro-Piquero, de Guevara-Miranda, et al., 2019).

Several types of drugs induce diverse kinds of alteration in brain morphology. Several brain regions are involved at various stages of the development of the

addictive disorder. Cigarette smoke has been found to cause mood elevation or euphoria by causing the release of neurotransmitters such as dopamine in the NA or prefrontal cortex in animals (Herman & Roberto, 2015; Nutt, 1996). Declines in the concentration of enzymes (such as sodium dismutase, catalase and glutathione reductase) and non-enzyme-based free radical scavengers (such as glutathione, vitamins A, C, E) were observed in rat model studies (Anbarasi, Vani, Balakrishna, & Devi, 2006; Méndez-Álvarez, Soto-Otero, Sánchez-Sellero, & López-Rivadulla Lamas, 1998). Therefore, the inability of these scavengers to quench free radicals generated by cellular processes, together with the elevated levels of unsaturated fatty acid in the brain, makes it vulnerable to oxidative damage. Smoking is found to reduce cerebral blood flow causing cerebral hypoperfusion, which, together with oxidative stress, makes the frontal and temporal lobes susceptible to damage (Kubota et al., 1983).

Cigarette smoking has been shown to reduce MAO-A and -B activity in the brain (Lewis et al., 2007). However, exposure to nicotine alone showed no MAO inhibitory activity. In one study, the concentration of nicotine required to produce about 20% inhibition in platelet MAO activity was found to be about 2000 times higher than the typical concentration of nicotine found in the blood of a heavy smoker (Oreland, Fowler, & Schalling, 1981). Thus, chemicals in the smoke other than nicotine must be responsible for the observed lower MAO activity in smokers. We can expect that the inhibition of MAO by cigarette smoke would increase levels of monoaminergic neurotransmitters such as dopamine and epinephrine in the synapse, thereby adding to the effects of nicotine, and would play some role in addiction (Benowitz, 2009). Moreover, smoking is influenced by polymorphisms in dopaminergic genes, which affect dopamine receptor function (Batra, Patkar, Berrettini, Weinstein, & Leone, 2003), giving further support to the widely accepted dopaminergic mechanism inducing addiction to nicotine.

2.5 Genetic and proteomic changes induced by smoking

It is a well-known fact that cigarette smoking causes several health problems and exposes humans to the risk of several diseases, including respiratory, cardiovascular and metabolic diseases, different types of cancers and premature death (detailed in Section 2.3). Smoking has been found to affect different regions of the lungs exposed to cigarette smoke directly and cause injury in different organs throughout the body (Tsai et al., 2018).

Different toxins are introduced in the human body due to smoking, and these toxins are detoxified by the endogenous defence system that includes lipids, proteins etc. Some effects imparted by the cigarette toxins on the human body are thought to be mediated by changes in the DNA sequence of the genes encoding this system. This effect is, however not unidirectional, as the toxins are also able to change the expression levels of different genes or cause DNA mutations (Armani, Landini, & Leone, 2010). Cigarette smoke aerosols have been found to cause the imbalance of histone acetylation/deacetylation, direct DNA damage, and activation of DNA methyltransferases. This causes changes in chromatin remodelling and changes in DNA methylation status, which in turn significantly modifies the transcriptome. Nicotine, which is the major addictive component of cigarette as well as other compounds, can also play direct or indirect roles in changing the gene expression profile (Kopa & Pawliczak, 2018).

2.5.1 Gene and protein expression analysis techniques

The genetic information present in DNA is transferred to RNA via the process called transcription, and the translation of mRNAs results in functional proteins. The analysis of gene expression is helpful in providing useful information on functional aspects such as biological pathways and protein function (Alberts et al., 2002; Polyak & Meyerson, 2003).

Gene expression analysis can be performed by methods such as quantification of RNA expression or protein expression. Molecular biology techniques such as quantitative PCR (qPCR), Northern blotting, serial analysis of gene expression (SAGE), DNA microarrays, RNA sequencing can be employed for the quantification of RNA expression. qPCR, Northern blotting and SAGE are based on a single-gene approach and provide information on the expression levels of specific genes. DNA microarrays and RNA sequencing, on the other hand, are able to quantify the expression levels of thousands of transcripts (Teo, Savas, & Loi, 2016). qPCR was chosen for this study as the aim is to understand the impacts of different treatment exposure on specific genes, which can be successfully achieved using the qPCR technique. Real-time polymerase chain reaction (rtPCR) or qPCR is a molecular biological technique widely used as a sensitive, rapid and accurate method for the quantitative analysis of gene expression. It is based on the principle of PCR, in which a single DNA sequence is exponentially amplified to several billion copies. Each amplification cycle comprises three major steps: Denaturation, annealing and extension. The overview of these steps is presented in Figure 1.

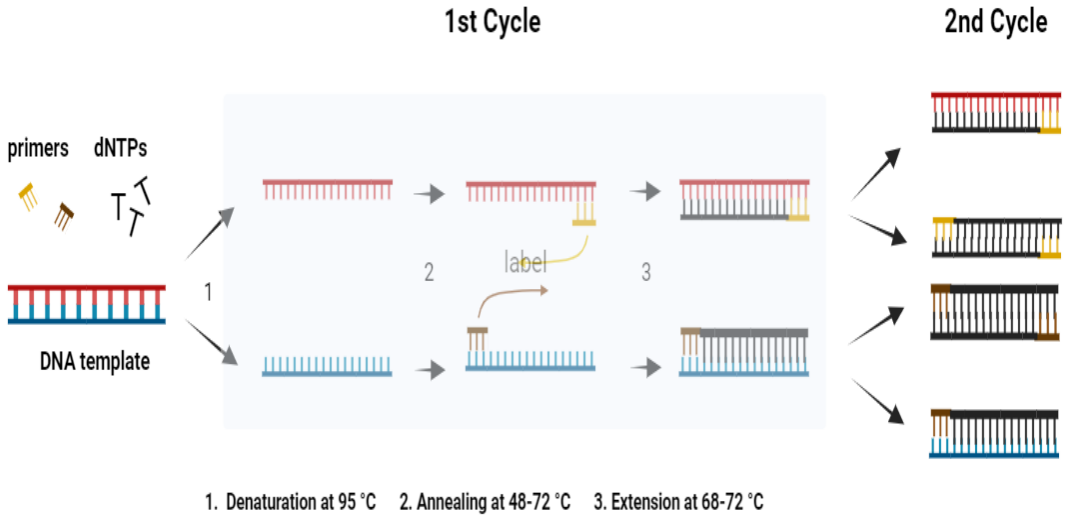

Figure 1: Basic principle of qPCR showing denaturation, annealing and extension steps. Reproduced from (Real-Time PCR (qPCR)), AAT Bioquest, n.d.).

The amount of PCR product produced is measured from the fluorescence of dyes that produce fluorescent signals proportional to the number of PCR products formed. qPCR offers advantages such as high sensitivity, accuracy, detection of low abundance transcripts, making it a preferred choice for the determination of change in expression levels of *MAOA* and *MAOB* (Smith & Osborn, 2009).

Similarly, analysis of protein expression includes techniques such as 2-D gel electrophoresis, ELISA, immunoassays, Western blotting, and mass spectrometry (Polyak & Meyerson, 2003). In this project, Western blots were employed, as this is a widely used molecular biology technique capable of detecting specific proteins in a mixture of proteins isolated from a cell sample. Western blotting is a technique based on three fundamental principles; separation of size, transfer to a solid membrane and detection of the protein of interest in order to visualise and quantify it (Mahmood & Yang, 2012). An overview of important steps in Western blot is shown in Figure 2. Lack of easy access to appropriate resources for other methods also prompted the use of Western blots in this PhD study.

Earlier gene expression techniques, such as qPCR and Western blots were limited to determination of a specific transcript of interest. The advancement in technologies in recent decades allowed the determination of genome-wide quantification of gene expression, termed transcriptomic, initially performed using hybridisation-based microarray technologies. These microarray techniques had limitations such as cross-hybridisation issues, poor quantification of genes with low and high expression levels and requiring pre-existing knowledge of the sequences of interest. Sequencing-based techniques have been developed to elucidate the transcriptome by directly determining the transcript sequence and offer distinct advantages over the earlier methods.

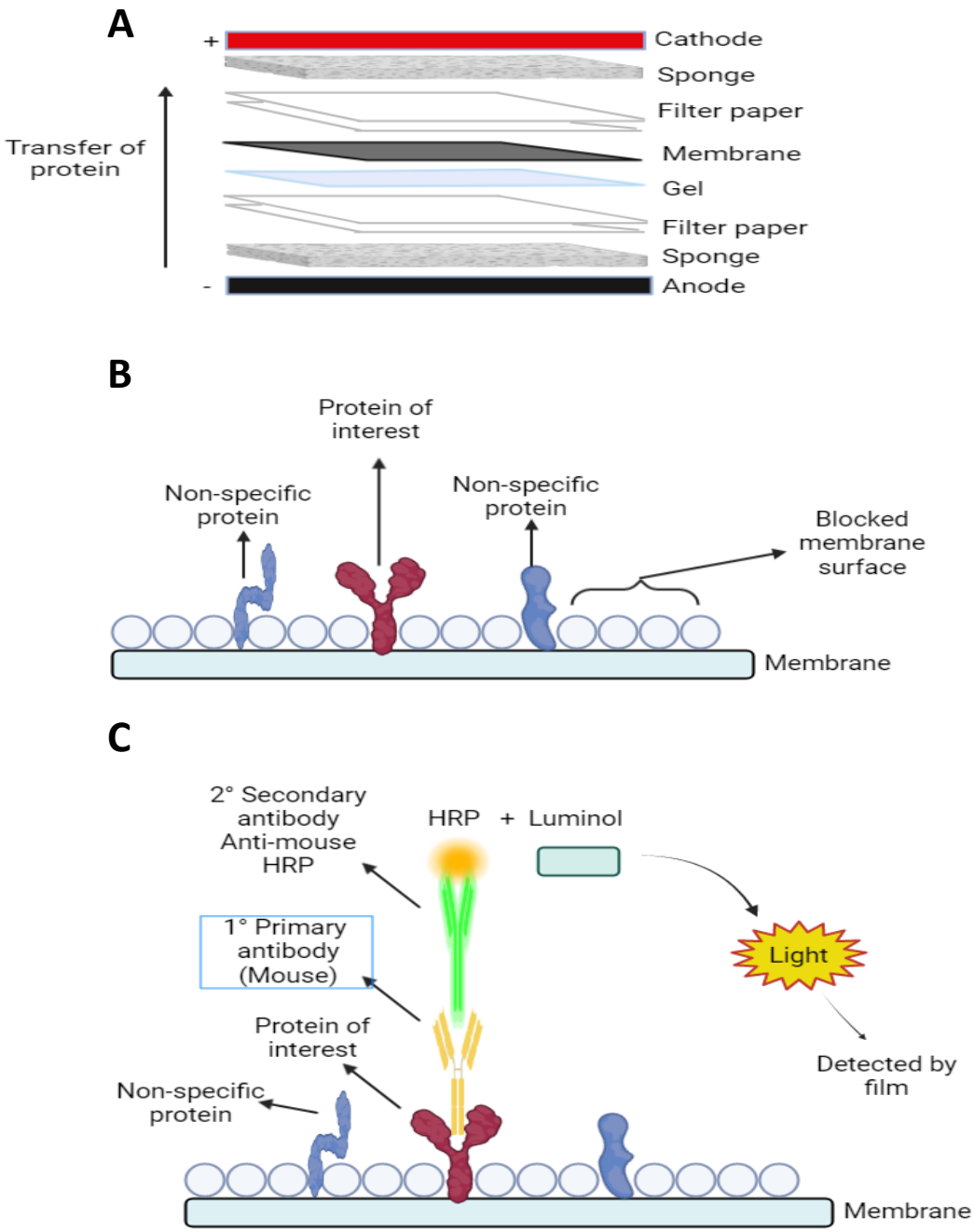

Figure 2: Setup of important steps in Western blot. A. Setup of Western blot transfer. B. Membrane blocked by blocking solution. C. Overview of antibody binding and detection.

RNA sequencing (RNAseq) is a widely used modern technique that enables the detection and analysis of mRNA molecules from any biological sample (detailed in Section 2.5.1.1). RNAseq helps researchers analyse the transcriptome (complete set of transcripts in a cell) and find out which genes are turned on or off and to what extent (Mackenzie, 2018). Thus providing

detailed information about gene expression, allele-specific expression, alternative splicing, elucidation of different physiological and pathological conditions (Kukurba & Montgomery, 2015; Wang, Gerstein, & Snyder, 2009). There are added benefits of RNAseq technology, such as RNA sequence data having less noise and higher specificity than microarray data and sequencing information of the entire population of polyadenylated mRNA being available (Hackett et al., 2012). This has probably encouraged more research related to the effect of smoking, nicotine and tobacco smoke on differential gene expression using RNAseq technology. Because of the advantages of the RNAseq method, it was chosen to determine genome-wide gene expression changes in differentiated SH-SY5Y cells post-exposure treatments.

2.5.1.1 The basics of RNA sequencing

RNAseq is an advanced technique used to analyse the expression of genes across the entire transcriptome. RNAseq comprises three main steps: sample and library preparation, RNA sequencing and data analysis. A basic workflow of steps involved in RNAseq is outlined in Figure 3. Total RNA is firstly isolated from the biological sample, which is purified in the next step to isolate specific RNA species. mRNA is then converted to complementary DNA (cDNA) by the process of reverse transcription. The cDNA molecules are then fragmented into short sequences, and specific sequencing adapters are added to each end of the cDNA fragments. These adapters serve as a barcode and help in sequencing. cDNA fragments are then amplified to facilitate detection before the sequencing. The amplified cDNA fragments are sequenced using the Next Generation Sequencing (NGS) platform of choice to the desired depth. The sequencing platform produces transcript data containing millions of short sequences, termed as reads. These reads are mapped into a reference genome or assembled de novo if a reference genome is not available.

Following the mapping of reads to a reference genome, the expression level of genes is determined by counting the total number of reads aligned with exons or full-length transcripts. The data are then analysed to determine differential gene expression between samples exposed to various conditions, detect allele-specific expression, and determine gene enrichment (Assefa, 2020; Kukurba & Montgomery, 2015; Wang et al., 2009). Exposure treatments can induce transcript levels of the same gene to vary significantly. This biological phenomenon is termed as differential expression. One of the major applications of RNAseq experiments is the determination of differential gene expression that provides information about the genes that have significant increase or decrease in expression following exposure to different experimental conditions (Assefa, 2020). In my thesis, I have focused on obtaining information on differential gene expression following different exposure treatments.

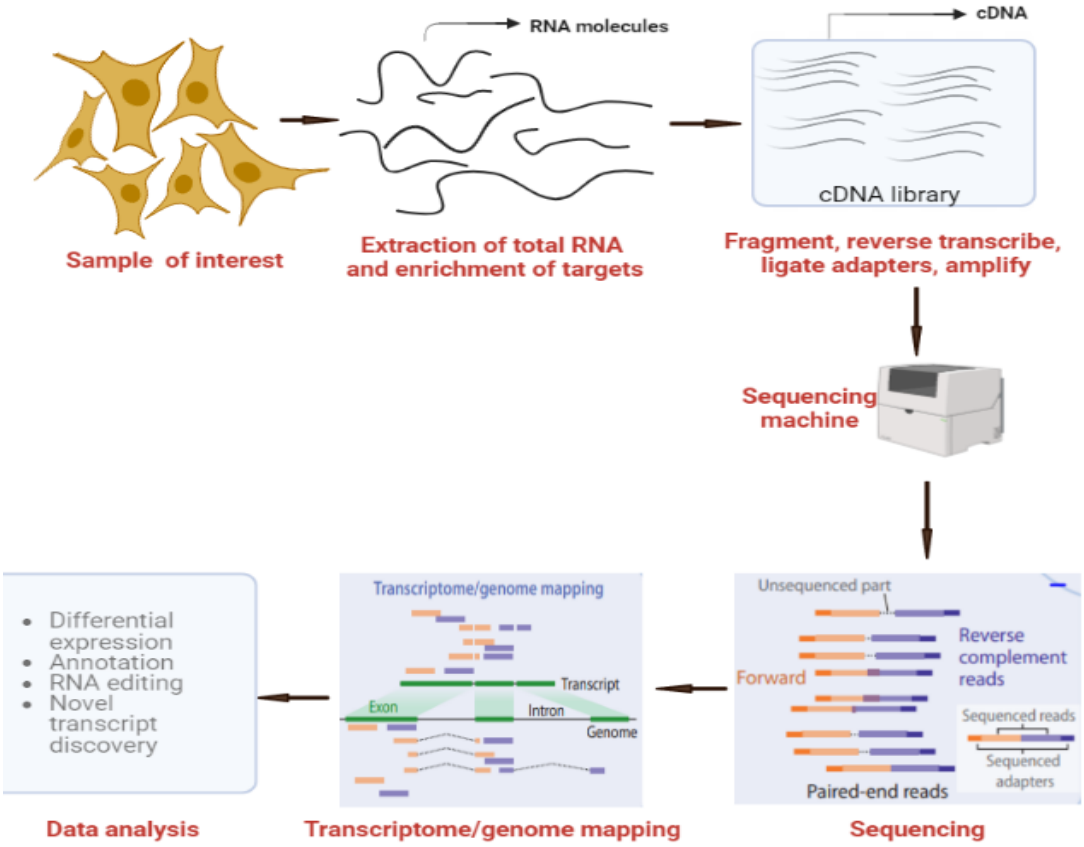

Figure 3: Overview of the experimental steps in the RNA sequencing protocol. RNAseq involves sample and library preparation, RNA sequencing and data analysis (Van den Berge et al., 2019).

2.5.2 Studies investigating the effect of smoking on gene and protein expression

Studies have shown smoking to affect the gene expression profile of a variety of genes (Büttner, Mosig, & Funke, 2007; Harvey et al, 2007; Turetz et al., 2009). A study of change in gene expression in small airway epithelium induced by smoking was performed to compare the gene expression from alveolar macrophages of smokers and non-smokers using RNA microarray analysis (Harvey et al., 2007). They showed up- and down- regulation of several genes that could be categorised to pathways for cytokines, mucin production, response to oxidants and xenobiotics, and general cellular processes that were related to chronic obstructive pulmonary disease. Büttner et al., (2007) found that the gene expression of 88 genes in heavy smokers to be significantly different compared to non-smokers when the gene expression profiles in the cells of the adaptive immune system of the subjects were analysed using RNA microarray analysis. Most of these genes were associated with responses to stimuli, cellular processes, regulation of biological processes when gene function groups were selected for the gene ontology analysis.

In another study, the effect of smoking on tracheal epithelium was studied by the analysis of bronchoscopy samples of small airway epithelium in healthy smokers and healthy non-smokers using Affymetrix microarray technology (Turetz et al., 2009). They found significant differences in gene expression (with a fold change greater than 1.5) of 500 genes in smokers compared to the non-smokers. They further found that genes in the tracheal epithelium were even more sensitive to smoking and had threefold more differentially expressed genes compared to the small airway epithelium. Trachea also had 156 out of 167 genes including genes such as alcohol dehydrogenase 7 (*ADH7*), carcinoem-bryonic antigen-related cell adhesion molecule 5 (*CEACAM5*), cytochrome P450 (*CYP*), malic enzyme 1 (*ME1*) significantly up- or down-regulated due to smoking. Hackett et al. (2012) used RNAseq to determine the complete transcriptome of human small airway epithelium

(SAE) in a group of six healthy smokers and five healthy non-smokers. They determined the changes in SAE gene expression in response to smoking and found that more SAE-enriched genes were upregulated as a result of smoking compared to ubiquitous genes. The comparison of transcriptome data between smokers and non-smokers thus helped determine the effect of cigarette smoke on small airway epithelium and was also helpful in identifying novel smoking-responsive genes such as aldo-keto reductase family 1, member B15 (*ALKR1B15)* and tetra-peptide repeat homeobox-like (*TPRXL*) that were induced by smoking and genes such as transcription factor paired box 1 (*PAX1*) and azurocidin (*AZU1*) that were repressed by smoking.

Boyle et al., (2010) investigated the effect of smoking on the oral mucosal transcriptome profile. They performed buccal biopsies on 40 current and 40 never-smokers who were age and gender-matched to study the change in transcriptome profiles. They found that smoking changed the gene expression of 41 genes, with 32 genes showing increased expression and the rest showing decreased expression in the oral mucosa of smokers compared to people who have never smoked. The genes that had changes in expression were related to nicotine signalling (e.g. cholinergic receptor, nicotinic, α3), xenobiotic metabolism (e.g. cytrochrome P 450 family, UDP glucuronosyltransferase 1 family, NAD(P)H dehydrogenase, quinone 1, aryl-hydrocarbon receptor repressor), cell adhesion (e.g. carcinoembryonic antigen-related cell adhesion molecule 7), and oxidant stress (e.g. aldehyde dehydrogenase 3 family, member A1, glutathione peroxidase 2). A study was performed to develop insight into the effect of smoking on lymphocytes (Charlesworth et al., 2010). Transcriptional profiles were obtained from 1240 subjects that included 297 current smokers using anti-sense RNA microarray. Correlation between smoking and gene expression levels was determined, and they found 323 unique genes significantly correlated with smoking behaviour. The affected genes were associated with immune response e.g. adenosinen deaminase (*ADA)* and C-type lectin domain containing 5A (*CLEC5A)*, natural killer (NK) cell activity e.g. cluster of differentiation 247 (*CD247*) and *CD300A*, cell death e.g. *CD38, CD300A*, and cancer e.g. acyl-

CoA oxidase 2 (*ACOX2*) and aquaporin 3 (*AQP3*). This study concluded that cigarette smoking affected the entire network of gene interaction rather than individual genes.

A meta-analysis of whole blood transcriptome-wide gene expression of current smokers, former smokers and people who had never smoked, totalling ~10,000 participants from six different cohorts, was performed (Huan et al., 2016). They analysed the effect of smoking on modification of the transcriptome and found huge changes brought about by smoking, with 1270 genes having altered gene expression compared to never-smokers. The researchers further determined change in the expression of 39 genes when a comparison of former vs never smokers was made. They also found that 12 genes including Leucine Rich Repeat Neuronal 3 (*LRRN3*), G-protein coupled receptor 15 (*GPR15*), and Claudin Domain Containing 1 (*CLDND1)* had increased gene expression levels even up to a period of 30 years post-smoking cessation, which would suggest that some molecular consequences of smoking last for decades.

Similarly, smoking also induces changes in the structure and functions of different proteins in the human body. Smoking produces several free radicals, including hydroxyl radicals, hydrogen peroxide, superoxide anion and reactive oxygen species (Valavanidis, Vlachogianni, & Fiotakis, 2009). Tobacco smoke components such as heavy metals are also able to catalyse the reaction that results in the formation of free radicals (Yan, 2014). These free radicals and reactive oxygen species may react with the protein backbone, thereby causing protein fragmentation and change in the primary configuration of proteins. This may further lead to distortion of the secondary and tertiary structure of proteins, which may lead to random conformation of protein as well as change in protein function. Oxidations of proteins may also cause the induction of disulphide or other intermolecular bridges, which may lead to protein aggregation and polymerisation. This in turn, can change the proteolytic properties and influence different physical and chemical properties

of protein (Zhang, Xiao, & Ahn, 2013). Reactive oxygen species are also able to modify amino acid residues (Yeh et al., 2008). The change in amino acid can, in turn, increase disulphides and carbonyl groups and decrease α-helices in the protein resulting in a conformational change of the protein (Ściskalska, Zalewska, Grzelak, & Milnerowicz, 2014).

Studies showing the effect of smoking on the expression level of different proteins have been previously done (Kelsen et al., 2008; Yang et al., 2018; Kokelj et al., 2020). Yang et al., (2018) found smoking to exert an impact on bronchoalveolar lavage cell proteome. They observed changes in expression levels of more than 500 proteins that represented 15 different molecular pathways as a result of smoking. A study was performed among healthy controls, ex-smokers and current smokers to observe the effect of smoking on proteins and pathways associated with smoking (Kokelj et al., 2020). It was found that smoking caused alterations in the levels of 112 proteins. They also performed gene set enrichment analysis (GSEA) to confirm that most of the proteins altered were associated with the vesicle-mediated transport pathway and the protein activation cascade pathway. In another study, smoking was shown to induce unfolded protein response in the human lung (Kelsen et al., 2008). They observed that proteomes from the lung samples of chronic smokers had 26 proteins with differential expression compared to non-smokers. Also, several UPR proteins such as chaperones, calreticulin, protein disulphide isomerase, and glucose-regulated protein 78 had increased expression in smokers compared to non-smokers and ex-smokers

2.5.3 Studies investigating the effect of cigarette smoke and its components on gene and protein expression

There has been research on determining the effect of cigarette smoke and its components on gene expression (Russo et al., 2011; Wright et al., 2012; Banerjee et al., 2017; Haswell et al., 2018). Russo et al. (2011) studied the effect of different concentrations of cigarette smoke condensate on the SH-

SY5Y human neuroblastoma cell line. A 24 h exposure to different concentrations of cigarette smoke condensate significantly reduced the gene expression of antioxidant enzymes, namely SOD1, SOD2, GPx and CAT. Wright et al. (2012) analysed the effect of cigarette smoke extract on THP-1 cells and primary human peripheral blood mononuclear cells (PBMCs), and found that exposing the cells to 10% v/v cigarette smoke extract for 8 hours caused a change in 117 genes with 80 genes having increased expression while the rest decreased expression by at least 1.5-fold in THP-1 cells. PBMCs had 199 genes with increased expression and 206 genes with decreased expression by greater than 1.5-fold. Banerjee et al. (2017) compared the change in gene expression profile in lung epithelial tissue post-exposure to cigarette smoke and e-cigarette aerosols using RNA sequencing. They also performed gene enrichment analysis to determine the biological function that could possibly be affected by exposure to cigarette smoke and found cigarette smoke exposure to affect inflammation and oxidative stress pathways. In another study examination of changes in transcriptome profile in airway tissue after exposure to an aerosol from commercial Tobacco Heated Products (THPs) compared to an aerosol from the standard research cigarette 3R4F found 2809 RNAs to be differentially expressed after the 3R4F treatment (Haswell et al., 2018).

Nicotine is recognised as the major addictive component in cigarettes. Many studies have demonstrated that nicotine has an impact on the expression levels of a wide range of genes (Dunckley & Lukas, 2003; Hosur, Leppanen, Abutaha, & Loring, 2009; Wang et al., 2011). Wang et al. (2011) observed the effect of acute nicotine exposure on gene expression of a SH-SY5Y cell culture system using a customised microarray. They found that 1 h nicotine treatment changed the expression of 295 genes. They also found that the altered expression in most genes occurred via signalling mediated through nicotinic acetylcholine receptors (nAChRs). They were also able to determine 14 different biochemical pathways that were modulated by nicotine, which included neuronal survival/death, neural development, cell metabolism, and immune response. In another study, hα4β2 SH-EP1 cells were exposed to 10

μM nicotine for varying time periods (Hosur, Leppanen, Abutaha, & Loring, 2009). RNA Microarray analysis was performed, and it was found that 41 genes showed a change in expression. Gene expression changes in pathways, including cytokines, transcription factors, chemokines, cytosolic proteins were observed, which might affect the hα4β2 up-regulation. Dunckley & Lukas (2003) found exposure to 1 mM nicotine for 1 hour changed the expression of several genes that coded for RNA binding proteins, transcription factors, plasma membrane associated proteins, and protein processing factors in SH-SY5Y cells. The result from cDNA microarray analysis showed 17 genes from the list of 5000 screened genes to have altered expression. The result was confirmed using quantitative polymerase chain reaction (qPCR), with 14 out of 16 genes tested showing altered expression. Increasing the exposure period caused additional changes to gene expression, as seen in a later study performed by these workers (Dunckley & Lukas, 2006). They found that exposing SH-SY5Y cells to 1 mM nicotine for a period of 1 day consistently changed the expression of 163 genes, and 13 out of 14 genes chosen for further study using qPCR showed a similar result, validating the cDNA microarray analysis.

Likewise, cigarette smoke and its components can also induce proteomic changes and are depicted by many studies (D'anna et al., 2015; Gugatschka et al., 2019; Paulo & Gygi, 2017; Kitamura et al., 2020). A proteomic analysis performed to observe the effect of cigarette smoke on the protein profile using left ventricles of spontaneously hypertensive (SHR) rats and control SHR showed significant alteration in 30 protein spots (14 up-regulated and 16 down-regulated) in the left ventricles of SHR exposed to cigarette smoke compared to control (Kitamura et al., 2020). They also used Western blot to confirm changes in the expression level of some proteins. D'anna et al., (2015) performed two-dimensional electrophoresis (2DE) and matrix-assisted laser desorption/ionisation time-of-flight mass spectrometry (MALDI-TOF-MS) to identify changes in protein expression levels after exposure to cigarette smoke extracts using human foetal lung cells (HFL-1). They found seven proteins with increased and four proteins with decreased expression at

different experiment points in cigarette smoke extract treatment compared to the control. They used mass spectrometry (MS) to conclude the differentially expressed proteins being involved in mitochondrial activity, ageing, stress response.

In another study, an analysis was conducted using mass spectrometry to evaluate the effect of nicotine treatment across four cell lines that included HEK, PaSC, HeLa, and SH-SY5Y (Paulo & Gygi, 2017). It was found that 31 proteins had 1.5-fold or greater increased expression across all the cell lines used. Similarly, 64 proteins were up-regulated in at least three of the four cell lines. They found proteins such as Amyloid-like protein 2 (APLP2), lysosomal-associated transmembrane protein 4A (LAPTM4B), Amyloid beta A4 protein (APP) to be dysregulated by nicotine treatment in all cell lines that could possibly be related with downstream signalling pathway such as autophagy. In another study by Gugatschka et al. (2019), human vocal fold fibroblasts were exposed with cigarette smoke extract for 24 h and 4 days. Quantitative mass spectrometry was performed, and cigarette smoke was found to increase expression levels of proteins that were typically involved in oxidative stress responses. They also observed an increase in the levels of UDP-glucose 6-dehydrogenase, a molecule responsible for the synthesis of hyaluronan, which is a component of the vocal fold lamina propria and a reduction in levels of fibrillar collagens, collagen alpha-1(I) chain (COL1A1) and collagen alpha-1(2) chain (COL1A2).

Though several studies have determined the effect of cigarette smoke and its components on several specific proteins and gene expression, these have seldom extended to investigating changes in MAO-A and MAO-B protein and gene expression. Lewis (2010) used SH-SY5Y cells and observed changes in MAO-A and MAO-B protein and gene expression levels after exposure to cigarette smoke using Western blot and RT-PCR, respectively. The change in gene and protein levels at different periods of time after the exposure were

also compared, and the result showed inconsistent changes in protein and gene expression at different time points.

2.6 Components of cigarette smoke

Tobacco contains many classes of compounds, including hydrocarbons, alcohols, ketones, aldehydes, nitriles, carbohydrates, amino acids, alkaloids, isoprenoids, sterols, acids, quinones, proteins, nucleic acids, peptides, starch, cellulose, hemicellulose. These compounds present in tobacco are exposed to temperatures of up to 950˚C in varying levels of oxygen during smoking, giving rise to different smoke components via several processes such as combustion, distillation, pyrolysis and pyrosynthesis (Baker, 2006). The temperatures in the burning cigarette range from 800-950˚C while puffing and about 700-800 ˚C between the puffs (Baker, 1974). Rodgman & Perfetti (2008) estimated cigarette smoke to have 7,357 chemical compounds that are from 21 different classes. Cigarette smoking, hence, produces a complex mixture of chemical compounds that are either bound to aerosol particles or remain free in the gas phase. The compounds in cigarette smoke can either distil into smoke directly or react to form other compounds which distil to cigarette smoke (Centers for Disease Control and Prevention, US, 2010).

With the objective of developing a priority list for monitoring the constituents of cigarette smoke, a list of almost all the known toxic chemicals present in cigarette smoke was prepared. Many of the chemicals found in tobacco smoke have been classified as human carcinogens by the International Agency for Research on Cancer (IARC). These chemicals are grouped into three categories: group 1 are known human carcinogens, group 2A are probably carcinogenic to humans, and group 2B are possibly carcinogenic to humans and listed in Appendix, Table A (Fowles et al., 2000). The IARC has categorised eight compounds in cigarette smoke as carcinogenic and at least ten compounds as probably or possibly carcinogenic (Smith & Hansch, 2000).

2.6.1 Nicotine

Nicotine is a major component of cigarette smoke, believed to have the main role in addiction. It is a bicyclic compound having pyridine and pyrrolidine rings and is dibasic (Figure 4). (S)-nicotine is the predominant form present, and a low quantity of (R)-nicotine is due to racemisation during the pyrolysis process (Benowitz, 1996). Nicotine is a water-soluble compound and is mainly absorbed through the oral mucosa, lungs, skin, and gut, depending on the pH of the solution. Increasing the pH of a solution increases the amount of uncharged lipophilic nicotine, which can pass through biological membranes easily and alter intracellular signalling. It can easily be metabolised by the liver through microsomal oxidation and glucuronidation. It is reported to affect important organs of the body, such as the heart, lungs and kidneys. Moreover, it has also been used as an insecticide (Mishra et al., 2015; Subramaniyan, 2015).

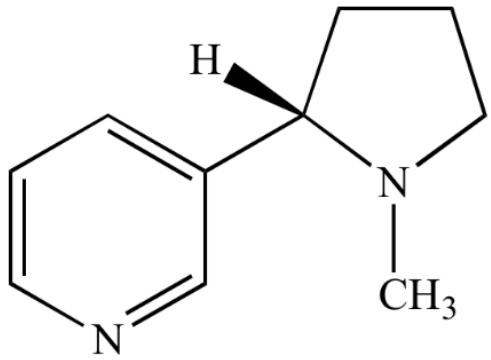

Figure 4: Chemical Structure of (S)-Nicotine.

2.6.1.1 Mode of action

(S)-nicotine is stereoselective for the nicotinic cholinergic receptor, and (R)-nicotine is a weak agonist of this receptor. These cholinergic receptors are referred as neuronal acetylcholine receptors (nAChRs) and are ligand-gated channels comprised of five subunits. nAChRs are present in both the central

and peripheral nervous systems (Barik & Wonnacott, 2009). There are nine α subunits (α2 to α10) and three β subunits (β2 to β4), and the most abudant receptor subtypes in the mammalian brain, are α4β2, α3β4, and α7 (homomeric). Among them, the α4β2 receptor subtype is predominant and is believed to be the receptor responsible for mediating nicotine dependence and the α3β4 nAChR subtype is believed to be the mediator for the cardiovascular effects induced by nicotine (Benowitz, 2009).

The neuropharmacology of nicotine is shown in Figure 5. Nicotine enters the systemic circulation in distilled cigarette smoke from the lungs via the pulmonary venous circulation and quickly enters the brain (Benowitz, 2009; Westfall & Brasted, 1972). After diffusing to the brain tissue, nicotine binds to ligand-gated nAChRs and opens them, allowing the influx of cations such as sodium and calcium. The entry of sodium and calcium activates voltage-dependent calcium channels allowing the entry of more calcium (Benowitz, 2009). An nAChR may exist as one of the several different interconvertible functional states, dominant ones of which are resting state (channel closed and agonist binding site occupied), activated state (channel open), desensitised state (channel closed and agonist bound with high affinity), and inactive state (long lasting desensitised state). Exposure to high concentrations of acetylcholine (ACh) or nicotine allow signal transduction to an activated state. (Barik & Wonnacott, 2009; Benowitz, 1996).

The activation of nAChRs releases growth hormone, prolactin and adrenocorticotropin, and a variety of neurotransmitters such as acetylcholine, norepinephrine, serotonin, β-endorphin, among which dopamine is the most prominent. Dopamine is released in the mesolimbic area, frontal cortex, and corpus striatum. Dopaminergic neurons in the ventral tegmental area of the midbrain and dopamine release in the NA are critical in drug-induced reward. The release of most of the nicotine-mediated neurotransmitters occurs by presynaptic nAChRs. However, the direct release of neurotransmitters also occurs.

Nicotine-mediated augmentation of glutamate release and long-term inhibition of GABA release facilitates dopamine release (Benowitz, 2009). The ERK1/2 signalling pathway has also been highlighted in the activation of nAChRs by nicotine. This pathway is related to associative learning processes and reward and reinforcing effects shown by drugs of abuse. Changes in ERK1/2 and the cellular transcription factor CREB following chronic oral nicotine administration in mice have been reported (Brunzell, Russell, & Picciotto, 2003). Genes involved in downstream targeting of ERK1/2 and CREB include c-Fos, FosB and Zif268, expressed in response to drugs of abuse (Valjent et al., 2006) and chronic nicotine use (Nisell et al., 1997; Pagliusi et al., 1996). FosB is demonstrated to be induced in the striatum of rats treated regularly with either cocaine or nicotine (Nestler, 2001; Pich et al., 1997). A study using SH-SY5Y cells suggested a complex role for nicotine in α7 and non-α7 nAChR signalling (Dunckley & Lukas, 2006). Also, *in vivo* acute and chronic nicotine treatments show specific patterns of changes in total and phosphorylated proteins such as ERK1/2 and their targets (Brunzell et al., 2003; Nuutinen, Barik, Jones, & Wonnacott, 2007).

The release of dopamine provides a pleasurable experience, increasing brain reward function, which reinforces the effects of nicotine (Nestler, 2005). With low agonist concentration due to the breakdown of dopamine by MAO, or nACHRs desensitised due to continued exposure to agonists (e.g. stable blood plasma nicotine level in smokers), receptor signalling is inhibited. This causes reduced reward, withdrawal symptoms and cravings, making a person want to smoke more cigarettes (Benowitz, 2009).

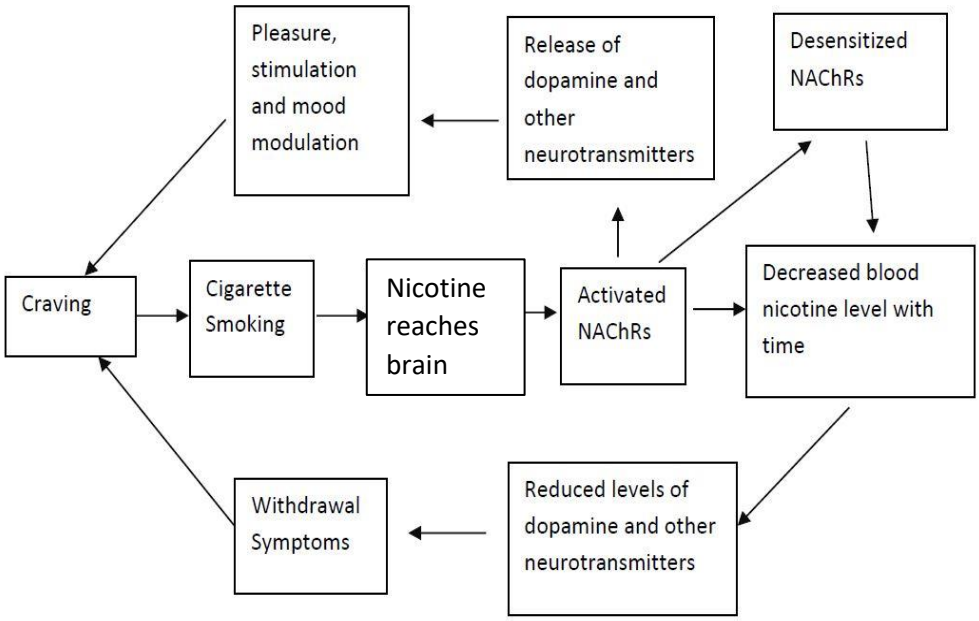

Figure 5: Overview of the neuropharmacology of nicotine.

2.6.2 Other components

Particulate matter or components other than nicotine in cigarette smoke include tar, carbon monoxide, nitrosamines, polynuclear aromatic hydrocarbons, chlorinated dioxins and furans. The component mixture varies depending on the source of tobacco (Fowles et al., 2000). MAOIs are an important group of compounds present in cigarette smoke relevant to this PhD project. Several MAOIs, including harman and norharman, have been reported to be present in cigarette smoke and have been shown to inhibit MAO isoforms (George & Weinberger, 2008). This is further discussed in Section 2.11.

2.7 Analysis of cigarette smoke components

The analysis of cigarette smoke involves three major steps: smoke collection, extraction of TPM and quantification. Numerous studies have been performed with different motivations for collecting cigarette smoke using smoking

machines. The earliest reports of smoking devices being used are believed to be from 1843 (Klus, Boenke-Nimphius, & Müller, 2016). Since then, smoking devices have gone through different modifications and advancements for the generation and collection of cigarette smoke using different puff parameters (Klus et al., 2016; Park et al., 2016). The extraction of TPM is another important part of the chemical analysis of cigarette smoke. A common method is the collection of particulates on a filter pad and extraction using solvent, but the use of a cold trap, bubbling through liquids, or electrostatic precipitation (Johnstone, Qual & Carruthers, 1962; Khalil, Davies & Castagnoli Jr, 2006; Klus et al., 2016; van der Toorn et al., 2019) are also possible. The method to be chosen for TPM extraction would depend on the requirements of the end user, and the equipment / chemicals available.

The final phase of analysing cigarette smoke is the quantification of the desired components present in the cigarette smoke. Quantification of ingredients that are present in the cigarette smoke is a very challenging task and several analytical techniques have been developed. The method to be employed for the quantification depends on the target substance to be analysed and includes GC-FID (Gas Chromatography-Flame Ionised Detector), GC-MS (Gas Chromatography-Mass Spectroscopy), IC (Ion Chromatography), HPLC (High Performance Liquid Chromatography), HPLC-MS (High Performance Liquid Chromatography-Mass Spectroscopy), IR (Infrared) (Geiss & Kotzias, 2007).

In this PhD project, the need was for a system which would be a reasonable representation of the major components of tobacco able to be collected on filters (since that was the part of tobacco smoke the inhibitors had been identified in by the Tobacco Research Group, Wellington), and for analysis of the key compounds of interest for this study in particular – nicotine, harman, norhaman and the six new MAO inhibitors.

2.8 Monoamine oxidase

2.8.1 General Introduction to Monoamine oxidase

MAO is an enzyme primarily found as an integral protein of outer mitochondrial membranes in the liver, kidney and brain and is responsible for oxidising amine substrates (biogenic and dietary amines) and xenobiotics (such as aniline) (Zhou, Wu, Kwan, & Abell, 1998). MAO has a key role in the metabolism of monoamine neurotransmitters released by neurons and glial cells in the Central Nervous System (CNS), including dopamine, serotonin, histamine, norepinephrine, benzylamine, and phenethylamine. The MAO family have similar structures with almost identical flavin adenine dinucleotide (FAD) binding domains (Figure 6), but the substrate binding site is different.

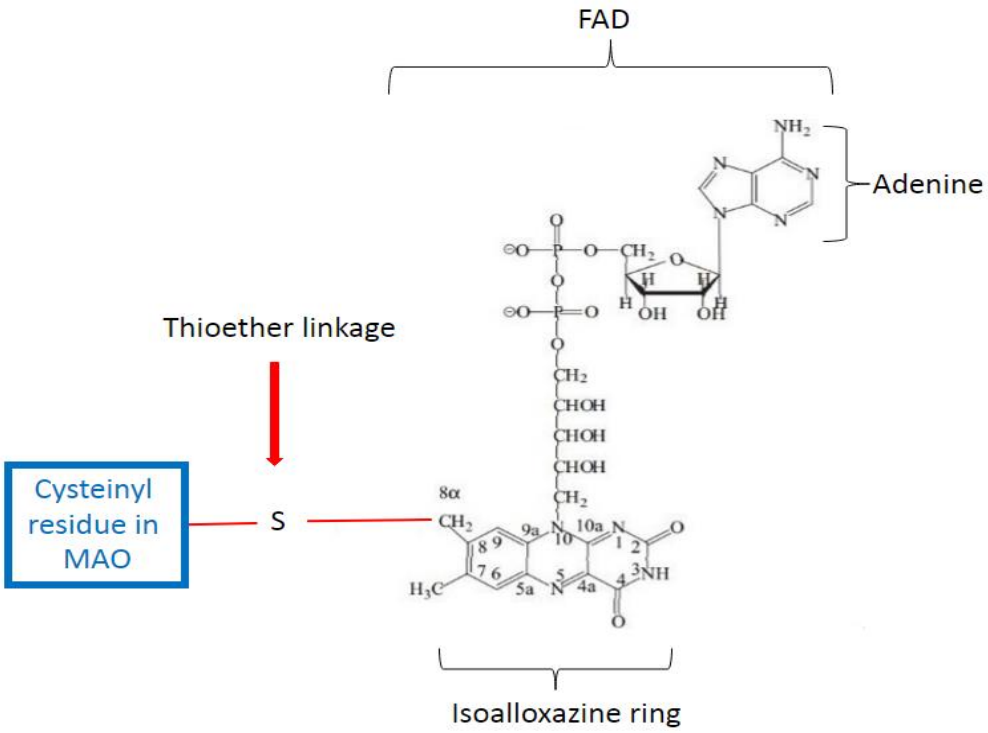

Figure 6: Structure of covalent FAD present in MAO enzyme (Edmondson, Mattevi, Binda, Li, & Hubalek, 2004).

The oxidation by MAO occurs via a 2-step reaction. Firstly, in the reductive reaction, the hydride equivalent of the substrate is accepted by the flavin cofactor, and it is reduced. Secondly, molecular oxygen is accepted by reduced flavin in the oxidative step (Chen, Wu, & Shih, 1993; Gaweska &

Fitzpatrick, 2011). The site for covalent linkage in MAO is towards the C-terminal, and the attachment to flavin occurs through a thioether linkage between a cysteinyl residue and the 8α-methylene of the isoalloxazine ring (De Colibus et al., 2005).

2.8.2 Types, Functions and Localisation

Based on substrate preference, MAO enzymes are categorised as MAO-A and MAO-B. MAO-A is predominantly found in catecholaminergic neurons, while MAO-B is in serotonergic and histaminergic neurons and astrocytes. MAO-A is also able to oxidise serotonin, whereas the MAO-B enzymes are also able to oxidize benzylamine and phenethylamine (Moraes & de Azevedo, 2012; Naoi, Maruyama, & Shamoto-Nagai, 2018). Dopamine, tyramine, and tryptamine can be metabolised by both MAOs. MAO-A is related to synaptic activity, development of neuronal architecture, and the onset of psychiatric disorders such as depression. MAO-B is associated with the production of hydrogen peroxide (H_2O_2) and plays a critical role in neuronal loss in neurodegenerative disorders such as Alzheimer's and Parkinson's (Naoi et al., 2018). Most human tissues co-express both MAO isoforms. However, they are expressed in differential levels in some tissues, summarised in Table 1.

Table 1: Localisation of Monoamine Oxidase in Human Tissues (Berry, Juorio, & Paterson, 1994).

Tissue type	**MAO isoform**
Lymphocytes	Higher MAO-B
Platelets	Higher MAO-B
Placental tissue	Higher MAO-A
Erythrocytes	Lack both isoforms
Lungs and intestine	Higher MAO-A
Brain, liver, adrenal, kidney and heart	High MAO-A and MAO-B

2.8.3 Structure

Both MAO isoenzymes consist of a FAD-binding domain, a substrate-binding site and a membrane-binding site (Figure 7) (Gaweska & Fitzpatrick, 2011). The MAO isoenzymes are 70% homologous, and both bind the mitochondrial membrane through a C-terminal α-helix along with membrane interactions with other hydrophobic residues. (Abell & Kwan, 2000; Gaweska & Fitzpatrick, 2011)

Corresponding amino acids in MAO-A (Lysine-305, Tryptophan-397, Tyrosine-407, and Tyrosine-444) and MAO-B (Lysine-296, Tryptophan-388, Tyrosine-398, and Tyrosine-435) are suggested to play an important role in catalytic activity. Most notably among these residues, Lysine and Tryptophan are observed to be involved in non-covalent binding to FAD and the Tyrosine residues form an aromatic sandwich within the substrate-binding site (Geha, Chen, Wouters, Ooms, & Shih, 2002). It has also been observed that Ile-335 in MAO-A and Tyr-326 in MAO-B are crucial in determining substrate and inhibitor specificities in human MAO (Geha, Rebrin, Chen, & Shih, 2001).

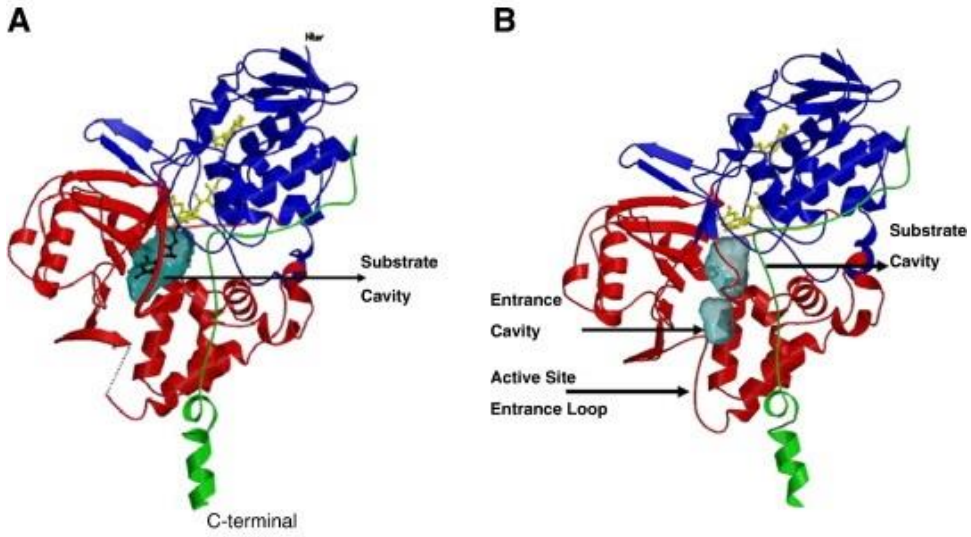

Figure 7: Three-dimensional structure of (A) MAO-A, (B) MAO-B and amine binding sites. The covalent flavin moiety is shown in yellow colour as a ball and stick model. The FAD-binding domain is shown in blue, the substrate-binding domain in red and the mitochondrial membrane-binding domain in green colours (Image by Edmondson et al., 2007 (copyright). Used by permission from Elsevier, Archives of Biochemistry and Biophysics; see Appendix)

MAOA and *MAOB* are derived from the same ancestral gene and are located in opposite orientations on the X-chromosome at Xp11.23 and Xp 22.1, respectively. Both MAOs have 15 exons, among which exon 12 codes for the FAD binding site. cDNA cloning of *MAOA* and *MAOB* established that the two forms of the enzyme are encoded by different genes (Grimsby, Chen, Wang, Lan, & Shih, 1991; Chen, 2004)

2.9 MAO Inhibition by cigarette smoke

Many studies have confirmed cigarette smoke to cause inhibition of MAO activity (detailed later in this section). MAO-A can be measured either directly in fibroblasts or indirectly in plasma or cerebrospinal fluid by determining catabolites of endogenous amines and can be estimated using Positron-emission tomography (PET) analysis. MAO-B can be assayed directly in platelets, and the activity reflects brain MAO-B activity (Bench et al., 1991; Chen et al., 1993).

A comparative analysis of MAO-A activity between smokers and non-smokers was performed, and some brain regions of smokers were observed to have 22-38% less MAO-A activity compared to non-smokers. MAO activity in the occipital cortex had the largest inhibition (38%), while the basal ganglia had the lowest inhibition (22%) associated with smoking (Fowler et al., 1996b). A similar study that compared MAO-B activity among brains and peripheral tissues of smokers, ex-smokers and non- smokers found MAO-B activity to be inhibited by an average of 40% in the brains of smokers compared to the ex-smokers and non-smokers (Fowler et al., 1996a).

Essman (1977) demonstrated dose-dependent deamination of serotonin (5-HT) in an *in-vivo* mouse model. Cigarette smoke and tobacco have been demonstrated to inhibit MAO activity irrespective of the substrate in rat lung mitochondria. However, MAO inhibition was about twice as high when 5-HT was used as a substrate compared to when other substrates, such as

tryptamine, tyramine, benzylamine, were used. Further, exposure of rat lung tissue to cigarette smoke was associated with decreased rat lung MAO activity (Yu & Boulton, 1987). Shahi, Das, & Moochhala (1991) also showed both brain and liver MAO inhibition by cigarette smoke in an *in-vivo* mouse model. When a biogenic amine is exposed to the aqueous extract of cigarette smoke, adducts, m-hydroxy substituted amines (tyramine, dopamine and norepinephrine), are formed, resulting in the formation of indolamines, cyanotetraisoquinolines, and eventually cyanotetra-β-carbolines (Boulton, Yu, & Tipton, 1988). They reported that the adducts 1,2,3,4 tetrahydroisoquinoline and 1,2,3,4 tetrahydro β-carbolines are reported to inhibit MAO-A and MAO-B. Exposure of single-isolated nerve cell bodies from the substantia nigra and nucleus reticularis *Pontis caudalis* to cigarette smoke inhibited MAO by 37% when one cigarette and 100% when four cigarettes were used, respectively. MAO-A was affected more than MAO-B. Animal exposure to cigarette smoke showed increased MAO inhibition dose-dependently, while exposure to smoke from burning cigarette paper showed no effect. (Berlin and Anthenelli, 2001).

Also, human saliva after smoking was shown to have MAO inhibitory activity (10-70%) on rat lung. However, the saliva before smoking did not have any effect on rat lung MAO activity. Smokers have reduced activity of MAO-A (28%) and MAO-B (40%) isoenzymes compared to non-smokers or former smokers (Abell & Kwan, 2000). Early phase of smoking withdrawal is followed by the elevation of MAO-A levels causing undue degradation of monoamine oxidases. This results in oxidative stress and disturbs the normal functioning of neural structures, thereby leading to a depressed mood (Dowlati, de Jesus, Selby, Fan, & Meyer, 2019; Herraiz & Chaparro, 2005).

2.10 Role of MAO inhibition in smoking addiction

MAO inhibition by components present in cigarette smoke in combination with nicotine may produce reinforcing properties exhibited in smoking addiction.

MAO enzymes present in the brain play a role in the degradation of monoamine neurotransmitters such as dopamine, serotonin, adrenaline, noradrenaline (Guillem et al., 2005). It can be hypothesised that when MAO is inhibited, a reduction in catabolism of neurotransmitters such as dopamine occurs resulting in the prolongation of the dopamine reward generated by nicotine. This can possibly contribute to the addictive property of smoking. MAO inhibition may therefore have a significant role in smoking addiction.

2.11 What causes MAO inhibition?

Although smoking causes inhibition of MAO activity, the mechanism behind this inhibition is not clear. Intravenous administration of nicotine (0.3 g) into the primate (baboon) brain was unable to inhibit MAO-B in any brain region (Fowler et al., 1998). Further, Carr & Basham (1991) conducted a study where mice were treated with nicotine, 4-phenylpyridine and hydrazine, all of which are tobacco smoke constituents and tested MAO activity in cerebral tissue. When analysed, none of the compounds inhibited MAO activity. In another study, rat brain mitochondrial MAO-A and MAO-B were measured after exposure to nicotine at physiological concentration for 28 days. No change in MAO-A and MAO-B activity was observed, suggesting a role for non-nicotinic components in MAO inhibition (Castagnoli et al., 2002). The group also isolated 2,3,6-trimethyl-1,4-napthoquinone from flue-cured tobacco, which was found to be a competitive inhibitor of MAO-A and MAO-B. However, the yield of this compound was only 0.8 mg for 1 kg of starting material (Khalil, Steyn, & Castagnoli, 2000). Another compound, 2-napthylamine found in concentrations of 1.0–20 ng/cigarette in cigarette smoke, has also been reported to inhibit both MAO-A and MAO-B, but to a 10-fold lesser extent than 2,3,6-trimethyl-1,4-napthoquinone (Hauptmann & Shih, 2001).

Harman and norharman are the most notable and potent MAOIs in cigarette smoke recognised so far (Herraiz & Chaparro, 2005; Truman et al., 2017).

Both harman and norharman are reported as potent MAO-A inhibitors, while MAO-B was shown to be inhibited by norharman only (Herraiz & Chaparro, 2005). The average amounts of norharman and harman, when quantified in several smoked cigarettes, were found to be 2192 ng/cigarette (range 1114–5846) and 853 ng/cigarette (range 453–2165), respectively. The absolute concentration of these compounds in smoke could differ depending on the cigarette and tobacco, brand, and smoking method (Herraiz & Chaparro, 2005). However, harman and norharman were shown to cause less than 10% of total MAO inhibition shown by tobacco smoke (Truman et al., 2017). This would suggest the possibility of other currently unidentified MAOIs in cigarette smoke (Hong, Teesdale-Spittle, Page, & Truman, 2022).

2.11.1 Candidate MAOIs (Monoamine oxidase Inhibitors)

Six candidate MAOIs have been isolated and quantified from a tobacco smoke preparation by the Tobacco Research Group, Wellington (Table 2), and are of particular interest for this PhD project. These are classified into two groups and have been proposed as key MAOIs present in cigarette smoke based on preliminary studies (SW Hong, pers. comm., manuscripts in preparation). The TPM collection for MAOIs' isolation and characterisation was performed by Dr Ali Heydari (Tobacco Research Group, Massey University) following the method described in Section 4.2.1. Each cigarette was however smoked in one long puff to maximise TPM collection, as over 1000 cigarettes were required to be smoked for the isolation and characterisation of MAOIs. A total of 126.5 g of TPM was collected using this method.

The candidate MAOIs were isolated from the tobacco smoke using bioassay-directed purification by testing each fraction for activity against human recombinant MAO-A (Sigma-Aldrich) and was performed by Drs Penelope Truman, Ali Heydari and Sa Weon Hong (Tobacco Research Group, Massey University). After the compounds were subjected to several purification steps

(Dr Hong), fatty acids present in the high activity fractions and TPM were identified by GC-MS (Kiril Lagutin, Callaghan Innovation), while the catechols were identified by Nuclear Magnetic Resonance by Dr Hong under the guidance of Dr R. Keyzers (Victoria University of Wellington). Major components in these high-activity, partially pure fractions were tested individually for MAO-A inhibitory activity by Drs Penelope Truman and Ali Heydari using the MAO activity assay described in Section 3.7. IC_{50} values for MAO-A and MAO-B inhibitory compounds (Table 3) were calculated by Dr Truman, P Watson, and confirmed by Dr Hong (SW Hong, pers. comm., manuscripts in preparation). The IC_{50} values for harman in Table 3 are obtained from a study by Herraiz & Chaparro (2005). The chemical structures of these candidate inhibitors are presented in Figure 8, and their physical properties are listed in Tables 4 and 5 (PubChem CID: 5280450, 5280934, 785, 289, 9958, 70761).

Table 2: List of candidate MAOIs isolated and quantified by the Tobacco Research Group, Wellington.

Group X – Poly unsaturated fatty acids (PUFAs)	**Group Y - Catechols**
Linoleic acid	Hydroquinone
Linolenic acid	Catechol
	4-Methylcatechol
	4-Ethylcatechol

Table 3: IC_{50} values of candidate MAOIs for MAO-A and MAO-B when tested without preincubation of enzyme with inhibitor.

MAOI	MAO-A IC_{50} (µM)	MAO-B IC_{50} (µM)
Linoleic acid	23.8 ± 8.7	71.7 ± 11.0
Linolenic acid	15.7 ± 1.5	31.9 ± 5.2
Hydroquinone	15.2 ± 2.6	20.5 ± 4.2
Catechol	34.3 ± 6.5	46.4 ± 8.2
4-Methylcatechol	14.1 ± 2.6	32.1 ± 5.5
4-Ethylcatechol	12.6 ± 3.6	21.9 ± 6.1
Harman	0.34 ± 0.009	No inhibition up to 25 µM
Norharman	4.23 ± 1.16	5.17 ± 0.35

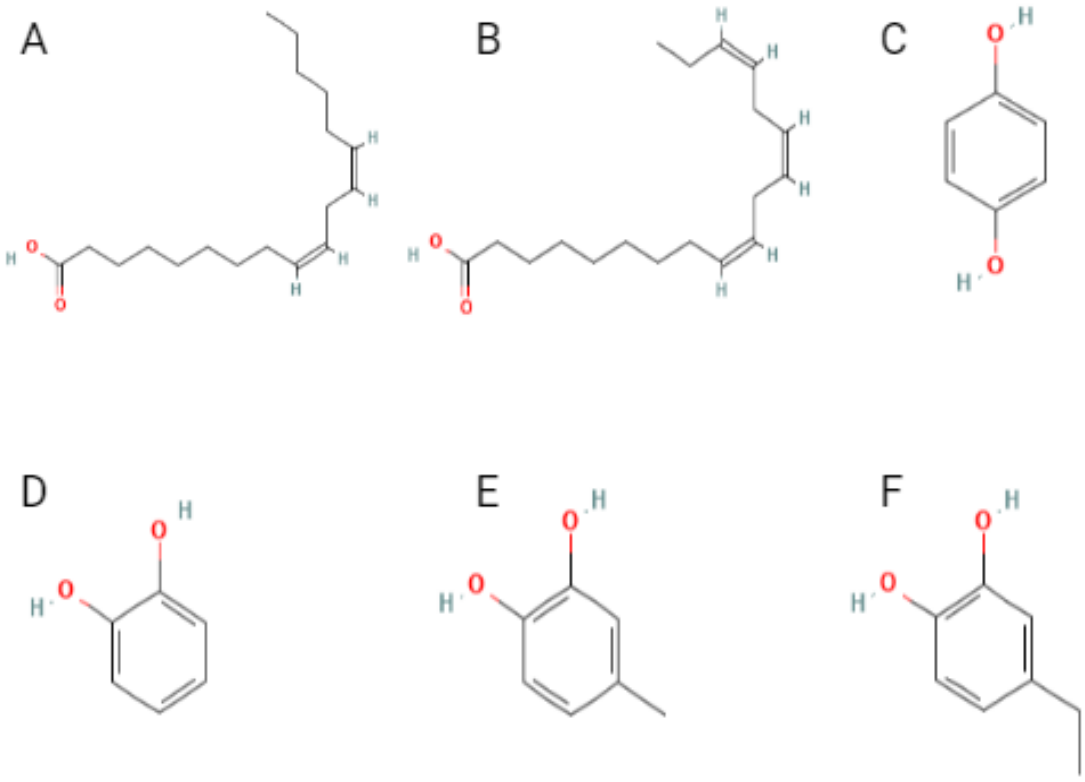

Figure 8: Chemical structure of candidate MAOIs (A) Linoleic acid (B) Linolenic acid (C) Quinol (D) Catechol (E) 4-Methylcatechol (F) 4-Ethylcatechol.

Table 4: Physical properties of Group X candidate MAOIs.

Property	**Linoleic acid**	**Linolenic acid**
IUPAC name	(9*Z*,12*Z*)-octadeca-9,12-dienoic acid	(9*Z*,12*Z*,15*Z*)-octadeca-9,12,15-trienoic acid
Molecular formula	$C_{18}H_{32}O_2$	$C_{18}H_{30}O_2$
Molecular weight	280.4	278.4
Colour	Colourless to straw coloured	Colourless
State	Liquid	Liquid
Boiling point	228.89 to 230 °C at 16 mm Hg	230 °C at 17 mm Hg
Melting point	-5 °C	-11.28 °C
Density	0.9007 at 22.22 °C	0.9164 at 20 °C
Solubility	Water – Insoluble Very soluble in acetone, benzene, ethyl ether and ethanol	Water - less than 1 mg/mL at 22.22° C

Table 5: Physical properties of Group Y candidate MAOIs.

Property	**Hydroquinone**	**Catechol**	**4-methylcatechol**	**4-ethylcatechol**
IUPAC name	benzene-1,4-diol	benzene-1,2-diol	4-methylbenzene-1,2-diol	4-ethylbenzene-1,2-diol
Molecular formula	$C_6H_6O_2$	$C_6H_6O_2$	$C_7H_8O_2$	$C_8H_{10}O_2$
Molecular weight	110.11	110.11	124.14	138.16
Colour	Light coloured	White	White or light brown	N/A
State	Crystal or solution	Solid	Solid	Solid
Boiling point	285 to 287.22 °C at 760 mm Hg	245 °C at 760 mm Hg	247.7 °C at 760 mm Hg	273 to 274 °C at 760 mm Hg
Melting point	173 °C	105 °C	65 °C	41 °C
Density	1.332 at 15 °C	1.344 at 20 °C	N/A	N/A
Solubility	Water - 10 to 50 mg/mL at 20° C	Water - ≥ 100 mg/mL at 21.5° C	Water - 24,900 mg/L at 25 °C	5520 mg/L at 25 °C

Only limited data related to the content of the six candidate inhibitors in cigarette smoke and their MAO inhibitory activity is available in the literature. Studies reported mainstream cigarette smoke and sidestream smoke (smoke coming from the lit end of the cigarette when not being smoked) to contain 88.2-119.70 µg/cigarette and 119.72 - 164.9 µg/cigarette of catechol, respectively. Similarly, the content of hydroquinone in mainstream smoke and sidestream smoke were reported to be 72.2 - 103 µg/cigarette and 149 - 183.5 µg/cigarette respectively (Fowles et al., 2000; Soleimani, Dobaradaran, De-la-Torre, Schmidt, & Saeedi, 2021). A study reported the content of 4-methylcatechol in different cigarette types, including Bright, Turkish, Burley and domestic tobacco, to be 29-80 µg/cigarette and 25-55 µg/cigarette for mainstream and sidestream cigarette smoke respectively. The study also found 4-ethylcatechol content to be 27-102 µg/cigarette and 19-68

µg/cigarette in mainstream and sidestream cigarette smoke, respectively (Sakuma, Kusama, Munakata, Ohsumi, & Sugawara, 1983). These data suggest that the MAOI content may vary depending on the type of cigarette used and the cigarette smoke collection method followed.

A study investigated the binding mode and interaction of omega-3 and omega-6 PUFAs, including linolenic acid, with the MAO-B binding site using Molegro Virtual Docking software. Molecular docking was performed, and the MAO-B inhibitory potential of these compounds was evaluated. (Masroor, Shireen, & Naeem, 2019). They concluded that linolenic acid binds the active site of MAO-B through a single hydrogen bond. They suggested that linolenic acid occupies MAO-B's active site through interaction with amino acid residue Tyr 326. This would, therefore, suggest that PUFAs including linolenic acid could inhibit MAO-B activity. No other research related to MAO inhibitory activity of the candidate MAOIs was found in a PubMed search.

While reversible inhibitors in cigarette smoke have been suspected for a long time, irreversible MAO inhibitors had not been previously linked to tobacco smoke (Herraiz & Chaparro, 2005). Yu & Boulton (1987) reported that MAO activity could be irreversibly inhibited by cigarette smoke. The time course of recovery of MAO activity to normal levels after quitting smoking was concluded to be several weeks, which is similar to that seen with the recovery of MAO levels with the use of known irreversible MAOIs (Fowler et al., 2003). Another study was done by Dr SW Hong in parallel to this PhD study to evaluate the nature of MAO inhibition of these candidate MAOIs. The study suggested that PUFAs are competitive inhibitors, while catechols could be irreversible inhibitors (SW Hong pers. comm., manuscripts in preparation). The presence of catechols (an irreversible inhibitor) in cigarette smoke could possibly explain what caused MAO activity to recover after several weeks of quitting smoking.

2.12 MAO assays

MAO is an enzyme involved in the oxidative deamination of primary amine substrates, including aliphatic, aromatic and some secondary tertiary amines. The MAO isoenzymes A and B are also involved in the degradation of amine neurotransmitters, including serotonin, dopamine, histamine, norepinephrine, benzylamine and phenethylamine (Tipton, Davey, & Motherway, 2000). The oxidation of these amines occurs, as shown in Figure 9.

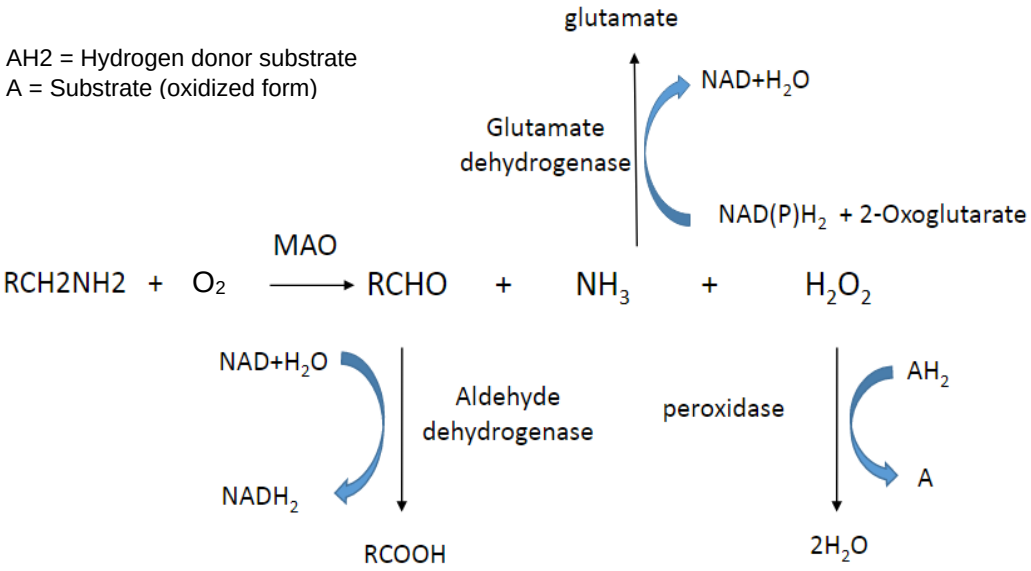

Figure 9: Pathway showing the oxidation of amines by MAO (Tipton et al., 2000).

To get an understanding of the effect of exposure treatment on MAO activity, a method suitable for the samples used in this project was required. Based on the chemical reaction showing the oxidation of amines by MAO (Figure 9), the methods of MAO activity determination may be broadly classified into two types. One measures the disappearance of oxygen or the amine substrate, and the other measures the appearance of the aldehyde product, hydrogen peroxide, ammonia or acidic and alcoholic metabolites (Tipton et al., 2000). Several assay protocols have been developed and validated based on these principles, each of which has its own pros and cons. The early assay protocols based on these principles have seen several modifications in recent times to develop more sensitive, rapid, and simple methods for the determination of MAO activity.

H_2O_2 being a common product in the reactions catalysed by MAO, detection of its production can help determine MAO activity for most substrates. Snyder & Hendley (1968) developed a simple and sensitive fluorometric method to assay MAO *in vitro.* The assay quantified the fluorescence produced from homovanillic acid and H_2O_2, when the substrate was added and oxidative deamination occured. They used liver and brain tissue samples from female Sprague-Dawley rats as an enzyme source and incubated them with horseradish peroxidase and homovanillic acid and an appropriate amine substrate. This gave rise to fluorescence quantified in a spectrofluorometer at an activation wavelength of 315 nm and fluorescence wavelength of 425 nm. Nakano, Kawai, & Nagatsu (1984) used glutathione and glutathione peroxidase to reduce the H_2O_2 formed in similar reactions and the estimation of glutathione was performed fluorometrically. They used mitochondrial fractions of rat liver or brain and incubated sample extracts along with glutathione peroxidase, reduced glutathione and the monoamine substrate tyramine. Oxidised glutathione was measured by measuring the fluorescence intensity at 460 nm with an excitation at 360 nm using a spectrofluorometer.

Zhou & Panchuk-Voloshina (1997) developed a fluorometric method for the assay of MAO in 96-well plates, which was much more sensitive than the previous methods. Their assay was based on the detection of H_2O_2 using N-acetyl-3, 7-dihydroxyphenoxazine (Amplex Red), a very sensitive and stable probe for hydrogen peroxide. Horseradish peroxidase and H_2O_2 convert Amplex Red to resorufin, a stable and fluorescent product. The fluorescence is then measured spectrofluorometrically to give an estimate of MAO based on the production of H_2O_2 in the reaction. They were able to assay MAO-A and MAO-B activity from cattle brain selectively. This assay could potentially be used in tissues, blood samples and body fluids. Amplex Red Hydrogen Peroxidase kits (Thermo Fisher Scientific, Auckland) have been developed as an advanced one-step assay method to measure MAO activity in different enzyme preparations, including extracts from cells and tissues. The problem with MAO assays based on measuring the production of hydrogen peroxide is the complexity created in data interpretation as MAO enzyme activity is

measured indirectly via a coupled reaction. The Amplex Red MAO activity assay kits sometime give inconsistent and unreliable results (Lewis, 2010).

Another method based on the formation of reaction products is based on measuring the amount of ammonia formed during the oxidative deamination of amine substrates by MAO. Nagatsu & Yagi (1966) assayed MAO activity in rat liver by incubating the homogenate together with serotonin creatinine sulphate. Ammonia liberated was measured by colour development using an indo-phenol method. Harada & Nagatsu (1973) also determined the MAO activity of rat brain regions such as the caudate nucleus, thalamus and hypothalamus with various amines and glutamate dehydrogenase (GLDH) assay mix. Ammonia was detected by fluorometric measurement of nicotine adenine dinucleotide hydrogen (NADH) conversion to NAD^+ in the GLDH assay system, which was used as a measure of MAO activity. However, this method is not applicable with secondary amines as deamination by MAO produces methylamine instead of ammonia and hence requires measurement of H_2O_2 formation.

Based on the principle of estimation of aldehyde and acid metabolites, Yu, Bailey, & Durden (1986) used High Performance Liquid Chromatography (HPLC) for the separation as well as electrochemical detection of the by-product aldehyde and acid formed as a result of oxidative deamination of amine substrate by enzymes. MAO activity in the mitochondrial fractions of rat liver was assessed by incubating together with the substrates using HPLC-electrochemical detection. In another study n-octylamine and n-decylamine were used as substrates, which were converted to n-octylaldehyde and n-decylaldehyde, respectively, by MAO (Tenne, Finberg, Youdim, & Ulitzur, 1985). They determined MAO activity in rat liver, rat brain and human platelets samples and n-octylamine or n-decylamine as substrate by recording the change in luminescence with time.

MAO assays can also be performed based on the consumption of oxygen during the deamination of a substrate by enzymes. Creasey (1956) identified

MAO activity by manometrically measuring the uptake of oxygen during the deamination of monoamines. MAO activity was determined in the mitochondrial fraction of homogenates obtained from rat liver, estimating the uptake of oxygen by taking manometric readings at different time intervals. The peroxidatic activity of catalase, cytochrome oxidase, aldehyde oxidase, which could all be present in the crude MAO preparations and might affect the oxygen uptake, was also measured. The same method was also used in another study to determine MAO activity in mitochondria from pig brains (Tipton & Dawson, 1968). The method was supplemented with an oxygen electrode which was connected to a strip chart recorder via a voltage divider and measured the oxygen consumed during the oxidation of tyramine by MAO.

Another common method of estimation of MAO activity is based on the measurement of the disappearance of amine substrates. A rapid spectrophotometric assay based on the rate of metabolism of kynuramine, a substrate, which is rapidly oxidised by MAO, was used in a study (Weissbach, Smith, Daly, Witkop, & Udenfriend, 1960). Liver homogenates were incubated together with the substrate kynuramine. The disappearance of kynuramine was determined as it had been proved earlier that kynuramine is readily metabolised by MAO to 4-hydroxyquinoline. Kynuramine is a non-selective substrate and has specificity for both MAO-A and MAO-B with Km values of 42 μM and 26 μM respectively (Wang et al., 2018; Yan, Caldwell, Zhao, & Reitz, 2004). An overview of the mechanism involved in the oxidation of kynuramine (I) by the MAO to form the product 4-hydroxyquinoline (III) is shown in Figure 10. An aldehyde (II) is formed as an intermediate product which either condenses to give 4-hydroxyquinoline or is further metabolised to an acid (IV) or lactam product (V). Condensation of the aminoaldehyde has been found to occur faster than oxidation of the aldehyde to form acid or lactam products (Weissbach et al., 1960).

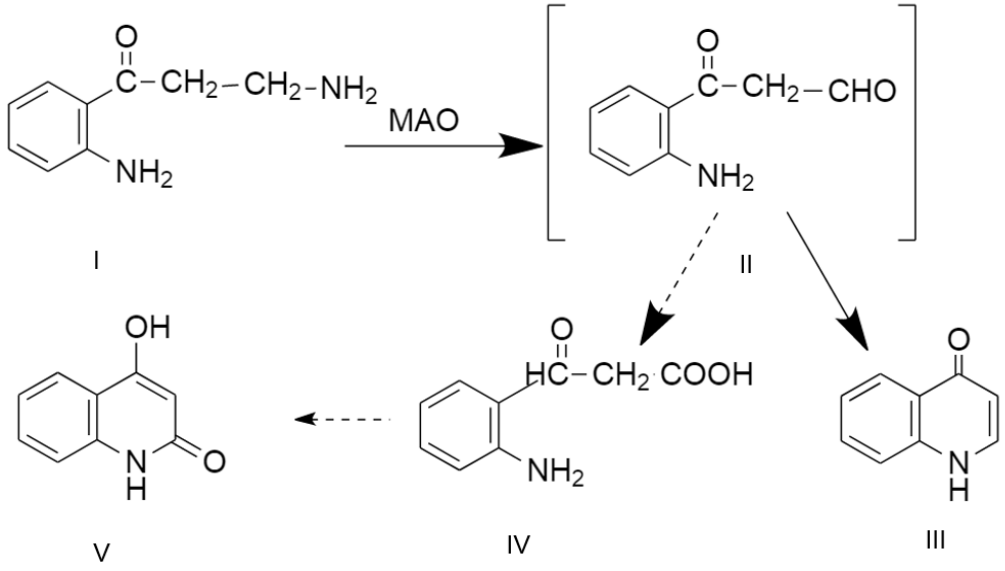

Figure 10: Mechanism of oxidation of kynuramine by MAO (Weissbach et al., 1960).

Krajl (1965) modified the method described by Weissbach et al. (1960) to develop a highly sensitive and convenient MAO assay. They monitored the appearance of 4-hydroxyquinoline formed by oxidative deamination of kynuramine instead of determining the disappearance of kynuramine. They incubated a variety of tissues, such as rat brain, guinea pig atria, and cat ganglia, with kynuramine and the fluorescence of 4-hydroxyquinoline was measured. 4-Hydroxychloroquine shows strong fluorescence in highly alkaline conditions, which can be measured using a spectrophotometer at an excitation wavelength of 318 nm and an emission wavelength of 380 nm (Massey & Churchich, 1977).

In another study, kynuramine was used as a substrate to determine MAO activity in different hybrid cells, which were derived by the fusion of liver or brain cells and were compared with that of parent/non-parent clones (Nagatsu, Nakano, Kato, & Higashida, 1981). The relative proportion of MAO-A and MAO-B activities in each cell type was also determined by developing an inhibition curve with the help of MAOIs clorgyline and deprenyl. Kynuramine has also been used as a substrate to measure MAO activity in

whole blood (van Kempen, van Brussel, & Pennings, 1985). They found that MAO activity in the total platelet population could be determined by using whole blood instead of preparing platelet-rich plasma, which is time-consuming. Morinan & Garratt (1985) modified the protocol for MAO assay described by Krajl (1965) to present a more sensitive and modified kynuramine assay method. They used perchloric acid to terminate the reaction instead of trichloroacetic acid (TCA) used in the earlier method, which prevented the quenching of the fluorescence by TCA, thereby increasing the sensitivity of the assay. They were also able to test the effect of six different MAOIs and were able to estimate MAO-A and MAO-B activity by the use of specific inhibitors. Kynuramine assays also were used to determine the MAO inhibitory effect of different cigarette brands and tobacco products (Lewis, 2010). MAO-A selective inhibitor clorgyline and MAO-B selective inhibitor pargyline was used to measure the inhibition of purified human recombinant MAO-A and MAO-B. In a study, 12 novel acetamide derivatives having MAO inhibitory properties were characterised (Kaya, Sağlık, Levent, Özkay, & Kaplancıklı, 2016). Kynuramine was used as a substrate to identify the MAO-A and MAO-B inhibitory effects of these compounds. Kynuramine assay was also used to determine MAO inhibitory activity for 12 different e-liquids (Truman, Stanfill, Heydari, Silver, & Fowles, 2019).

A review of the literature demonstrates several methods for the measurement or assay of MAO activity. Accurately measuring the change in the MAO activity after exposure treatments is a major requirement for this PhD project. Kynuramine assays are relatively simple and also devoid of interference due to other cellular processes that might generate H_2O_2. Many samples were required to be assayed, which was applicable to the kynuramine assay. The cost of using the kynuramine assay compared to using other kit-based assays was nominal (Lewis, 2010). More importantly, supervisor Dr Truman had also successfully used and validated the method and all the reagents and equipment required were available at Massey University, School of Health Sciences, Wellington, which encouraged the choice of the kynuramine assay over others. Lewis (2010) successfully used the kynuramine assay to identify

MAO activity in SH-SY5Y cells treated with tobacco extracts, which was similar to the current project. All these factors supported the choice of the kynuramine assay for this PhD project, which was modified slightly to determine MAO activity from the cell lysates.

2.13 Cell culture as a model for brain research

The use of cell culture as a model for neuroscience research has gained popularity because of the advantages it offers compared to using *in vivo* models. Cell culture systems are very simple in nature, so they can be easily manipulated to have differential gene or protein expression, eliminating the need for suitable *in vivo* models that can simulate the disease or condition that is of interest to the researcher (Gu, 2017). Cell culture has also provided scientists with an alternative approach to the use of animals in research. Several cell lines expressing specific neurotransmitters have been developed, which are used as neural cell lines. Additionally, glial cell lines that have been derived from gliomas or glioblastomas are available. Altogether, these cell culture systems are being used for neuroscience research, including neural growth, differentiation, plasticity, gene expression, protein expression, toxicity etc. Some of the commonly used cell lines in brain research include SH-SY5Y, PC12, N1E-115, Neuro 2a, and HCN-2 (Gu, 2017; Gordon & Amini, 2021). In this PhD project, I used the SH-SY5Y cell line because of the properties explained in Sections 2.13.1 - 2.13.2.

2.13.1 SH-SY5Y human neuroblastoma cells

The SH-SY5Y human neuroblastoma clone cell line was derived by cloning a subline of SK-N-SH cells three times; first to SH-SY, then to SH-SY5, and finally to SH-SY5Y. SK-N-SH cells originated from a bone marrow biopsy of a neuroblastoma patient with sympathetic adrenergic ganglial origin in the early 1970s. Among the different phenotypes of SK-N-SH cells; neuronal (N-type), Schwannian (S-type), and intermediary (I type); SH-SY5Y cells are

homogeneous with N-type and therefore possess many biochemical and functional properties of a neuron. Cells with N-type morphology are positive for tyrosine hydroxylase (TH) and express dopamine β-hydroxylase, characteristic of catecholaminergic neurons. Cell culture of this cell type includes both adherent and floating cells, both of which are viable. Most studies discard the floating cells and use the adherent cells, while few studies are conducted on floating cells (Kovalevich & Langford, 2013). Adherent cells were used in this study to conform to the approach used in most other studies.

2.13.1.1 Type and function

SH-SY5Y cells can be differentiated with the aid of differentiating agents such as retinoic acid, phorbol esters and neurotrophins (Xie, Hu, & Li, 2010). Differentiated cells have synchronised cell cycles, which fluctuate dramatically in undifferentiated cells. Several studies suggest that floating cells are more likely to adhere and differentiate into a N-type phenotype than adherent cells (Kovalevich & Langford, 2013). The morphology of undifferentiated cells is neuroblast-like, and has non-polarised bodies and few truncated processes. They grow in clusters and forms clumps where the cells seem to grow on top of one another. This cell type continuously proliferates, expresses immature cell markers and lacks mature neuronal markers. They are also considered to be reminiscent of immature catecholaminergic neurons. The morphology of differentiated cells is similar to primary neurons with long exquisite processes, which are randomly distributed and distinctly polarised. Differentiation of SH-SY5Y cells decreases their proliferation rate and increases neuron-specific enolase (NSE) activity (Kovalevich & Langford, 2013; Xie, Hu, & Li, 2010)

2.13.2 Rationale behind choosing the SH-SY5Y cell model

The SH-SY5Y cell line is a commonly used model of neuronal cell behaviour and physiology, as it exerts several biochemical and functional characteristics

of a neuron. Some reports suggest the use of SH-SY5Y cells for determining the level of endogenous MAO-A and MAO-B enzymes (Jiang, Jiang, Liu, & Feng, 2006; Ren, Jiang, Ma, Nakaso, & Feng, 2011) and a few studies have determined the response of SH-SY5Y cells when treated with nicotine and tobacco extracts (Dunckley & Lukas, 2006; Sokolova, Matteoni, & Nistri, 2005). The differentiation method for the generation of N-type SH-SY5Y cells has been revolutionary for neurological studies, as the method is relatively easy, has low cost compared to primary human neuronal cell lines and is devoid of the ethical concerns associated with primary human neuronal cell lines (Xie et al., 2010). Since the SH-SY5Y cell has neuronal characteristics, the results obtained can also be closely correlated with *in vivo* methods. There are some limitations associated with cell culture models, such as higher chances of contamination and the requirement of frequent passage. Hence, attention to following the standard protocols along with strict aseptic cell handling practices is required (Arango, Quintero-Ronderos, Castiblanco, & Montoya-Ortíz, 2013).

2.14 Cell differentiation

Cell differentiation is a process that enables cells to become specialised for a specific function. The differentiation of cells enables cells from the same lineage to produce cell groups that are different in morphology and functions. The human body is composed of trillions of cells, each of which is derived from stem cell precursors. Specialised cells develop from progenitor cells, which are descendants of stem cells. Pluripotent stem cells and progenitor cells have the potential to become any type of specialised cell. This capacity, however is slowly lost as cells differentiate and gain specialised functions. Different mechanical and chemical stimuli trigger the process of cell differentiation, which causes the cells to undergo major changes in shape, metabolic activity, and overall function. The cells also start expressing certain sets of genes more than others at various stages of cell differentiation (Ng, Pawijit, Tan, & Yu, 2019).

2.14.1 Rationale behind Differentiation of SH-SY5Y cells

Both differentiated and undifferentiated SH-SY5Y cells have been used in neuroscience studies and this cell line is an important neuronal cell model (Cheung et al., 2009). Differentiated SH-SY5Y cells offer some advantages compared to the undifferentiated ones. Firstly, differentiation dramatically reduces cell proliferation, which is helpful in maintaining an almost constant cell number, making experiments involving cell exposures or cellular toxicity studies relatively easy to carry out (Kovalevich & Langford, 2013). Secondly, undifferentiated SH-SY5Y cells do not usually exhibit the markers that are typical of the mature neurons. Differentiation enables SH-SY5Y cells to reduce their proliferation as well as to develop extensive neurite outgrowths that are similar to the neurons in the living brain (Xie et al., 2010). Since the differentiated cells demonstrate morphological as well as biochemical properties similar to those of neurons, transformation to more pronounced neuronal phenotype makes studies using differentiated SH-SY5Y cells more comparable with the actual phenomena in the human brain.

2.14.2 Differentiating agents

Different differentiating agents have been in use for the differentiation of cell lines to cholinergic, adrenergic or dopaminergic phenotypes. Retinoic acid (RA) is one of the common agents used for differentiation. It binds to retinoid X receptors (RXR) and retinoic acid receptors (RAR) and regulates the transcription of neurotrophin receptor genes and pathways involving type II protein kinase A. RA causes the transformation of SH-SY5Y cells to a cholinergic neuronal phenotype. Phorbol esters are another type of differentiating agent that causes a significant reduction in cell growth and transformation to an adrenergic neuronal phenotype. Neurotrophins have also been shown to induce cell differentiation and modulate survival. Other agents include staurosporine, guanosine, guanosine-5'-triphosphate etc. (Xie et al., 2010). Two or more agents have also been used to induce differentiation.

Examples include a combination of RA and dibutyryl cyclic adenosine monophosphate (dbcAMP), RA and one of tissue plasminogen activator growth/differentiation factor 5 (GDF5), recombinant bone morphogenetic protein 2 (BMP2), staurosporine glial cell line-derived neurotrophic factor (GDNF) (Xicoy, Wieringa, & Martens, 2017).

2.14.3 Retinoic acid induced SH-SY5Y cell differentiation

The decision to use RA in this study to induce cell differentiation was based on its induction of the cholinergic neuronal phenotype characterised by expression of nicotinic acetylcholine receptors, which are the binding sites for nicotine, which is of significance in this study (Kovalevich & Langford, 2013). The most visible and common change in SH-SY5Y cells after treatment with RA is the extension of neurites. This can be seen as early as one day post-treatment. Differentiation is very distinctly visible, as undifferentiated cells have very short neurites (Cheung et al., 2009). RA has been shown to greatly reduce cell proliferation (Jahn et al., 2017). RA differentiated cells show a significant increase in the expression of neuronal markers such as tyrosine hydroxylase (TH), neuron-specific enolase (NSE), synaptophysin, SAP97 (Post synaptic associated protein 97) and NeuN (Neuronal nuclei) (Cheung et al., 2009; Lopes et al., 2010; Wang et al., 2018). RA treatment has also shown to increase the expression of expression of choline acetyl transferase (ChAT) activity and vesicular monoamine transporter (VMAT) (Adem, Mattsson, Nordberg, & Påhlman, 1987; Presgraves, Ahmed, Borwege, & Joyce, 2003). Similary, reduction in expression of inhibitor of differentiation 1 (Id1), cyclinD1 and cyclin-dependent kinase 4 (CDK4) (Cheung et al., 2009; Wang et al., 2018) and no significant change in the expression of neurofilament (NF), microtubule-associated protein 2 (MAP2) and dopamine transporter (DAT) (Cheung et al., 2009) have been found in previous studies.

2.15 Cytotoxicity Assays

Cigarette smoke consists of many harmful compounds. A report confirmed that at least 250 compounds, out of more than 7000 compounds present in cigarette smoke, are potentially harmful (Suarez-Torres, Alzate, & Orjuela-Ramirez, 2020). This includes compounds such as hydrogen cyanide, ammonia and carbon monoxide. Toxicity tests can be performed on cell systems *in vitro*, which has the associated benefit of being able to get quick results at a relatively low cost. Such tests are helpful to determine whether a chemical, or a mixture of chemicals, has any cytopathic or cytotoxic properties using a cell system rather than a whole animal or human health statistics (Stratton, Shetty, Wallace, & Bondurant, 2001). Toxicants can induce toxicity in cells by stimulating the increased production of chemicals such as nitric oxide and reactive oxygen species, which subsequently result in oxidative stress. The toxicants may also induce mitochondrial dysfunction as a result of oxidative stress or cause the production of compounds that can cause DNA damage resulting in cell toxicity (Zhang, 2018). Cytotoxicity assays are used to determine the ability of compounds to induce toxicity in cells resulting in cell damage or cell death (Adan, Kiraz, & Baran, 2016). Though cytotoxicity tests have the limitation of having results based on the response depicted by a single cell type, they can be important in identifying whether or not any compound or product is worth further development or research (Stratton et al., 2001).

Different methods are available for the assessment of cytotoxicity based on a variety of functions, such as cell membrane permeability, enzyme activity, ATP production. The use of membrane impermeable fluorescent dyes to selectively stain dead cells is one of the common methods to determine cytotoxicity. Trypan blue, propidium iodide, and ethidium homodimer-1 are some examples of dyes that are used based on the principle of membrane permeability. These dyes are not able to penetrate inside live cells as the cell membrane of the live cell membrane is intact. However, they can seep through the non-intact cell membranes of dead cells and stain them (Coder,

2001; Fang & Trewyn, 2012). Another method for cytotoxicity assay by estimating the number of dead cells is based on determining the activity of enzymes that leak from the cytoplasm to the cell culture medium. Lactase dehydrogenase assay, adenylated kinase assay, and glyceraldehyde-3-phosphate dehydrogenase (GAPDH) are common examples of assays based on this principle. These enzymes leak from the cytoplasm to the cell culture medium and catalyse the formation of coloured, luminogenic or fluorescent products from suitable substrates. (Riss, Niles, Moravec, Karassina, & Vidugiriene, 2019)

Another method involves the measurement of different aspects of general metabolism or enzyme activity that exists in a viable cell. Examples include tetrazolium reduction, protease activity assay, and resazurin reduction, in which reagents are incubated with live cells and converted to a substrate that can be detected using instruments such as a plate reader or spectrophotometer (Riss et al., 2016).

2.15.1 MTT assay

The MTT (3-(4,5-dimethylthiazol-2-yl)-2,5-diphenyl tetrazolium bromide) assay is one of the many cytotoxicity test methods, which is based on colorimetric measurement of cell metabolic activity. It is based on the principle that metabolically active cells can reduce the yellow tetrazolium dye MTT to the insoluble product formazan, which is purple (Figure 11). Metabolically active cells have NAD(P)H-dependent oxidoreductase enzyme, which is responsible for this reaction. The insoluble formazan product is then made soluble with solubilising agents such as dimethyl sulfoxide (DMSO) or acidified ethanol solution. The absorbance of this solution is then quantified using a spectrophotometer set at a wavelength usually between 500 and 600 nm. The result of which will be dependent on the number of metabolically active cells present in the sample, as dead cells will be unable to contribute to oxidative reduction of MTT to formazan. (Kuete, Karaosmanoğlu, & Sivas, 2017). The

MTT assay is considered as one of the well-established methods for determining cytotoxicity. Some advantages of the MTT assay are that it is easy to perform and a quick result is achieved. It is versatile as it can be used with several cell lines and is a reproducible method with demonstrated clinical correlation between *in vitro* and *in vivo* testing (Kuete et al., 2017; Supino, 1995; Winikoff, Zeh, DeMarco, & Lotze, 2011).

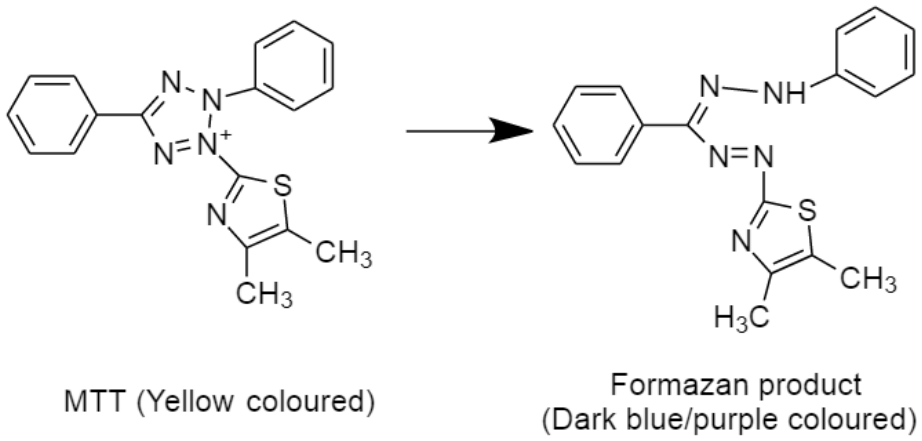

Figure 11: Schematic diagram showing chemical reaction involved in MTT assay. Yellow-coloured MTT is converted into purple-coloured formazan by the enzyme mitochondrial reductase. (Kumar, Nagarajan, and Uchi, 2018).

In a previous study, SH-SY5Y cells were treated with different concentrations of salsolinol and the MTT assay was performed to determine the dose-response relationship of salsolinol-induced toxicity (Copeland, Leggett, Kanaan, Taylor, & Tizabi, 2005). Further, SH-SY5Y cells were treated with nicotine as well as nicotine antagonist and a MTT assay was performed to determine if nicotine had any neuroprotective effect. In another study, SH-SY5Y cells were treated with different concentrations of areca nut extracts and arecoline to determine the dose that would induce cytotoxicity in the cells (Chen et al., 2012). Another report described the effect of cigarette smoke condensate on gene expression of different antioxidant enzymes by exposing SH-SY5Y cells to different concentrations of cigarette smoke extract (Russo et al., 2011). They performed a MTT assay to determine concentrations that would produce toxic effects and checked if exposure to the toxic concentration

was also marked by an increase in the production of free radicals and a change in the gene expression of antioxidant enzymes. Therefore, the use of MTT was deemed appropriate for this study as results could be assessed in relation to that of other similar studies.

2.16 Conclusion

Smoking is a global health problem responsible for the death of millions of people. A better understanding of smoking addiction and its underlying mechanism is helpful in supporting smoking cessation efforts. Though many studies indicate cigarette smoke to have MAO inhibitory potential, the literature lacks sufficient research on the primary components of cigarette smoke causing this effect. Similarly, the effect of smoking on gene and protein expression changes has been investigated in earlier research, but research on the effect of cigarette smoke and MAOIs on MAO gene and MAO protein expression is very limited. These gaps identified in the literature serve as a foundation for this PhD study.

Chapter Three: General Methods

3.1 Introduction

An overview of this PhD project is shown in Figure 12, which includes the layout of different experiments conducted throughout the PhD study, including TPM collection and extraction, preparation of human neuroblastoma SH-SY5Y cells and cell exposure (Chapter 4), determination of MAO activity and examining toxicity (Chapter 5), qPCR and Western blotting examining MAO gene and protein expression respectively (Chapter 6) and RNA sequencing examining genome wide expression under the different treatment conditions (Chapter 7). This chapter provides information on general methods employed for this project, which include cell culture (Section 3.2), cell differentiation (Section 3.3), preparation of cell lysate (Section 3.4), assay of protein concentration (Section 3.4), mRNA extraction (Section 3.5), MAO activity assay (Section 3.7), Western blotting (Section 3.8), qPCR (Section 3.9) and statistical analysis (Section 3.10). The specific methods for individual experiments are described in the Method sections of the individual Chapters 4-7.

3.2 Cell culture

The human neuroblastoma cell sub-line SH-SY5Y was used as a model for the study of the effect of nicotine, TPM and cocktail of the six candidate MAOIs in this research, with the control group exposed to ethanol, the solvent for the other treatment compounds. The detailed cell culture method and maintenance of the cells are explained below.

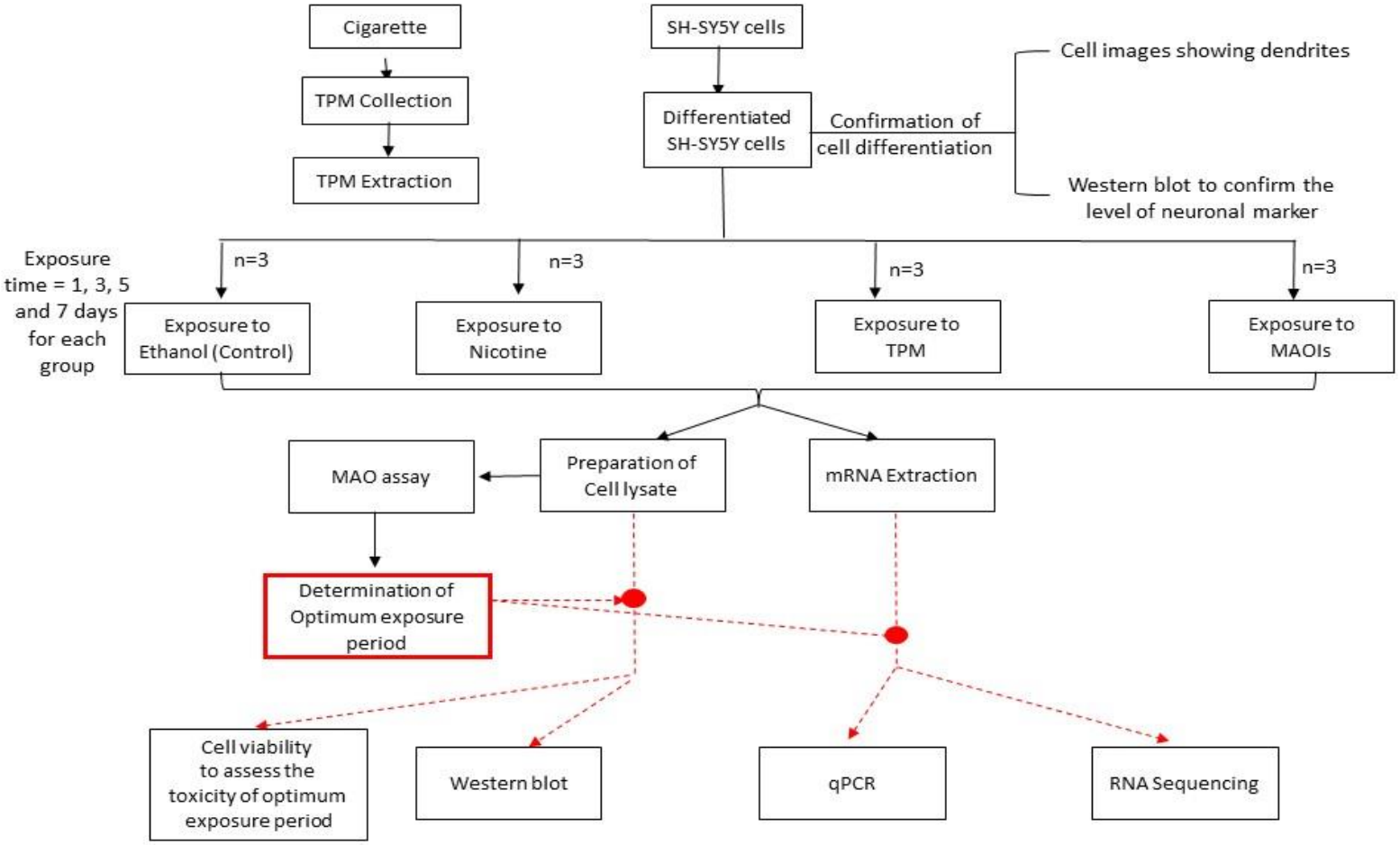

Figure 12: Overview of the PhD study comparing the impact of Nicotine, TPM and MAOI exposure on MAO activity, protein and gene expression of SH-SY5Y cells. Exposure time = 1, 3, 5 and 7 days for each group. The optimum time period of exposure was determined from the result of the MAO assay and the rest of the experiments were carried out only for the optimum time period exposure, which is denoted by red dashed lines. TPM collection & extraction, preparation of cell culture and cell exposure is detailed in Chapter 4, determination of optimum exposure period from the results of MAO assay and toxicity of exposure treatment is detailed in Chapter 5, qPCR and Western blotting is detailed in Chapter 6 and RNA sequencing is detailed in Chapter 7.

3.2.1 Culture condition

The SH-SY5Y (human bone marrow neuroblast) cell line, purchased from ATCC (American Type Culture Collection), was available in a frozen state stored at -80°C at Massey University and it was used throughout this project. It was cultured in Roswell Park Memorial Institute 1640 medium (RPMI 1640) (GIBCO, Invitrogen) with 10% v/v heat inactivated Foetal Bovine Serum (FBS) (Sigma) and 1% v/v Penicillin-Streptomycin (P/S) (10,000 Units Penicillin and 10 mg streptomycin per mL) (Sigma). The SH-SY5Y cells were maintained in a 75 cm^2 (T-75) Nunc ™ cell culture flask (ThermoFisher) in a cell culture CO_2 incubator (Esco). The incubator was set at 37˚C in a humidified atmosphere of 5% CO_2. Cells were differentiated as detailed in Section 3.3. Cell passaging, media refreshment etc were carried out in an aseptic environment in a horizontal biological safety cabinet. The cabinet was sterilised by UV irradiation for 15 minutes, and wiping the surfaces with 70% ethanol before and after each use.

3.2.2 Cell passaging and medium refreshment

Frozen cells were rapidly thawed by placing them in the incubator at 37˚C. Once cells were thawed, they were carefully pipetted into the cell culture medium and kept in a 25 cm^2 (T-25) Nunc ™ cell culture flask (ThermoFisher). About 10 mL of cell culture medium had been pre-warmed at 37 °C for 2 hours before thawing the cells. The medium was refreshed within 24 hours to avoid toxicity from the dimethyl sulfoxide (DMSO) present in the cell culture medium containing frozen cells. To refresh the cell culture medium, the cell culture flask was taken out from the incubator and the medium was removed with the aid of a pipette. About 10 mL of fresh and pre-warmed cell culture medium was added carefully with the aid of a pipette, touching the walls of the cell culture flask taking consideration not to disturb the cells.

Cells were transferred to a T-75 cell culture flask after they reached ~ 90%

confluence, which was estimated using a microscope. Cell culture medium and PBS (Phosphate-Buffered Saline) were pre-warmed in the incubator at 37 ˚C for 2 hours. To transfer the cells to a T-75 cell culture flask, the cell culture medium was removed, and 5mL pre-warmed PBS (Phosphate-Buffered Saline) was added to the T-25 cell culture flasks containing confluent cells and cells were allowed to detach for about 1 minute. The flask was tapped at the edge against the floor of biological safety cabinet to encourage cell detachment. The cells were collected with the aid of a pipette and transferred to a 50 mL centrifuge tube. About 5 mL of pre-warmed medium was added to the flask to ensure almost all cells were transferred to the centrifuge tube. It was then centrifuged at 1500 RPM for 3 minutes and then the supernatant was carefully removed. The cell pellet was dissociated by trituration in 1 mL of medium. Cells were then transferred to a new T75 cell culture flask containing 15-20 mL pre-warmed cell culture medium.

Maintaining the cells prior to beginning the experiments involved passaging cells every time they reached ~ 90% confluency at intervals of approximately one week. For the cell passage, cells were detached from the cell culture flask and centrifuged as described in the previous paragraph. Supernatant was removed after the centrifugation, and the cell pellet was resuspended in 1 mL of medium by triturating with the aid of a pipette. A cell count was performed using a hemocytometer and 2 x 10^6 cells were transferred to a new T75 cell culture flask containing 15-20 mL pre-warmed cell culture medium. The cell culture medium was refreshed every 3-4 days while maintaining the cells prior to beginning the experiments.

3.2.3 Freezing cells

Reserve vials of cells were generated to maintain cell line stocks in case of contamination or the need to discard the cell culture due to high cell passage number. Cells were cultured as described in Section 3.2 and grown to ~ 90% confluence. The medium was removed, and 5 mL of pre-warmed PBS was

added as above. Detached cells were centrifuged at 1500 RPM for 3 minutes, and then the supernatant was carefully removed. The cell pellet was resuspended in 1 mL of medium. Cell count was measured using a hemocytometer, and cell culture medium was added to adjust the cell concentration to 5 x 10^6 cells per mL, and 10% v/v DMSO was added dropwise with gentle swirling. The cells were aliquoted to 1 mL cryovials and frozen in a Mr Frosty freezing container (ThermoFisher) at – 80 °C. The cryovials were transferred to a storage box and stored at – 80 ° C until required. A reserve stock of cells was maintained in liquid nitrogen, and the cells stored in the freezer were used as working stock.

3.3 Cell differentiation

An aliquot of 4 x 10^6 cells were seeded in a T-25 cell culture flask in RPMI medium with 10% FBS and 1% P/S. The medium was replaced with a differentiation medium comprised of RPMI medium with 3% FBS, 1% P/S and retinoic acid two days later. Retinoic acid (10 µM in the final solution) was used as a differentiation agent. A stock solution of 5 mM retinoic acid was prepared by dissolving retinoic acid (Sigma) in 95% ethanol. This stock solution of retinoic acid was stored at 4°C in a light-protected container for a maximum of 6 weeks from preparation. The differentiation medium was refreshed every other day after the first addition of the differentiation medium. The differentiation was completed 7 days after the addition of retinoic acid. Differentiation of cells was confirmed using cell images showing dendrites taken with the aid of a camera and Western blot comparing the changes in neuronal marker level in differentiated and undifferentiated cells. Confirmation of cell differentiation is detailed in Chapter 4.

3.4 Preparation of cell lysate

SH-SY5Y cells were detached from the surface of the flask, and the concentration of cells was determined as described in Section 3.2.2, except that cold PBS was used instead of warm PBS. Once the cell concentration was determined, the cell suspension was centrifuged, and the supernatant was discarded. The cells were resuspended in 200-500uL of lysis buffer (1mM $MgCl_2$ (Sigma), 2mM EGTA (Sigma), 1% Nonidet P40 (Sigma), 50mM Tris (Sigma)) depending on cell number (about 200 uL per $5X10^6$ cells). The cell suspension was homogenised by trituration with a pipette and vortex machine, taking care to produce as few bubbles as possible. The cell suspension was centrifuged at 13,000 g for 1 minute at 4°C using a benchtop centrifuge machine (Eppendorf), and the supernatant was collected. The supernatant was immediately stored at -80 ˚C until further use. The protein concentration of the lysate collected using this method was determined using a protein assay (see below) and utilised to perform MAO activity assays and Western blot analyses.

3.5 Assay of protein concentration

Protein assays were carried out for all the lysates prepared using a Pierce Bicinchoninic acid (BCA) Protein Assay Kit (ThermoFisher) following the manufacturer's protocol. Briefly, BCA reagent was prepared by mixing BCA reagents 'A' and 'B' in the ratio 50:1. A range of bovine serum albumin (BSA) standards with concentrations of 2, 1.5, 1, 0.75, 0.5, 0.25, 0.125, 0 mg/mL and 10-fold diluted samples were prepared by dilution with water. Aliquots (10 µL) each of standard and samples were pipetted into the respective wells of 96 well plates in triplicate. After the addition of the standard and sample, 200 µL of BCA reagent was added to each well and allowed to mix thoroughly using a plate shaker for 30 seconds. The microplate was covered and incubated at 37˚C for 30 minutes. The plates were cooled to room temperature for 5 minutes before measuring the absorbance at 562 nm using a spectrophotometer. A standard curve was prepared by plotting the known

concentrations of the standard on the X-axis against the value of absorbance obtained on the Y- axis. A linear fit was performed using Excel, and the equation of the line of best fit was calculated. The concentration of protein in the sample was obtained using the equation obtained from the standard curve.

3.6 mRNA extraction

Cells grown to near confluence were detached, and cell number was assessed as described in Section 3.4. An RNeasy Mini kit (Qiagen) was used to extract total RNA from SH-SY5Y cells following the manufacturer's protocol, with a slight modification to the centrifuge speed. Cells were transferred to a sterile RNase-free microfuge tube and centrifuged at 1500 RPM for 3 mins at 4°C in a benchtop centrifuge. The supernatant was removed by aspiration. An appropriate volume (350 µL for less than 5 x 10^6 cells and 700 µL for 5 x 10^6 – 1 x 10^7 cells) of buffer RLT was added to a microfuge tube containing the cell pellet. The cell pellet was homogenised by trituration followed by the addition of 1 volume of 70% ethanol and pipetting to mix well. A 700 µL volume of the mixture was then transferred to RNeasy Mini spin column, placed in a 2 mL collection tube, and centrifuged for 15 s at 8,000 g. The eluent was discarded, and 700 µL of buffer RW1 was added to the RNeasy spin column. This was centrifuged for 15 s at 8,000 g, followed by the addition of 500 µL of buffer RPE and centrifuging for 15 s at 8,000 g. The flow-through was discarded in each of the above steps. Another volume of 500 µL of buffer RPE was added and centrifuged for 2 min at 8,000 g. The RNeasy spin column was then placed in a new 1.5 mL collection tube, and 30 - 50 µL RNase-free water was added directly to the spin column membrane, paying attention not to add water to the walls of the spin column. It was then centrifuged for 1 min at > 8,000 g for the RNA to be eluted into the collection tube. The isolated RNA was stored at -80°C until required for further analysis.

3.7 MAO activity assay

A modified kynuramine assay was performed using the method described previously, with slight modification (Morinan & Garret, 1985; Lewis, 2010). Briefly, SH-SY5Y cells were exposed to different treatments or subjected to experimental conditions, and cell lysate was collected using the method described in Section 3.4. The protein concentration of the sample was determined as described in Section 3.5, and samples were diluted to a specific protein concentration using cell lysis buffer. The protein concentration used depended on the specific experiment. Aliquots (25 µL) of samples were added in a microfuge tube that contained 217.5 µL of sodium phosphate buffer (50 mM sodium phosphate (Sigma) and 150 mM sodium chloride (Sigma), pH 7.4). The samples were incubated at 37°C for 5 minutes to equilibrate the sample and buffer mixture to the reaction temperature. A 7.5 µL volume of 0.307 mM of kynuramine dihydrobromide (Sigma) solution in sodium phosphate buffer was added to each of the reaction tubes to initiate the reaction. The reaction tube was then placed in an incubator for 30 minutes at 37°C. The reaction was terminated with 75 µL of 0.4 M perchloric acid, and the tubes were centrifuged at 13,000 x g for 30 sec at 4°C. Aliquots (100 µL) of supernatant were pipetted into the wells of a sterile black polystyrene 96-well microwell plate (Nunc) in triplicate. In order to fluoresce the 4-HQ product, 50 µL of 2 M NaOH (Sigma) was added to each well and, fluorescence was immediately measured immediately using a spectrophotometer (Omega) at 318 nm excitation and 380 nm emission wavelength.

For Standard curve preparation, 100 µL of 4-HQ reference standard was added to each well of the 96 well plates in triplicate in the concentration range of 0-5000 nM. A volume of 50 µL of 2M NaOH was added to each well, and fluorescence was immediately measured using a spectrophotometer at 318 nm excitation and 380 nm emission wavelengths. The standard curve was developed by plotting values of fluorescence of the 4-HQ reference standard on the Y-axis and concentration of the 4-HQ reference standard on the X-axis.

The amount of the 4-HQ product from tested samples in each well was calculated from the standard curve.

3.8 Western blotting

3.8.1 Gel Electrophoresis

The cell lysates previously collected, as described in Section 3.4, with protein concentration assayed as explained in Section 3.5 and stored at -80˚C, were thawed on ice. The protein amount in cell lysates was adjusted to 2.5-10 µg, diluting with lysis buffer where necessary. Six µL of Pierce™ Lane Marker Reducing Sample Buffer 5X (ThermoFisher) was added to 24 µL of cell lysate sample and samples were heated at 95°C for 1 min on a dry bath incubator (Major Science) and allowed to cool to room temperature. Three µL of pre-stained protein ladder (ThermoFisher) was used as a size standard and loaded into the first well, and 28 µL of each of the samples were loaded into the following wells of a 4-20% tris-glycine gel (Invitrogen). The setup was electrophoresed in a Mini gel tank (Life Technologies) with 1X 2-(N-morpholino) ethanesulfonic acid (MES) Running Buffer (Invitrogen) for 1 hr at 100 V.

3.8.2 Immunoblotting

Firstly, 1x transfer buffer was prepared by diluting 20x transfer buffer (Sigma) using distilled water and methanol (dilution scheme detailed in Appendix). A nitrocellulose membrane (Invitrogen) cut to a similar dimension as the mini gel was soaked for 5 min in the transfer buffer. The membrane, blotting paper (3 mm thickness), and blotting pads were soaked in Western transfer buffer for 15 min, and the blotting apparatus was assembled with a membrane between the gel and the positive electrode. Blotting paper and blotting pads were put in the transfer apparatus, and it was placed inside the Western blot blotter (Bio-

Rad). A frozen icepack was added to the tank to help with the cooling of the apparatus, as heat is produced during the transfer process. The transfer was then performed in a 4°C walk-in cold room for 45 minutes at 90V. Once the transfer process was completed, the nitrocellulose membrane was carefully removed using a tweezers and then blocked for 25 minutes in a blocking buffer solution (Sigma) on a rocker platform.

3.8.3 Incubation

After completion of blocking, the membrane was washed in Tween-Tris-buffered saline (T-TBS) thrice for 5 minutes each on a rocker platform. The membrane was then incubated overnight at 4°C with 15 mL of primary antibody solution. The primary antibody solution was prepared by diluting the primary antibodies in T-TBS as per the manufacturer's specification and dilution recommendation. This was followed by washing with T-TBS thrice for 5 minutes each. After the primary incubation, the membrane was incubated with the appropriate horseradish peroxidase (HRP) conjugated secondary antibody with the aid of a rocker platform for one hour at room temperature. The secondary antibodies were prepared by diluting secondary antibodies in T-TBS as per the manufacturer's recommendation. The details of the antibodies, and the dilutions used are explained in Chapters 4 and 6.

3.8.4 Detection of protein

The PVDF membranes were washed three times with T-TBS before being visualised using an iBright Chemiluminescent reader (ThermoFisher) located at the School of Medicine, University of Otago, Wellington. The chemiluminescence substrate mix was prepared by mixing equal amounts of chemiluminescence substrates A and B (ThermoFisher), and 1 mL of chemiluminescence substrate mix was added to the surface of the membrane. It was incubated in the dark for 2 minutes and then analysed using the

chemiluminescence reader. The molecular weights of resolved bands were estimated by comparison with the known sizes of the pre-stained protein ladder.

3.8.5 Data analysis using Image J

Quantitation of image intensity was performed using the software Image J (Version 1.47T, National Institutes of Health, USA). Images of bands to be analysed were opened, and then peaks relative to the intensities of each band were developed. The Area Under the Curve (AUC) for each peak of the treatments and control was calculated, and the AUC of the peaks of the treatments was expressed as a percentage of the control.

3.9 Quantitative real-time PCR

Analysis of mRNA expression of the *MAOA*, *MAOB*, *GAPDH* and *POLR2F* genes was performed utilising the quantitative real-time reverse transcriptase PCR or qPCR. This allowed relative quantitation of the changes in expression of these genes of interest following exposure to control, nicotine, TPM, and MAOI treatments.

3.9.1 Reverse Transcription

The concentration of the RNA samples collected according to methods described in Section 3.6 was checked using a spectrophotometer / fluorometer (Denovix). Some samples were sent to Massey Genome Services, Palmerston North, for the determination of concentration and purity. A Quantitect reverse transcriptase kit (Qiagen) was used to synthesise first-strand cDNA from the purified RNA samples following the manufacturer's protocol. Briefly, gDNA Wipeout Buffer, Quantiscript® Reverse Transcriptase,

Quantiscript RT Buffer, RT Primer Mix and RNase-free water were thawed at room temperature, and RNA samples were thawed in ice before beginning the reverse transcription procedure. The DNA elimination reaction was set up as shown in Table 6. A specific concentration of RNA was set for each of the samples in an assay, which is discussed in the individual sections of Chapter 6.

Table 6: Genomic DNA elimination reaction components.

Component	Volume / reaction
gDNA Wipeout Buffer, 7x	2 µL
Template RNA, up to 1 µg	Variable
RNase-free water	Variable
Total reaction volume	14 µL

The reaction components were incubated for 2 minutes at 42°C using a dry bath incubator. Reverse transcription master mix was prepared according to Table 7.

Table 7: Reverse-transcription master mix components.

Component	Volume / reaction
Quantiscript Reverse Transcriptase	1 µL
Quantiscript RT Buffer, 5X	4 µL
RT Primer Mix	1 µL
Total master mix component volume	6 µL

Fourteen µL of the genomic DNA elimination reaction containing template RNA and 6 µL of reverse transcription master mix components were mixed well and incubated for 30 min at 42°C. Reverse transcription reactions were terminated by incubating the tubes at 95°C for 5 min, then chilling on ice. Synthesised cDNA was stored at -20°C for up to 3 months before being used for qPCR analysis.

3.9.2 Gene expression assays

Gene expression assays were performed to compare the expression level of specific genes in the sample and were conducted using the LightCycler96 (Roche) PCR system. TaqMan Gene Expression assays that comprised predesigned primer and probe sets and TaqMan fast advanced master mix (ThermoFisher) were used to perform quantitative gene expression studies on different samples. The cDNA samples and master mix were thawed on ice and resuspended with gentle vortexing. Appropriate PCR reaction mixes containing 5 µL Master mix, 0.5 µL TaqMan gene expression assay system and 3.5 µL of RNase-free water were prepared per sample in microfuge tubes, vortexed well to mix and transferred to LightCycler® 8-Tube Strips (Roche). One µL of template DNA was added to each reaction mixture. The tubes were vortexed and centrifuged using a mini-centrifuge. Samples were amplified in a Lightcycler96 using a pre-set protocol with the following cycling conditions: an initial step of 50°C for 2 min, followed by pre-incubation at 95 °C for 10 min, and 40 cycles of amplification at 95 °C for 15 s and 60°C for 1 min (Gene Expression Assays User Guide, 2019). Gene expression was determined using the $2^{-\Delta\Delta Ct}$ method (Livak & Schmittgen, 2001).

3.10 Statistical analysis

Statistical analyses and tests on all data were performed using GraphPad Prism v5.0 (GraphPad Software Inc., San Diego, CA). Tests performed included Student's t-tests, one and two-way Analysis of Variance (ANOVA), with relevant post-hoc tests including the Bonferroni multiple comparison post-test and Dunnett's post-test. Dose-response relationships and enzyme reactions were analysed by non-linear regression analysis, as noted. GraphPad Prism v5.0 and Microsoft Excel 2011 were used for graphing and data manipulation. The details of the tests performed are described in the Results Sections of the individual experimental chapters of this thesis.

Chapter Four: Preparation of exposure condition, cell line and exposure to different treatments

4.1 Introduction

This chapter describes the preparatory works required to perform the major experiments like examining changes in MAO activity, MAO gene expression, MAO protein levels and whole genome expression after exposing human neuroblastoma cells SH-SY5Y to the different exposure treatments (Chapters 5-7). In order to determine the effect of TPM and its components on MAO activity, protein levels and gene expression, firstly, it was essential to collect and extract TPM (Section 4.2.1). The TPM extracted into ethanol was sent to ESR, Christchurch and Callaghan Innovation, Wellington, for assaying the content of nicotine and six candidate MAOIs in the TPM (Section 4.2.2). This result was helpful in determining the concentration of treatments suitable for exposure to cells. Stock solutions for exposure treatments were prepared (Section 4.2.4) to save time, chemicals and improve accuracy. Cells were prepared for exposure (Section 4.2.5) and then exposed to treatments (Section 4.2.6).

4.2 Methods

4.2.1 TPM collection and extraction

TPM, which is considered to contain equivalent combustion products to inhaled tobacco smoke, was collected using a smoking machine purchased from Teague Enterprises and modified by Thomas J. Sheehan (Sheehan, Hamnett, Beasley, & Fitzmaurice, 2019) on loan from the Institute of Environmental Science and Research Ltd. (ESR), Porirua. TPM collection and extraction was performed according to the method described by Ambrose et al. (2007) with slight modification. Briefly, about 1 g of loose tobacco (Holiday

Red) was rolled in Silver Tip Cigarette filter papers (Gizeh) with the aid of a cigarette rolling machine (Aztec). Each cigarette was combusted using the smoking machine (Figure 13) with puff duration and interval maintained in a way to imitate a smoker's cigarette smoking pattern. The puff duration was approximately 2 to 3 seconds, and the puff interval was between 40 and 60 seconds. The cigarette smoke from five cigarettes was collected onto a single 44 mm Whatman filter paper (Cerulean). The filter pads with cigarette smoke were then immediately wrapped in aluminium foil and stored at -80˚C in a box to prevent degradation of volatile compounds until required for further use.

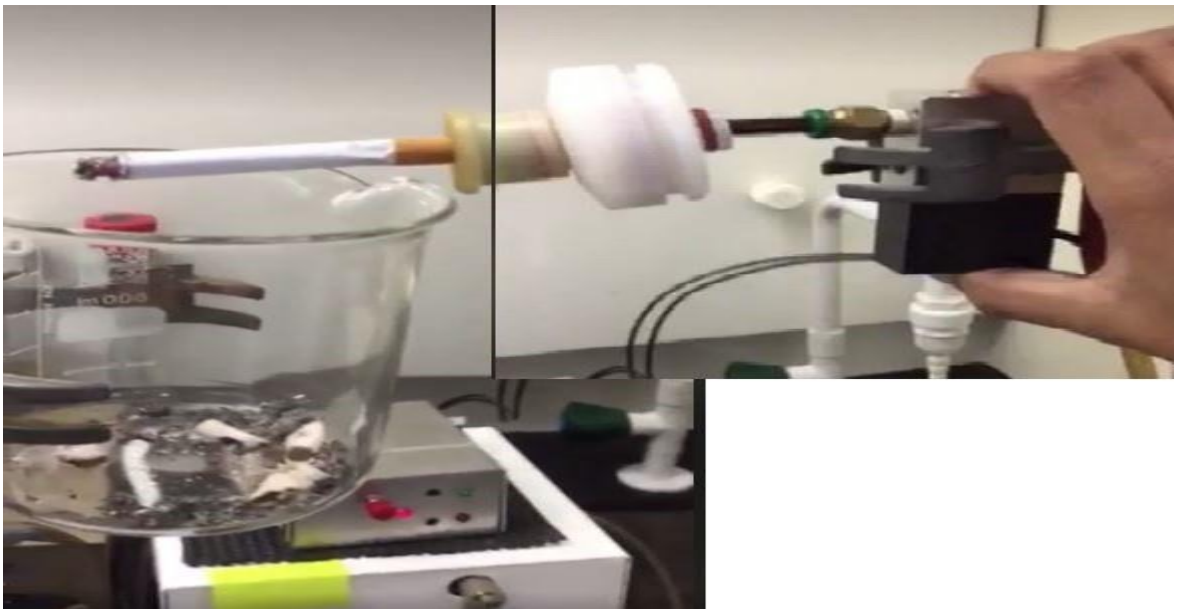

Figure 13: TPM collection using a smoking machine.

TPM extraction from Whatman filter paper containing absorbed cigarette smoke (Figure 14) was achieved by placing a filter paper inside a syringe barrel with no plunger. The syringe barrel with filter paper was placed in a 50 mL centrifuge tube. A total of 5 mL of absolute ethanol was added to the syringe in 4 aliquots, allowing the filter to soak in ethanol for a minute. The tube was centrifuged each time at 1500 RPM for 1 minute, and total eluents from each lot were recovered and divided into microfuge tubes in aliquots of 30 µl each. The aliquots were immediately taken to ESR, Porirua, on dry ice for vacuum centrifugation to remove the ethanol, leaving behind TPM pellets.

Ethanol was chosen as an extraction agent in order to obtain as many organic components as possible from cigarette smoke. All the candidate MAOIs were soluble in ethanol, and the ethanol could be removed easily, making it a preferable solvent. Vacuum centrifugation was performed at low temperature and maximum speed to remove solvent from the TPM and collect TPM, which was stored at -80°C. TPM aliquoted and stored was used later for the treatment of SH-SY5Y cells for the main experiments.

Figure 14: TPM collected in Whatman filter paper.

4.2.2 Assay for nicotine and candidate inhibitors

TPM collected and stored at -80˚C were sent to ESR, Christchurch, for the analysis of nicotine, harman and norharman and to Callaghan Innovation, Wellington, for analysis of candidate MAOIs (linoleic acid, linolenic acid, quinol, catechol, 4-methyl catechol, 4-ethylcatechol).

Nicotine analysis was performed using a Liquid Chromatography Tandem Mass Spectrometry (LC/MSMS) following in-house methods (ESR, Christchurch). Lipomed L-Nicotine 10 mg free base/1mL methanol was used as a reference standard, and 500 parts per billion (ppb) D4-nicotine was used as an internal standard. Nicotine precursor ion (m/z 163) was used, and daughter ions (m/z 84, 130 and 132) were obtained with a retention time of 0.8 minutes. A range of standard concentrations of nicotine (2, 20, 200, 1000, 2000 ppb) was used to prepare a standard curve and nicotine content in the

sample was determined by comparison with the standard curve (A Chappell, pers. comm.). Harman and norharman were analysed as previously described (Truman et al., 2017).

Quantification of the new candidate inhibitors was performed by Kiril Lagutin (PUFAs) and Kevin Mitchell (catechols) from Callaghan Innovation, Wellington. It was carried out using an LCMS (Waters, H-Class UPLC and Xevo g2-XS QTof) according to [Callaghan Innovation report No.816, Analysis of selected MAOIs and polyunsaturated fatty acids (PUFAs), Method development]. To generate a single ion chromatogram, a mass window of 0.1 m/z was employed for each analyte (quinol, 108.02 m/z, RT 1.3 minutes; catechol, 109.03 m/z, RT 3.0 minutes; 3-methyl catechol, 123.05 m/z, RT 5.3. minutes; 4-ethyl catechol, 137.06 m/z, RT 7.4 minutes; 18:3n-3, 277.22 m/z, RT 16.3 minutes; 8:2n-6, 279.24 m/z, RT 16.7 minutes).

4.2.3 Stability study of Catechol

The stability study of MAOIs was performed by Callaghan Innovation, Wellington since it had been observed that inhibitory activity was being lost on the storage of these reagents in solution. Four different models were used – TPM extracts in saline, TPM extracts in ethanol, solution of analytical standards in saline, and solution of analytical standards in ethanol. In order to assess stability, samples were analysed multiple times over the period of 6-20 hours while stored at 37 °C. Quantification of all analytes in samples was carried out following the method for assay of candidate MAOIs (Section 4.2.2) using LCMS and is presented in Table 8. The results of these stability studies suggested that the stability of MAOIs in solution were variable, and MAOIs were likely to degrade quickly in solution. A key consideration for the exposure method to be used was achieving a balance between decreasing medium change to reduce disturbance to the cells and changing the medium in order to prevent the degradation of both RA and MAOIs.

Table 8: Estimated half-life for quinol, catechol, 4-methly catechol and 4-ethyl catechol.

MAOI	$T_{1/2}$ in saline (h)	$T_{1/2}$ in ethanol (h)	$T_{1/2}$ in TPM in ethanol (h)
Quinol	0.9	11	15
Catechol	7.5	60	60
4-methylcatechol	0.5	19	19
4-ethylcatechol	0.9	202	20

4.2.4 Preparation of stock solutions

Stock solutions for each exposure treatment were prepared to avoid frequent preparation and wastage of chemicals as the exposure concentrations were extremely low and to maintain consistency in the exposure treatment with each medium change. Stock solution aliquots were stored at -80 ˚C and diluted immediately prior to the addition to cell culture flasks. The stock solutions were prepared such that the final concentration required (Table 10) for the exposure treatments could be obtained with simple dilution steps.

- **Nicotine**:

A stock solution of 2 mM of nicotine in PBS was prepared and stored at -80 ˚C until further use. Prior to use, the contents of one vial were dissolved and diluted in ethanol.

- **TPM**:

TPM was stored dry, immediately after the vacuum centrifugation procedure, as explained in Section 4.2.1. Prior to use, the contents of one vial were dissolved and diluted in ethanol.

- **MAOI:**

Two different stock solutions were prepared, one for PUFAs and the other for catechols. For PUFAs, a concentration of 34.12 µM linoleic acid and 32.59 µM linolenic acid was prepared using ethanol in a microfuge tube and stored at -

80 ˚C. A stock solution of catechols had a concentration of 115.85 µM quinol, 166.24 µM catechols, 25.75 µM 4-methylcatechol and 22.29 µM 4-ethylcatechol, which was dried using a vacuum centrifuge machine at ESR, Porirua and stored at -80 ˚C. Prior to use, the contents of one vial were dissolved and diluted in ethanol as for the TPM sample.

4.2.5 Preparation of cells for exposure

In order to prepare cells for the exposure experiments, stock SH-SY5Y cell line stored at -80°C at Massey University, School of Health Sciences, Wellington was used, and appropriate cell culture condition explained in Section 3.2.1 was maintained. Cells were passaged every 3-5 days as described in Section 3.2.2. Cells were then required to be differentiated to perform the exposure experiments in a controlled cell growth environment. A concentration of 10 µM retinoic acid was used to differentiate the cells following the protocol of Shipley, Mangold, & Szpara (2016). After some preliminary trials were performed, the method described by Cheung et al. (2009) was used with slight modifications detailed earlier in Section 3.3.

4.2.5.1 Confirmation of cell differentiation

Once the differentiation was complete, confirmation of cell differentiation was done by observing the change in cell morphology from cell images and measuring the protein expression level of neuronal marker synaptophysin using Western blot. To perform Western blot, cell lysates were collected as described in Section 3.4. Cell lysates were stored at -80°C until further use. The protein content of the lysates collected was determined as described in Section 3.5.

Cell Images

Images of cells were taken using a digital camera (Olympus, C-5050) mounted on the microscope (Olympus, CKX41SF) using the 20X objective

lens. The length of dendrites was used to confirm differentiation. Differentiated cells have elongated dendrites, while the neurite length of undifferentiated cells would be comparatively much shorter. Images were taken on Day 1 to observe changes in the morphology of the dendrites and their cells upon differentiation.

Western blot confirmation of synaptophysin expression

Western blots were performed as described in Section 3.8. Firstly, a range of protein amounts (5, 10, 20 and 40 µg) from differentiated and undifferentiated cell lysate samples were used to determine the optimal concentration of protein that would give well-resolved bands after gel electrophoresis so that equal amounts of protein could be loaded in each well. Electrophoresis, transfer and blocking was then carried out. For primary incubation, anti-synaptophysin mouse monoclonal antibody (Abcam ab8049) diluted 1:2000 in TBST and anti-β tubulin rabbit polyclonal antibody (Abcam ab6046) diluted 1:2000 in TBST were used. The membranes were then incubated overnight at 4°C, and washed thrice with TBST for 5 minutes each time. Goat anti-rabbit IgG (H&L) HRP (Abcam Ab205718) and Goat anti-mouse IgG H&L HRP (Abcam ab205719), both diluted 1:2000 in TBST, were used as secondary antibodies for the quantitation of β-tubulin and synaptophysin respectively. The membranes were again washed thrice with TBST for 5 minutes each time. The membrane was covered in 2 mL of chemiluminescence substrate mix and incubated in the dark for 2 minutes. Imaging was performed using an iBright chemiluminescent reader, and images were stored as JPEG files. Densitometry of the detected bands was performed with Image J software (version 1.53m, National Institutes of Health, USA) and a one-way ANOVA test was performed to determine whether there were any significant differences in synaptophysin levels.

4.2.6 Cell exposure

SH-SY5Y cells were exposed to different exposure treatments in order to study the effect of TPM and MAOI after the completion of seven days of the differentiation cycle. The medium was then removed and replaced with a

differentiation medium (RPMI 1640, 3% FBS, 1% P/S and 10 µM RA) and one of the exposure treatments. The weight of MAOIs relative to nicotine and concentrations of individual MAOIs for cell exposure were determined based on the assay of nicotine and MAOIs in TPM samples (Section 4.3.1) and the molecular weight of individual MAOIs. These calculations were made relative to the 0.2 µM nicotine final concentration. The weights of MAOIs relative to nicotine and the concentration of candidate inhibitors required for exposure to SH-SY5Y cells was calculated and are listed in Tables 9 and 10.

Three replicates of SH-SY5Y cells were cultured in 75 cm^2 culture flasks and exposed to the treatments for a period of 1, 3, 5 and 7 days, with medium replaced every other day. Cell lysates were collected at the end of the exposure period, as explained in Section 3.4, and utilised for main experiments such as determination of MAO activity, MAO protein level, MAO gene expression and whole genome expression . The media were replaced every other day to maintain the concentration of retinoic acid and catechols in the medium, which tend to degrade over time.

- **Ethanol**:

The ethanol treatment was considered a control group to offset the effect of ethanol used as a solvent in other treatments. Treatment with ethanol concentrations up to 0.5% of ethanol has been found to be non-toxic for SH-SYY cells (Ekblom, Zhu, Chen, & Shih, 1996; Lewis, 2010). For the exposure experiment, a constant ethanol concentration of 0.05% in the differentiation medium was used, which is much less than the safe limit.

- **Nicotine:**

The nicotine treatment contained ethanol in the final concentration of 0.05% in the differentiation medium and nicotine in the final concentration of 0.2 µM. A nicotine concentration of 0.2 µM was used as it is reported to be the biological concentration of nicotine found in the blood of smokers (Alkondon, Pereira, Almeida, Randall, and Albuquerque, 2000). The stock solution of nicotine prepared as explained in Section 4.2.4 was diluted to the required

concentration (Table 10) using absolute ethanol, and added to the differentiation medium.

- **TPM**:

The TPM exposure treatment contained ethanol in the final concentration of 0.05% in the differentiation medium, and TPM equivalent to 0.2 µM of nicotine. The stock solution of TPM prepared as explained in Section 4.2.4, was diluted to obtain a final concentration of 0.2 µM nicotine using absolute ethanol and added to the differentiation medium. The required dilution was based on the amount of nicotine present in each TPM sample and obtained from the assay of nicotine (Section 4.3.1).

- **MAOI**:

The MAOI treatment contained ethanol in the final concentration of 0.05% in the differentiation medium, and the MAOIs (1.32 nM linoleic acid, 1.26 nM linolenic acid, 4.48 nM quinol, 6.43 µM catechol, 0.99 µM 4-Methylcatechol, 0.86 µM 4-Ethylcatechol). The required concentration of MAOIs (Table 10) were calculated from the assays of nicotine and MAOIs in TPM (Section 4.3.1) based on the weight of individual MAOIs relative to that of nicotine in the TPM sample. The stock solution of MAOIs was prepared as detailed in Section 4.2.4. It was diluted to the required MAOI concentration using absolute ethanol and added to the differentiation medium immediately before use.

4.3 Results

4.3.1 Assay of TPM components

Two representative TPM samples that were extracted from the Whatman filter paper using ethanol, and vacuum dried, were sent to ESR, Christchurch, for the analysis of nicotine, harman and norharman content (Section 4.2.2). The content of nicotine in tube A was 240 µg and 243 µg in tube B. Therefore, an average nicotine concentration of 241.5 µg per tube was used for further experimentation in this project. ESR also analysed these samples for harman and norharman.

Two representative TPM samples were also sent for analysis of their content of candidate MAOIs to Callaghan Innovation, Wellington. The result for the assay of the individual MAOIs is listed in Table 9.

Table 9: Assay of MAOIs in TPM sample.

Compound	µg / TPM sample	Amount relative to 1 µg of nicotine
Harman	0.08	0.0003
Norharman	0.25	0.001
Linoleic acid	2.76	0.011
Linolenic acid	2.61	0.011
quinol	3.68	0.015
catechol	5.27	0.022
4-Methylcatechol	0.92	0.004
4-Ethylcatechol	0.89	0.004
Nicotine	241.50	1

Based on these results, the concentration of individual MAOIs for cell exposure was determined (Table 10) such that exposure treatments contained MAOIs in the same ratio as found in the TPM samples extracted earlier (Section 4.2.1). These results are roughly in accord with literature values for these compounds in TPM (Section 2.11.1).

Table 10: Concentration of MAOIs for cell exposure.

Compound	Molecular weight	Concentration for cell exposure (μM)	Stock Solution (μM)	Dilution factor
Linoleic acid	280.45	1.321×10^{-3}	13.21	10,000
Linolenic acid	278.43	1.261×10^{-3}	12.61	10,000
quinol	110.11	4.484×10^{-3}	44.84	10,000
catechol	110.11	6.434×10^{-3}	64.34	10,000
4-Methylcatechol	124.14	0.997×10^{-3}	9.97	10,000
4-Ethylcatechol	138.16	0.863×10^{-3}	8.626	10,000
Nicotine	162.23	0.2	2000	10,000

Harman and norharman were not included in the cocktail to observe the effects of the previously unknown MAOIs without the influence of harman and norharman. Since the candidate MAOIs were proposed to be the major MAOIs, it was expected that the MAO inhibition due to MAOIs would be similar to MAO inhibition due to TPM.

4.3.2 Cell differentiation

4.3.2.1 Protein assay

The protein content of the cell lysates obtained from differentiated and undifferentiated cells was calculated using the standard curve and are listed in

Table 11. A representative standard curve obtained by using different concentrations of BSA is shown in Figure 15. When lysis buffer was used as a control, no change in the absorbance was observed compared to when water was used as a control. This suggested that lysis buffer does not influence the absorbance of the samples.

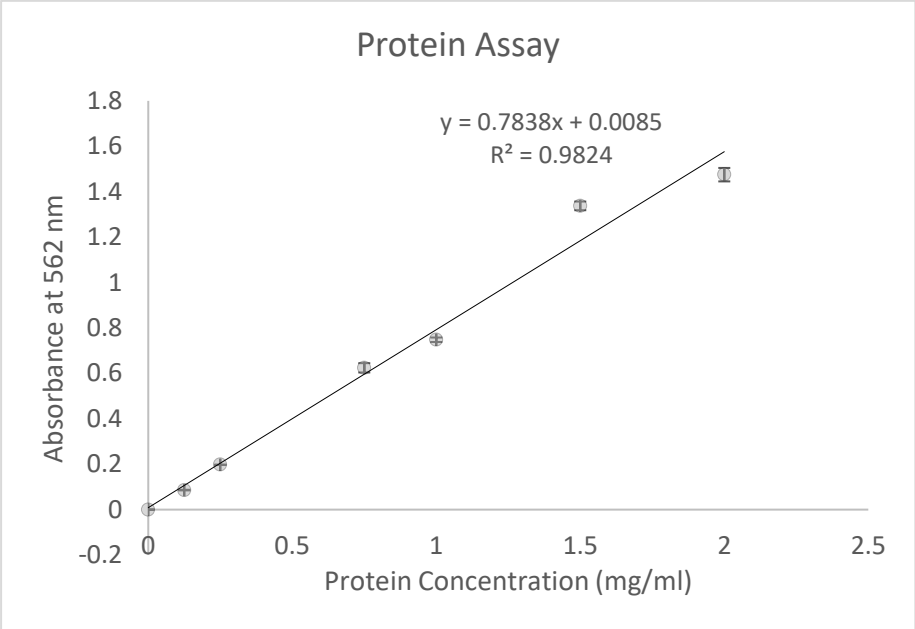

Figure 15: Representative graph showing a standard curve for protein assay with concentration of BSA in the X-axis and Absorbance at 562 nm on the Y-axis.

Table 11: Protein content of cell lysates obtained from differentiated and undifferentiated cells.

Sample	**Protein Concentration (mg/mL) ± SD**
Differentiated replicate 1	2.16 ± 0.063
Differentiated replicate 2	2.07 ± 0.0128
Differentiated replicate 3	6.50 ± 0.132
Undifferentiated replicate 1	8.27 ± 0.092
Undifferentiated replicate 2	9.68 ± 0.0893
Undifferentiated replicate 3	9.34 ± 0.162

4.3.2.2 Cell Images

To demonstrate the differentiation of SH-SY5Y cells by RA, images of cells in the cell culture flask were photographed under 200x magnification. The cell images taken 24 hours after the addition of the differentiation medium from differentiated and undifferentiated cells are shown in Figure 16. As shown in the figure, RA-induced differentiated cells (Figure 16B) clearly showed extension of neurites, while the undifferentiated cells (Figure 16A) had very short neurite lengths compared to the former. Also, undifferentiated cells seemed to grow in clusters, while the differentiated cells were more spread throughout the cell culture flask. The differentiation was maintained until 14 days after the addition of the differentiation agent. The cells started growing on top of each other after 14 days.

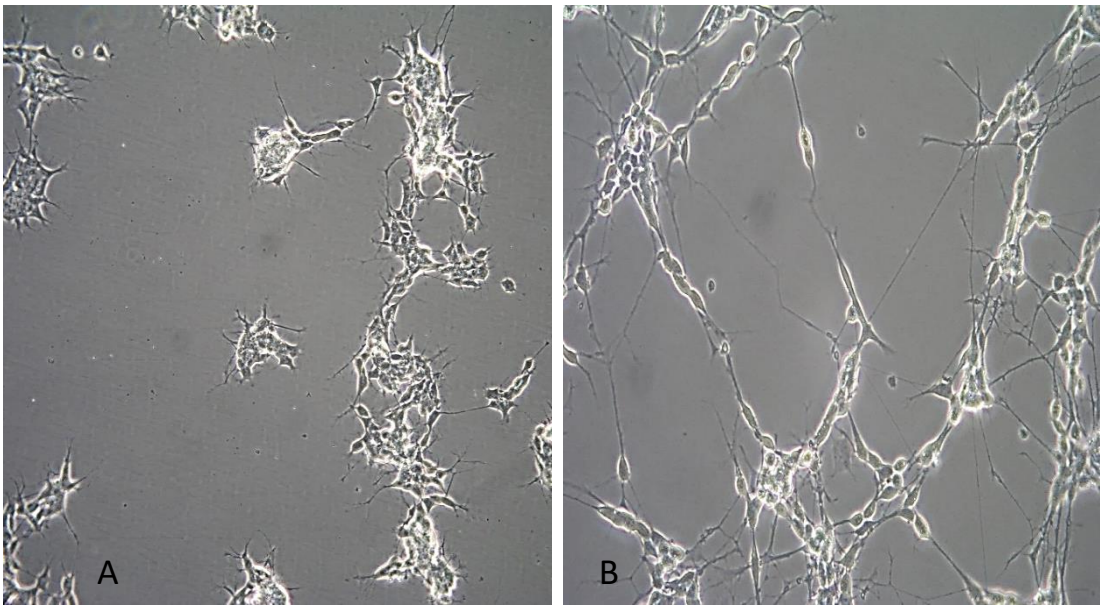

Figure 16: Images of SH-SY5Y cells showing A) undifferentiated and B) differentiated cells. Both images are in 20X magnification one day post-addition of differentiation medium containing 10 µM retinoic acid

4.3.2.3 Western blot confirmation of differentiation

Western blots were performed to analyse the protein levels of the neuronal marker synaptophysin in differentiated and undifferentiated SH-SY5Y cells. A representative blot showing synaptophysin and β-tubulin bands in undifferentiated and differentiated SH-SY5Y cells is shown in Figure 21a. The quantification of the protein abundance performed using densitometry analysis of the detected bands using Image J software is shown in Figure 21b. The band density values of synaptophysin obtained from Image J were normalised to the band density of β-tubulin (a common housekeeping protein), and then expressed as a percent of control. Western blots showed higher expression of protein synaptophysin in differentiated SH-SY5Y cells compared to the undifferentiated ones. Three replicates were performed to confirm the change in protein levels.

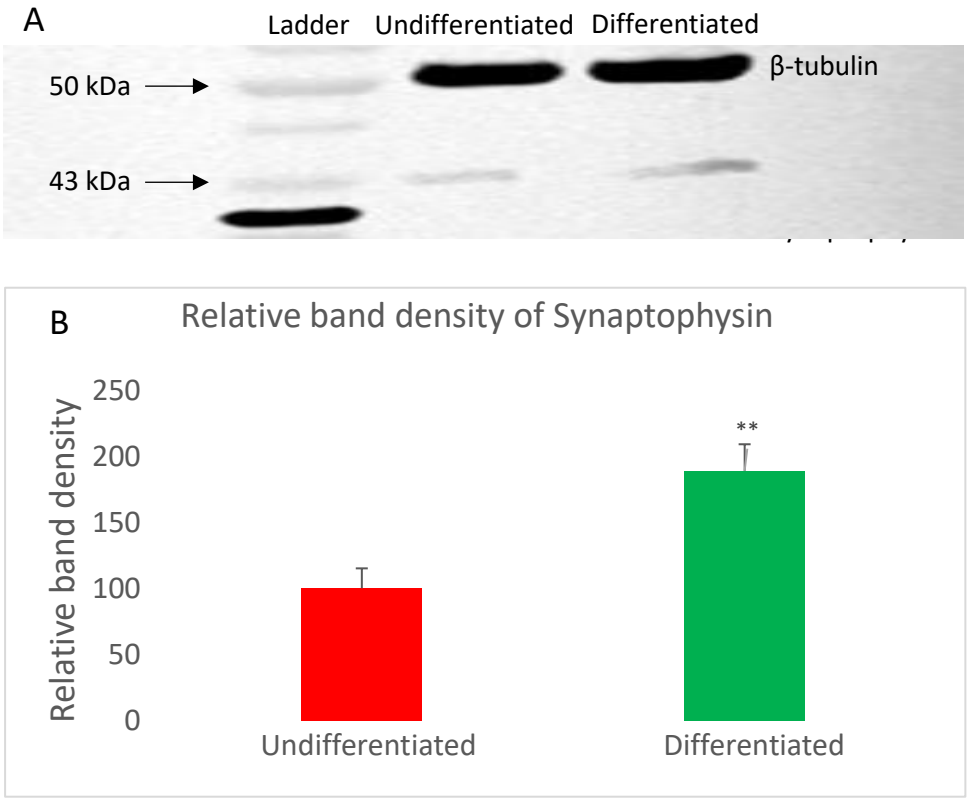

Figure 17: A) Representative Western blots of synaptophysin and β-tubulin in undifferentiated and differentiated SH-SY5Y cells. SH-SY5Y cells were differentiated using 10 µM retinoic acid for a period of seven days. Synaptophysin and β-tubulin bands are at 50kDa and 43 kDa, respectively. B) Electrophoretic band density of the protein synaptophysin relative to β-tubulin in differentiated SH-SY5Y cells is expressed as percent of the band density of the undifferentiated cells (one-way ANOVA with Bonferroni's post-test; α=0.05; n = 3 blots from 3 independent preparations.

4.4 Discussion

This study was carried out in order to collect cigarette smoke using an appropriate method to extract TPM for use in different experiments in this project. The ability to collect cigarette smoke using a specific method that would represent the cigarette smoking behaviour of the general human population is near to impossible. Different people tend to have different smoking styles (Park et al., 2016). However, a method needs to be followed that can be considered to generate smoke most similar to what a normal human smoker would inhale. Therefore, smoke was collected by combusting cigarettes using the smoking machine, imitating a normal smoker's smoking pattern.

The gaseous vapour phase (GVP) has also been collected by researchers in some studies (Pankow, Kim, Luo, & McWhirter, 2018; Kim et al., 2018). However, studies also found that the gaseous vapour phase tended to have very little nicotine present compared to that trapped in TPM. They also found that relatively heavy compounds with a molecular weight greater than 100 g/mole were mostly detected in TPM rather than in GVP. All our six candidate MAOIs have relatively high molecular weight, providing some support to leaving behind the GVP in our study. Van der Toorn et al. (2019) have confirmed in their study that TPM inhibits both MAO-A as well as MAO-B, while the GVP has no significant effect on MAO inhibition. Similar results were seen in the studies conducted by (Khalil et al., 2006) and (Herraiz & Chaparro, 2005). Since MAO inhibition from candidate MAOIs is the main emphasis of the overall research in our group, the collection of TPM and omission of GVP is justified.

Another factor to be considered was the stability of the compounds. The stability study showed that the half-life of the catechols ranged from 0.5 to 7.5 hours in saline solution at 37 ˚C, and from 11 - 60 h in ethanol at the same temperature. With this in consideration, the stock solution of catechols was prepared in ethanol, dried down and stored at -80 ˚C. Fresh stock was added

along with the differentiation medium every other day. This prevented degradation of the compounds during long-term storage, reduced batch-to-batch variability and wastage of time and sample required if fresh solutions were to be made before every exposure.

Several protocols are available for the differentiation of SH-SY5Y cells. Based on a reading of the literature (Section 2.14), differentiation using RA was chosen as it induces a cholinergic neuronal phenotype. RA binds to cell nuclear receptors, RAR and RXR. These receptors act as a DNA-binding transcription regulator. Once, RA binds to these receptors, conformational changes in the receptors occur that modulate complex receptor functions. The receptors' activity is also modulated by different coactivators and corepressors of the receptors (Das et al., 2014). Several procedures have been used for the differentiation of SH-SY5Y cells using RA. Shipley, Mangold, & Szpara (2016) used 10 µM RA and continued the cell differentiation with RA for 14 days. In my study, however, the differentiated cells started growing on top of each other, forming clumps towards the end of the cycle. For the other experiments, such as MAO activity assays, SH-SY5Y cells had to be exposed to different treatments for periods of 1, 3, 5 and 7 days, as explained in Section 4.2.6. Therefore, it was thought that 14 days of cell differentiation was too long and impractical for this project. Instead, a slight modification of the method of Cheung et al. (2009) was used. In this method, the differentiation was continued for 7 days using 10 µM RA in RPMI medium with 3% FBS and 1% P/S. It was observed that the cells started showing extended neurites as early as Day 1, similar to the results obtained by Cheung et al. (2009).

We confirmed the RA-induced differentiation of SH-SY5Y cells by observing changes in their morphology and by observing a change in the expression of neuronal marker protein synaptophysin after differentiation. RA has been shown to increase the expression of neuronal markers NSE, synaptophysin, SAP97 and NeuN (Cheung et al., 2009). It was not feasible to measure the

change in the protein level of all the neuronal markers. Therefore, a change in the expression of synaptophysin was measured. The choice of synaptophysin was made as the change in its expression level was the greatest of the markers measured by Cheung et al. (2009). Synaptophysin is an integral membrane protein that is abundant in synaptic vesicles and is involved in the release of neurotransmitters (Rehm, Wiedenmann, & Betz, 1986). The increased level of synaptophysin confirms the differentiation and is in agreement with Cheung et al. (2009). It was also observed that there was a very slow growth of the SH-SY5Y cells after the addition of the differentiation medium. This slow and consistent growth was very helpful in getting enough cells at the end of the exposure regime.

4.5 Conclusion

Cigarette smoke was successfully collected using a smoking machine and filter paper, and then extraction of TPM using ethanol. Samples were sent to be analysed at ESR, Christchurch and Callaghan Innovation, Wellington, Their results allowed a comparison between the effects of the new MAOIs in ethanol and the same MAOIs in tobacco smoke. A protocol for the differentiation of SH-SY5Y using RA was developed. Using 10 µM RA for 7 days, cells were stimulated to differentiate to a neuronal phenotype. The addition of RA controlled the proliferation of the cells, which was essential to perform the exposure experiments in a controlled manner without overgrowth of the cells. Confirmation of the cell differentiation was observed by examination of changes in the cell morphology and measuring the change in the expression of the neuronal marker synaptophysin.

Chapter Five: Impact of exposure treatments on MAO activity and determination of optimum exposure period

5.1 Introduction

This chapter highlights the measurement of MAO activity (Section 5.2.3) after the differentiated SH-SY5Y cells are exposed to different treatments (Chapter 4). Determination of MAO activity is utilised to identify the optimum duration of exposure in order to perform other major experiments for this PhD study, as shown in Figure 12, which includes MAO gene and MAO protein expression (Chapter 6) and whole genome RNA expression (Chapter 7). The MTT viability assay is also performed (Section 5.2.5) to confirm that the optimum exposure period identified does not impart any overt toxicity on SH-SY5Y cells.

5.2 Methods

5.2.1 Sample preparation

SH-SY5Y cells were cultured and differentiated as described in Sections 3.2 and 3.3. The cultured cells were then processed to collect cell lysate after the completion of the differentiation cycle or after the completion of exposure treatments using the method described in Section 3.4. Briefly, the cell culture medium was removed using a pipette and about 10 mL of cold PBS was added. Cells were detached from the cell culture flask by tapping the flask on the bench. Cells suspended in the PBS were sedimented by centrifugation, and the supernatant was discarded. Cell pellets were homogenised by triturating with an appropriate amount of cell lysis buffer (~ 200 µL lysis buffer

per 1X10^7 cells). Cell lysates were stored at -80 ˚C until required for MAO assay.

5.2.2 Protein assay

The protein content of the lysates collected was determined using the method described in Section 3.5. Briefly, 10 µl each of standard or sample and 200 µl of BCA reagent were added to wells in a 96-well plate. The reaction was incubated at 37˚C for 30 minutes, cooled to room temperature, and absorbance was measured at 562 nm. The concentration of protein in the sample was obtained using the standard curve obtained from absorbance from a range of BSA concentrations (0, 0.125, 0.25, 0.50, 0.75, 1, 1.5, 2 mg/mL).

5.2.3 MAO assay after exposure treatments

Treated cells were thawed immediately before MAO assay at room temperature for about 15 minutes and assayed for total protein content using the BCA assay. Sample concentrations for individual assays (Section 5.3.3.1-5.3.3.4) were then adjusted as necessary with sodium phosphate buffer (50mM sodium phosphate, 150 mM sodium chloride, pH 7.0) by using results obtained from the protein assay.

A modified kynuramine assay was performed using the method described in Section 3.7. Briefly, cell lysate samples were thawed immediately before MAO assay at room temperature for about 15 minutes. Cell lysates were diluted to a specific protein concentration depending on the type of experiment being performed using cell lysis buffer. Aliquots of 25 µL samples were taken in a 1.5 mL microfuge tube that contained 217.5 µL of sodium phosphate buffer (50 mM sodium phosphate, 150 mM sodium chloride, pH 7.4). The samples

were incubated at 37°C in an incubator for 5 minutes to equilibrate the sample and the buffer mixture to the reaction temperature. The addition of 7.5 µL of kynuramine hydrobromide to each of the reaction tubes initiated the reaction. The microfuge tube was then placed in a 37°C incubator for a specific time range. The reaction was terminated with 75µL of 0.4 M perchloric acid, and the tubes were centrifuged at 13,000 x g for 30 sec at 4°C. Aliquots of supernatant, 100 µL, were then pipetted into the wells of a sterile black polystyrene 96-well plate in triplicates. To induce fluorescence, 50 µL of 2 M NaOH was added to each well. Fluorescence was then measured immediately using a spectrophotometer (BMG Labtech, FLUOstar Omega) at 318 nm excitation and 380 nm emission wavelength.

For the standard curve, 100 µL of 4-HQ reference standard was added to the 96-well plates in duplicate/triplicate at a concentration range of (0-5000) nM. Aliquots of 50 µL 2M NaOH were added to each well, and fluorescence was measured spectrophotometrically at 318 nm excitation and 380 nm emission wavelengths. The standard curve was developed, and it was used to determine the MAO activity of the cell lysates.

5.2.4 Determination of MAO-A and MAO-B activity from total MAO activity using clorgyline

The percentage of MAO-B activity in samples was determined from total MAO activity using clorgyline as described in similar research (Jiang, Jiang, Liu, & Feng, 2006) with slight modification. Clorgyline is a selective MAO-A inhibitor and inhibits MAO-A with a very low IC_{50} value. However, a much larger concentration of clorgyline is required to inhibit MAO-B (Lewis, 2010). A range of clorgyline concentrations (0.01 nM – 0.75 µM) and (1nM – 75 µM) were incubated with human recombinant MAO-A and MAO-B enzyme (Sigma) respectively. The result of the MAO assay from these two experiments was used to determine the concentration of clorgyline that completely inhibited

MAO-A without any change in MAO-B activity. Two aliquots of equal volumes of cell lysate were taken in a microfuge tube for each exposure treatment. One aliquot of cell lysate was incubated with clorgyline, and the other one without it. Total MAO activity in samples incubated with and without clorgyline was determined as described in Section 3.7. The percentage of MAO-B activity was determined from the total MAO activity, and the remainder was identified as MAO-A activity.

5.2.5 Assessing toxicity from exposure to treatments

MTT assays were performed to assess the possible toxicity on the cells from the three-day exposure regime. Out of all the treatment regimes, the three-day regime for each of the treatments was selected for this study, as this was concluded to be the optimum time period for assessing the effect of treatment as detailed in Sections 5.4 and 5.5. The MTT assay was firstly trialled in 96-well plates. However, it did not seem to work well as the medium change disrupted cell adhesion. Therefore, an approach was used to grow and expose cells in 6-well plates and then perform the final step of the assay by transferring the solubilised formazan into 96-well plates to measure the absorbance.

5.2.5.1 Determination of optimum seeding concentration

In order to determine the optimum cell seeding concentration, a range of cell concentrations ($3x10^4$ – $3x10^5$ cells per well) were used for initial seeding in 6-well plates. The objective of this experiment was to determine the optimum cell seeding level such that 90% confluency was achieved at the end of ten days (seven days of the differentiation, followed by three days of exposure to the different treatments). The volume of medium used in 6-well plates was 2 mL, and differentiation with RA was initiated two days after seeding, as described in Section 3.3. Once the differentiation cycle was completed, exposure to different treatments was performed as described in Section 4.2.6

for a period of three days. Cells were examined with a microscope to estimate the level of confluency on Day 10.

5.2.5.2 Exposure to range of concentrations for each treatment

Once the optimum seeding concentration was determined, equal concentrations of cells determined were seeded in 6-well plates. Cells were firstly differentiated using the method explained in Section 3.3 for a period of 7 days. Cells were then incubated with the exposure treatments (listed in Table 12) for three days after completion of the differentiation cycle.

Table 12: Exposure treatments to assess their possible toxicity.

Treatment	Detail
Negative Control	RPMI differentiation medium with no ethanol
Ethanol Control	0.05% of Ethanol in differentiation medium
1 x Nicotine	0.2 µM Nicotine
10 x Nicotine	2 µM Nicotine
50 x Nicotine	10 µM nicotine
250 x Nicotine	50 µM Nicotine
1 x TPM	Concentration of TPM relative to 0.2 µM Nicotine
10 x TPM	Concentration of TPM relative to 2 µM Nicotine
50 x TPM	Concentration of TPM relative to 10 µM Nicotine
250 x TPM	Concentration of TPM relative to 50 µM Nicotine
1 x MAOI	Concentration of MAOI in TPM relative to 0.2 µM Nicotine
10 x MAOI	Concentration of MAOI in TPM relative to 2 µM Nicotine
50 x MAOI	Concentration of MAOI in TPM relative to 10 µM Nicotine
250 x MAOI	Concentration of MAOI in TPM relative to 50 µM Nicotine

A total of 14 different treatments were used (Table 12). These comprised control and exposure treatments (nicotine, TPM and MAOIs) at concentrations 1-, 10-, 50- and 250- fold compared to those used in the main experiments (Section 5.2.3). The medium was changed every other day. A total of 3 replicates for each treatment were set up.

5.2.5.3 MTT assay

The MTT assay was used to assess the toxicity of the treatments according to a well-established method with slight modification (Riss et al., 2016). Briefly, at the end of the exposure experiment, as described in Section 5.2.5.2, the medium was removed from the wells and replaced with 600 µL of 0.5 mg/mL MTT solution. The 6-well plates were incubated at 37 ˚C for 1 hour after the addition of MTT solution. Following the incubation step, the MTT solution was removed, and 1 mL of DMSO was added as a solubilising agent. The plates were then tapped and gently shaken on the bench. Samples of 200 µL of the liquid from each well were pipetted into 96-well plates in triplicate. The absorbance of the solutions was measured at 580 nm using a spectrophotometer.

5.3 Results

5.3.1 Protein assay

Figure 18 shows the standard curve for the protein assay generated by plotting absorbance for a range of protein concentrations. The content of protein in the lysates was determined as described in Section 5.2.2. The samples were assayed in triplicate. The average protein content of the samples is listed in Table 13.

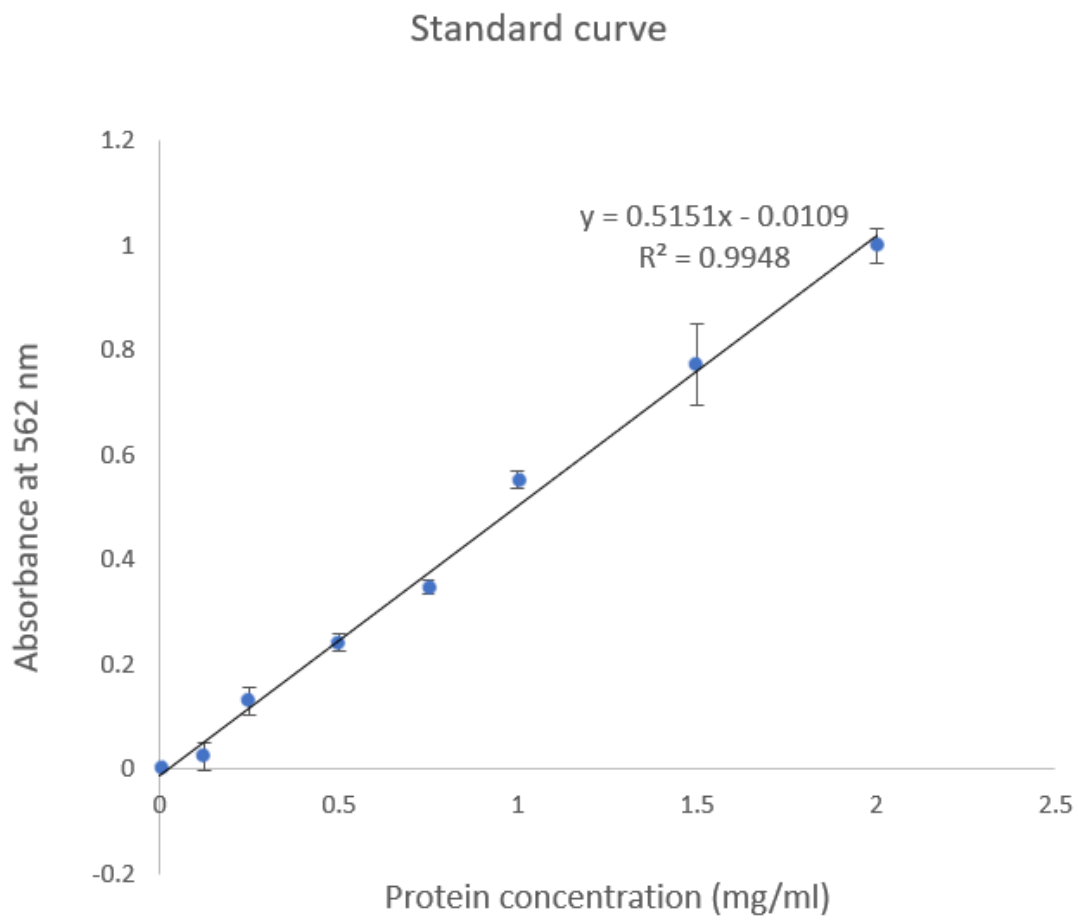

Figure 18: Representative standard curve for calculation of protein concentration at absorbance of 562 nm.

Table 13: Protein content of cell lysate samples obtained from different exposure treatments.

Sample	Replicate 1 Protein Content (mg/mL) ± SD	Replicate 2 Protein Content (mg/mL) ± SD	Replicate 3 Protein Content (mg/mL) ± SD
Day 1 Control	1.82 ± 0.059	1.29 ± 0.263	5.72 ± 0.199
Day 1 Nicotine	1.99 ± 0.176	1.95 ± 0.182	5.22 ± 0.128
Day 1 TPM	1.78 ± 0.124	2.12 ± 0.319	4.99 ± 0.0697
Day 1 MAOI	3.03 ±0.455	2.71 ± 0.414	5.62 ± 0.178
Day 3 Control	2.18 ± 0.154	3.49 ± 0.255	5.93 ± 0.195
Day 3 Nicotine	3.48 ± 0.388	3.37 ± 0.212	5.79 ± 0.390
Day 3 TPM	3.30 ± 0.081	2.60 ± 0.169	7.20 ± 0.139
Day 3 MAOI	2.79 ± 0.185	2.99 ± 0.192	7.32 ± 0.153
Day 5 Control	2.74 ± 0.0297	2.69 ± 0.242	6.88 ± 0.376
Day 5 Nicotine	1.12 ± 0.0489	1.54 ± 0.179	6.61 ± 0.125
Day 5 TPM	1.17 ± 0.178	2.64 ± 0.191	6.75 ± 0.0836
Day 5 MAOI	2.09 ± 0.0404	3.14 ± 0.211	6.85 ± 0.0836
Day 7 Control	4.35 ± 0.216	4.23 ± 0.13	7.43 ± 0.0139
Day 7 Nicotine	3.39 ± 0.189	4.66 ± 0.191	7.27 ± 0.613
Day 7 TPM	5.45 ± 0.096	4.60 ± 0.635	7.90 ± 0.167
Day 7 MAOI	3.68 ± 0.242	5.10 ± 0.263	7.85 ± 0.0139

5.3.2 4-Hydroxyquinoline Standard Curve

MAO enzymes deaminate kynuramine to 4-hydroxyquinoline (4-HQ), which fluoresces under basic conditions. In order to develop a standard curve, a range of dilutions (0-1000nM) of 4-HQ was used. 2M NaOH was added, and the fluorescence was measured using 320 nm excitation and 380 nm emission wavelengths. A linear increase in fluorescence with an increase in 4-HQ concentration throughout the entire range tested was observed. A representative standard curve is shown in Figure 19. It was used to convert the fluorescence units to the amount of 4-HQ produced during the reaction involving oxidative deamination of kynuramine by cell lysates.

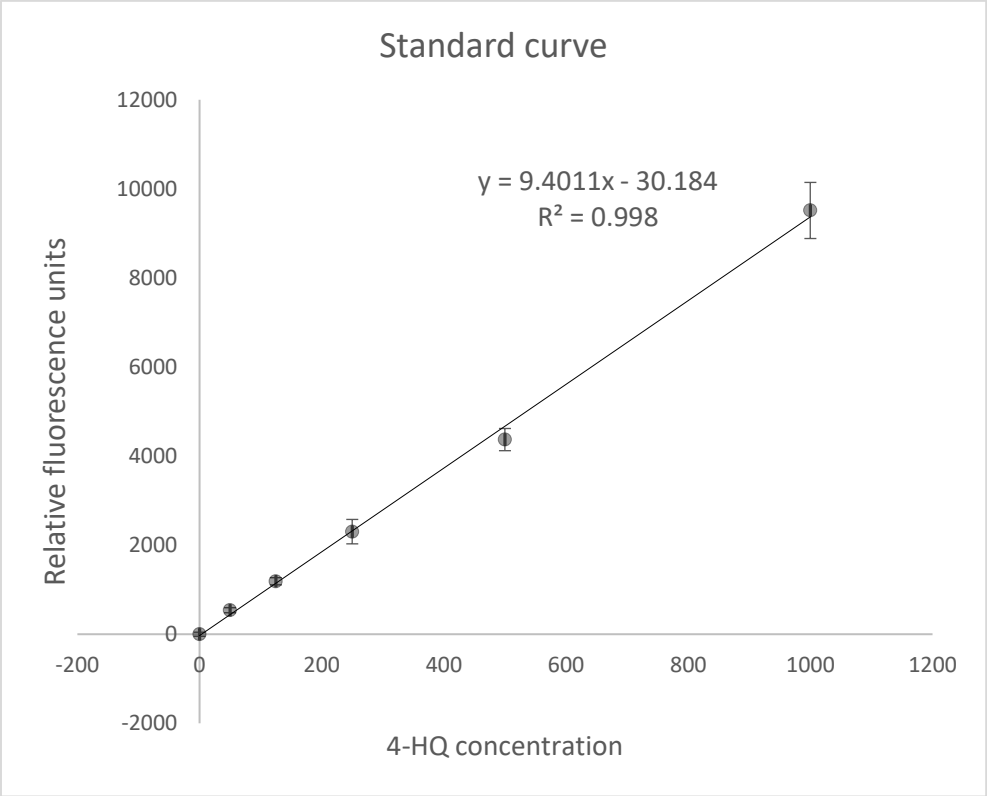

Figure 19: Representative standard curve of 4-HQ concentration versus fluorescence. 4-HQ concentration versus fluorescence is linear over the range of the assay, fitting the straight-line equation y=9.4011x-30.184 (R^2 = 0.998).

5.3.3 Determination of MAO activity after exposure treatment

5.3.3.1 Determination of Optimum Substrate Concentration

To determine the optimum substrate concentration to be used in MAO assays, a range of concentrations of kynuramine were trialled. Differentiated SH-SY5Y cell lysate with a protein concentration of 1.0 mg/mL was used as an enzyme source to react with substrate concentrations ranging from 1 – 7 mM. Cell lysate samples with a protein concentration of 1.0 mg/mL were prepared by diluting with cell lysis buffer, while kynuramine was diluted using sodium phosphate buffer. As seen in Figure 20, the fluorescence increased rapidly with an increase in substrate concentration and plateaued at concentrations higher than 3 mM. The result obtained looked similar to previous results (Lewis, 2010) and based on this, a concentration of 3 mM kynuramine was selected to be used in MAO assays. With concentrations of kynuramine higher than 3mM, the fluorescence increased with an increase in kynuramine concentration. However, the increase was very slow and not linear, suggesting substrate approaching saturating conditions. With the concentration of 3 mM kynuramine, it is expected that enzymes would not reach saturation and would be sufficient to show proportional increases in fluorescence with increases in enzyme concentration and small variations in kynuramine concentration would not affect the result.

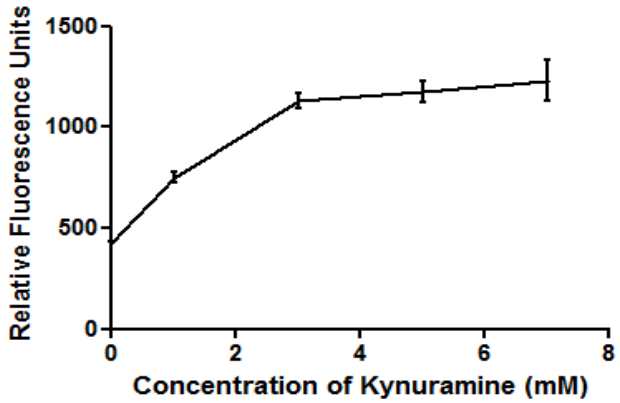

Figure 20: A curve of range of kynuramine concentrations (1-7) mM versus the fluorescence at 380 nm emission wavelength. Each data point represents the mean of three independent samples taken in triplicate.

5.3.3.2 There is a linear increase in fluorescence with an increase in enzyme concentration

To determine the optimum concentration of protein that could be used for MAO assays, a range of concentrations of the cell lysate was used. Cell lysates obtained from SH-SY5Y cells differentiated for a period of 7 days were used as a source of enzyme. Different concentration ranges of cell lysate were prepared by diluting the cell lysate using cell lysis buffer. Based on the earlier result, a concentration of 3mM kynuramine was selected for these assays. Fluorescence showed a linear increase with an increase in the concentration of protein tested over the range of 0-8 mg/mL using lysates of differentiated SH-SY5Y cells (Figure 21). This suggested that any protein concentration in the range of 0-8 mg/mL could be used in the MAO assay as each of these protein concentrations fell in the linear range and the amount of kynuramine in the assay was sufficient during incubation.

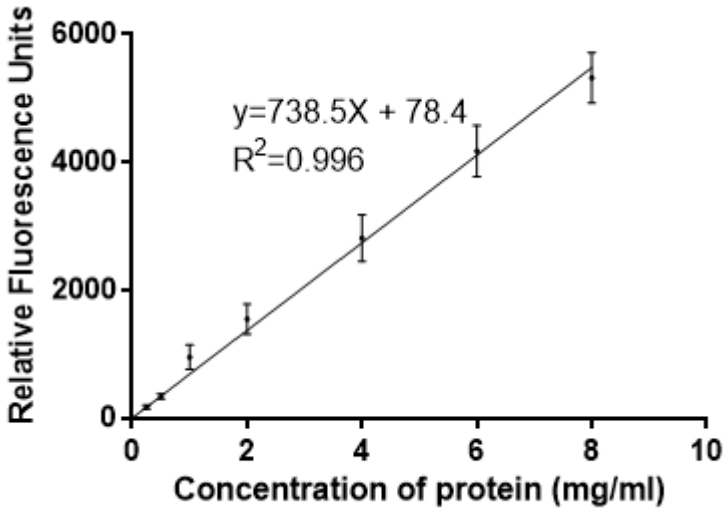

Figure 21: A curve of range of protein concentrations (0 - 8) mg/mL of differentiated SH-SY5Y cell lysates versus fluorescence at 380 nm emission of wavelength. Each data point represents the mean of three independent samples taken in triplicate

5.3.3.3 The Kynuramine Enzyme Reaction is Linear Over Time

In order to determine the optimum enzyme reaction time, 3mM of kynuramine substrate was used to react with SH-SY5Y cell lysate with a concentration of 1 mg/mL and incubated for a range of time between 0 and 60 mins. The concentrations of the protein sample and substrate were chosen based on the result obtained from 5.4.3.1-5.4.3.2. A linear increase in fluorescence was seen with an increase in incubation time (Figure 22). Based on this result, 30 minutes of incubation was selected as it fell within the linear range.

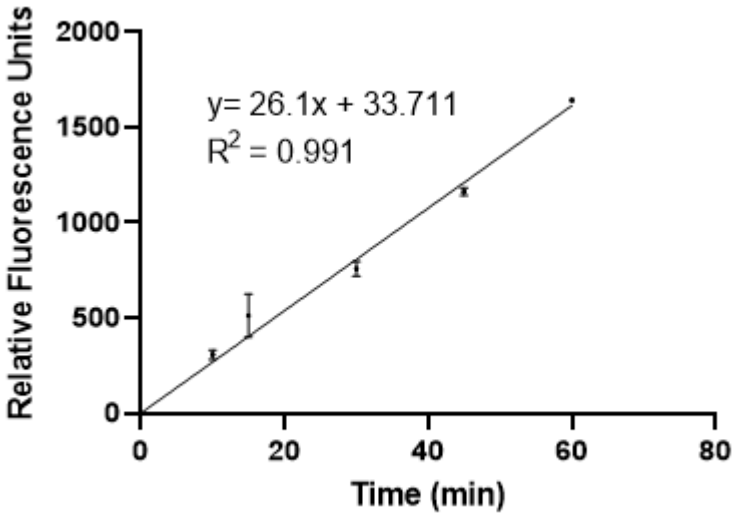

Figure 22: A curve of range of incubation time (0 – 60) min versus fluorescence at 380 nm emission wavelength. Differentiated SH-SY5Y cell lysate (1 mg/mL) was incubated with 3mM kynuramine. Each data point represents the mean of three independent samples taken in triplicate.

5.3.3.4 Exposing differentiated SH-SY5Y cells to different treatments for 1, 3, 5 and 7 days.

Differentiated SH-SY5Y cells were exposed to the four different exposure treatments: ethanol (the control), nicotine, TPM and MAOIs in a CO_2 incubator for 1, 3, 5 and 7 days as detailed in Chapter 4. The medium was replaced every other day until the end of the exposure period. At the end of the exposure period, cell lysates were collected using the method described in Section 3.4. MAO activities from these samples are shown in Figure 23.

When cells were exposed to the treatments for 1 day (Figure 23A), there was no significant change in total MAO activity in the cells exposed to nicotine ($p > 0.999$). TPM exposure for 1 day caused a significant decrease in total MAO activity compared to the control ($p = 0.0053$). MAOIs also caused a significant decrease in the total MAO activity of the cells compared to the control ($p = 0.0012$). The inhibition induced by MAOI was greater than TPM, but this difference was statistically insignificant ($p > 0.999$).

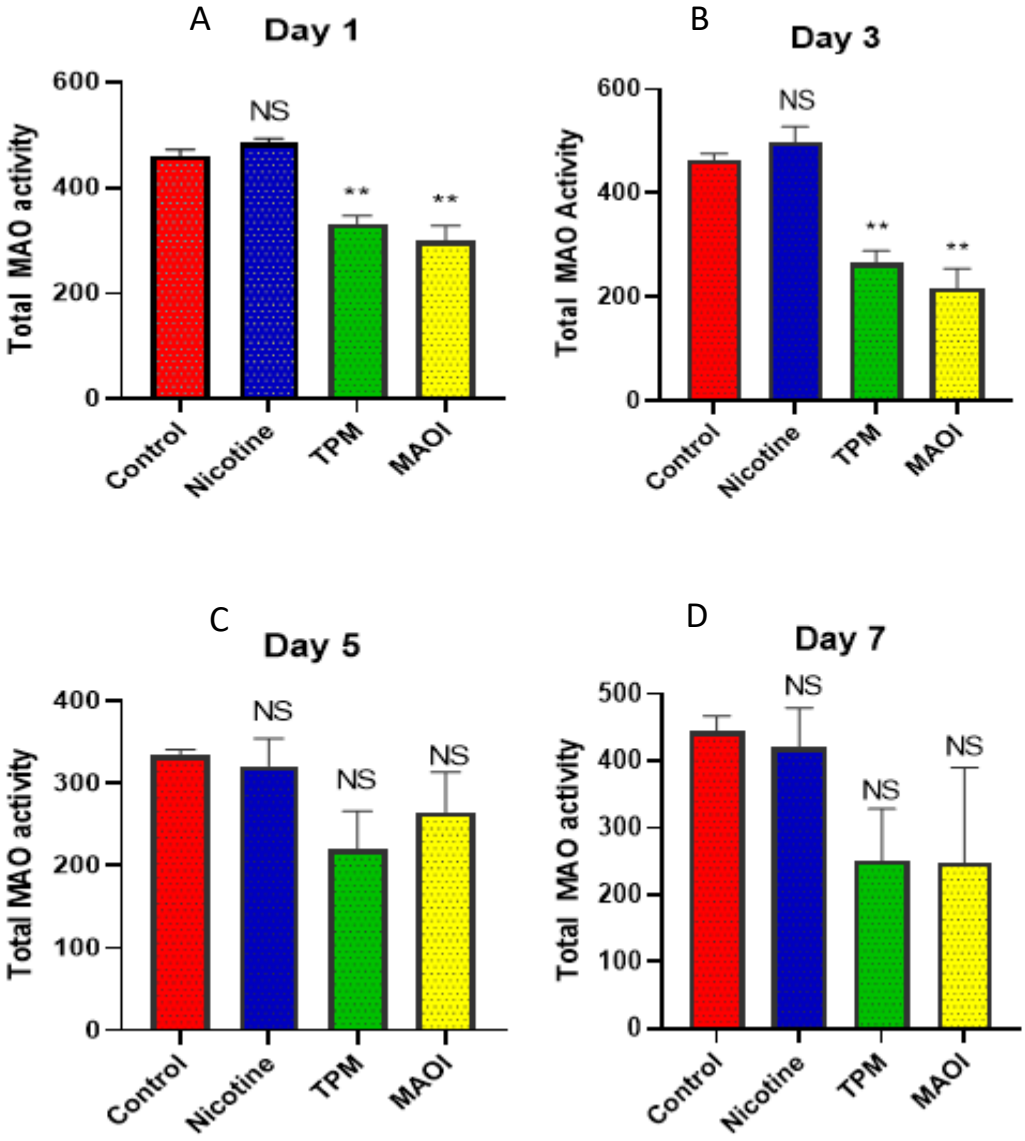

Figure 23: Total MAO activity in the differentiated SH-SY5Y cell lysates exposed to the exposure treatments: control, nicotine, TPM and MAOI for A) 1 day. B) 3 days. C) 5 days. D) 7 days. (n = 3) for each sample.

When cells were exposed to nicotine for 3 days (Figure 23B), there no significant change in total MAO activity ($p > 0.999$). Exposure to TPM and MAOIs for 3 days caused a significant decrease in total MAO activity compared to the control (p: 0.0059 and 0.0015, respectively). Similar to Day 1, the decrease induced by MAOI was more than that of TPM exposure treatment but statistically insignificant ($p > 0.999$).

Treatment for 5 days (Figure 23C) did not cause any significant change in total MAO activity in the cells exposed to nicotine compared to the control ($p > 0.999$). TPM exposure for 5 days caused a decrease in total MAO activity compared to the control. However, the decrease was not statistically significant ($p = 0.382$). MAOI also did not impart any significant change in the total MAO activity of the cells compared to the control ($p > 0.999$).

With exposure treatment for 7 days (Figure 23D), there was no significant change in total MAO activity in the cells exposed to nicotine ($p = 0.999$). TPM exposure, as well as MAOIs cocktail exposure, decreased the total MAO activity compared to the control ($p = 0.157$ and 0.147, respectively). However, sample-to-sample variation was very high, which might have resulted in statistically insignificant differences.

5.3.4 Determination of MAO-A and MAO-B activity from total MAO activity using clorgyline

5.3.4.1 Inhibition of MAO-A and MAO-B by clorgyline

The logarithmic concentration of the clorgyline was plotted against total MAO activity, and non-linear regression analysis was performed (Figure 24). The IC_{50} of clorgyline for MAO-A was found to be 5.20 nM. MAO-B was not well inhibited by clorgyline, and concentrations as high as 75 µM resulted in inhibition of only about 15% of MAO-B activity. Therefore, a concentration of 100 nM clorgyline was chosen to determine MAO-B activity from total MAO

activity as it caused almost complete inhibition of MAO-A but no inhibition of MAO-B.

A

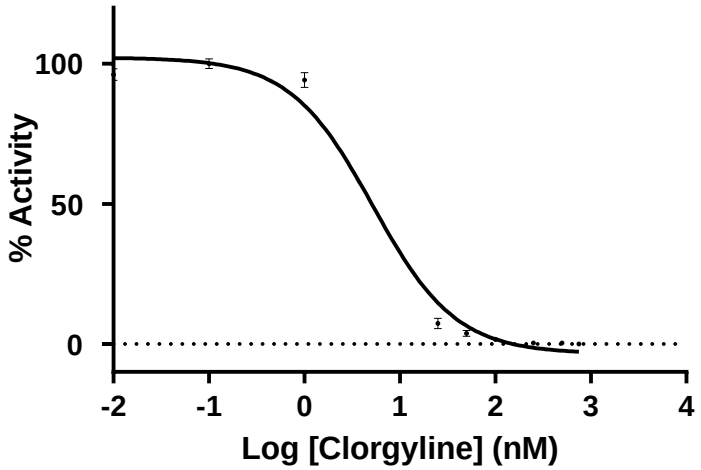

B

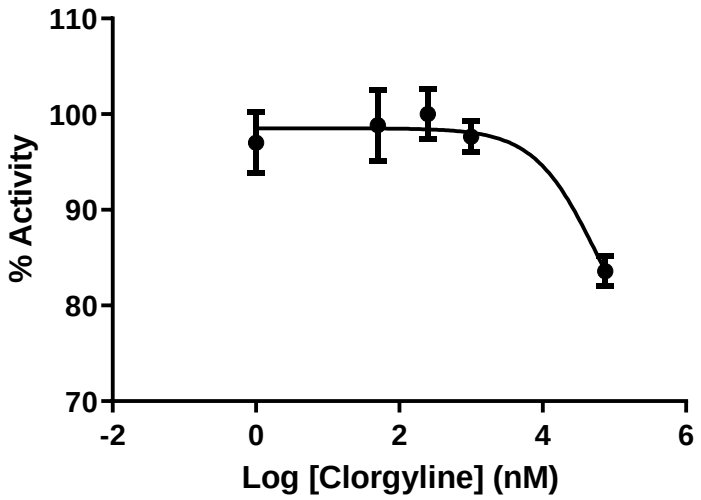

Figure 24: Activity of purified recombinant human A) MAO-A and B) MAO-B in the presence of clorgyline.

5.3.4.2 MAO-A and MAO-B activity from total MAO activity

MAO-A and MAO-B activity was determined from total MAO activity and presented in Figure 25 as a percentage of total MAO activity. MAO-B activity comprised 66.3-86.9% of total MAO activity compared to MAO-A activity in each of the exposure treatments (1, 3, 5 and 7 days).

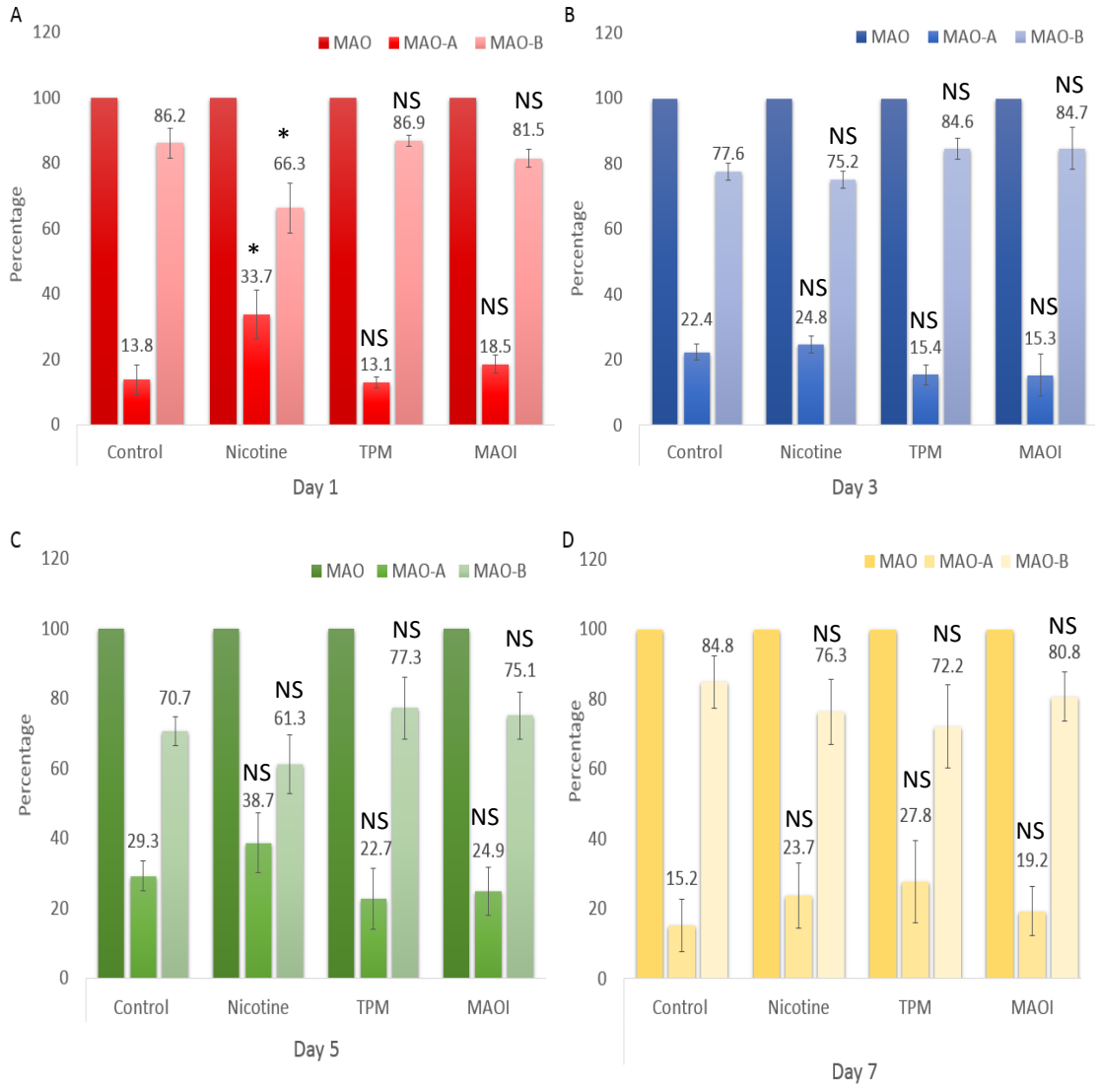

Figure 25: MAO A- and -B activity from different exposure treatments expressed as percentage of total MAO activity ± SD for A) 1 day. B) 3 days. C) 5 days. D) 7 days. Arithmetic means of relative activity are shown above each bar. No significant difference was found in the percentage of MAO-A and MAO-B activity compared to the control for any time period except the nicotine group, which showed a significant change in day 1 compared to the control. (One way ANOVA with Bonferroni's multiple comparison post-test; $p < 0.05$, n=3).*

5.3.5 Assessing cytotoxicity of exposure treatment

5.3.5.1 Determination of optimum cell seeding concentration

Based on the observation of cell confluency from the range of seeding concentrations tested, a seeding concentration of 1.8×10^5 cells per well was selected. This seeding concentration resulted in differentiated cells with 80-90% confluency as observed visually by microscope at the end of Day 10 of culture. Seeding concentrations higher than 1.8×10^5 cells per well resulted in close to 100% confluency or cells starting to grow on top of each other. Concentrations less than 1.8×10^5 cells per well resulted in cells not being suitably confluent at the end of 10 days of incubation.

5.3.5.2 Toxicity assessment of exposure groups

Cell viability for the treatments was calculated as a percentage of the control and is presented in Figure 26. Nicotine had no toxicity up to 250 times the concentration used in the main experiment. For TPM exposure there was no toxicity up to 10 times the concentration used in the main experiment. Slight toxicity was seen at 50 times the original concentration, and the toxic effect at 250 times was found to be very high. Some dead cells were seen at 50 x TPM concentration, and cell viability was found to be about 80%. However, the decrease in cell viability was statistically insignificant ($p = 0.819$). Toxicity at 250 x TPM concentration seemed to kill almost all the cells ($p < 0.0001$). The MAOIs had no toxicity up to 50 times the original concentration. At 250 times the original concentration, viability decreased to about 88%, but this change was non-significant ($p = 0.997$). These results show that the concentration of nicotine, TPM and MAOI used in the main experiment were well below the toxic range.

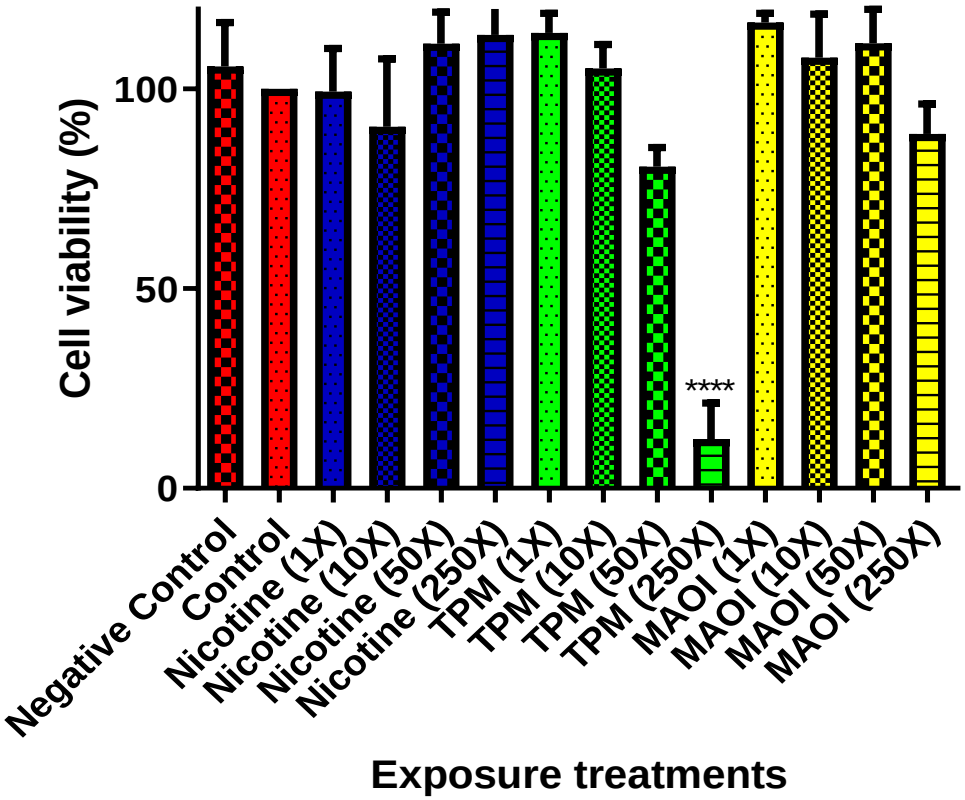

*Figure 26: Cell viability after exposure treatments. Mean cell viability for control, nicotine (1X, 10X, 50X, 250X), TPM (1X, 10X, 50X, 250X) and MAOI cocktail (1X, 10X, 50X, 250X) for 3 days. (n = 3). No significant difference was found in the cell viability of any of the exposed groups compared to the control except the 250 x TPM, which had a significant decrease in cell viability. (**** One way ANOVA with Bonferroni's multiple comparison post-test; $p < 0.0001$, n=3).*

5.4 Discussion

The kynuramine assay displayed linearity in samples with protein concentrations ranging from 0-9 mg/mL and hence allowed the flexibility of choosing any protein concentration within the tested range for standard MAO assays in cell lysates from different treatments. Therefore, while performing the MAO assay, a fixed protein concentration (1 mg/ml) was chosen, which was the lowest protein concentration among all the replicates of 12 different sample types, as it would allow the simplest comparison. Use of up to 0.5% of ethanol has been reported to have no effect on the total MAO activity in SH-SY5Y cells (Lewis, 2010; Ekblom, Zhu, Chen, & Shih, 1996). Therefore, the use of ethanol as a solvent in exposure treatments would not affect the MAO activity in the SH-SY5Y cells in these experiments. The effect of ethanol, if any would be similar in all the treatments as all samples and controls were matched for ethanol concentration.

This study showed a significant decrease in total MAO activity in SH-SY5Y cells exposed to TPM as well as the MAOI exposure treatments on day 1 and day 3. MAOIs were able to inhibit MAO activity at a similar or higher level than TPM, which indicated that these candidate inhibitors have significant inhibitory properties and can be claimed as major inhibitors present in tobacco smoke. TPM and MAOI exposure treatments for 5 and 7 days also caused a decrease in total MAO activity compared to the control, but these changes were not statistically significant. This may be in part due to the high variance between samples and a low number of samples. The inhibition of the MAO activity was inconsistent in the exposure treatments for the period of 5 and 7 days. Further, it was observed that cells started growing on top of each other as the length of exposure was increased, especially around 7 days.

Overall, Day 3 exposure treatment induced the most significant MAO activity inhibition in the SH-SY5Y with more consistent results. This dictated using Day 3 as the optimum exposure period for assessing other parameters such as changes in MAO gene and protein expressions. In another similar study, two different types of TPM caused a decrease in MAO activity to about 62%

and 63% of control when undifferentiated SH-SY5Y cells were exposed for 1 day (Lewis, 2010). However, other exposure regimens produced inconsistent results, such as 3 days of exposure not causing any significant change in the activity and 5 days of exposure causing a decrease in activity to about 82% and 78% of control. One of the reasons for the discrepancy in the Day 3 exposure treatment effect could be the use of a continuous medium (no change of medium), unlike ours, where medium was replaced every other day. The MAO inhibitory effect obtained in that study may not include the effect of catechols, since these have a shorter half-life (listed in Table 3) and could be one of the reasons for the MAO inhibitory effect not being prominent in 3 days exposure. Catechols are found to demonstrate an irreversible MAO inhibitory effect (Unpublished data, SW Hong, pers. comm.) and, therefore should have a prominent role in MAO inhibitory effect shown by TPM and MAOI.

MAO-B activity was determined from total MAO activity using clorgyline to inhibit MAO-A activity, and MAO-A activity was calculated as a difference between total MAO activity and MAO-B activity. It was found that total MAO-B activity had a much greater contribution towards total MAO activity compared to MAO-A activity. The expression levels of MAO-A and MAO-B, however, may vary depending upon the species and tissues analysed. Rodents have been shown to have higher MAO-A levels, while the human brain has higher MAO-B levels than MAO-A (Richards, Saura, Ulrich & Da Prada, 1992; Van Amsterdam, Talhout, Vleeming, & Opperhuizen, 2006).

Studies have shown MAO-A to be predominantly expressed in catecholaminergic neurons in areas such as NA, substantia nigra, and ventral tegmentum, while MAO-B predominates in serotonergic and histaminergic neurons in areas such as substantia nigra, dorsal and medial raphe complex, hypothalamus as well as astrocytes and glial cells (Westlund et al., 1985; Riederer et al., 1987; Westlund et al., 1988). MAO activity measured in a similar study using SH-SY5Y cells showed much higher levels of MAO-A compared to MAO-B (Jiang, Jiang, Liu, & Feng, 2006). However,

undifferentiated SH-SY5Y cells were used in that study, while our study used differentiated SH-SY5Y cells. Another reason for this disparity could be the use of RA to differentiate SH-SY5Y cells. RA has been found to activate MAO-B in human neuronal cells and downregulate MAO-A in different studies (Korecka et al., 2013; Wu, Chen, Ou, & Shih, 2009). Though it was found in our study that total MAO activity comprises a greater contribution from MAO-B activity, the use of a selective MAO-B inhibitor in future studies would be encouraged to compare and confirm the result in this study.

MTT assays have been used in several investigations, including the study of toxicity induced by nicotine or cigarette smoke with SH-SY5Y cells as a model neural cell culture (Jung, Choi, & Oh, 2021; Russo et al., 2011). This makes the method a suitable one for this study. Also, the availability of all the reagents required for MTT assay in the lab prompted the choice of MTT assay over other cytotoxicity assays. MTT assay was first performed using 96-well plates and following the standard protocol for MTT Cell Viability Assays (Riss et al., 2016). However, this created problems, including the loss of a substantial proportion of cells from the wells during medium changes, as well as the clumping of cells on top of each other. The results obtained could not be trusted. Therefore modifications were made to the MTT assay by culturing the plates in 6-well plates instead of 96-well plates. After induction of differentiation and treatment exposures, cells were found to be well differentiated, and no clumping was seen for the duration of the exposure period.

An ethanol concentration of 0.05% was used in each of the treatments as TPM and MAOI were soluble in ethanol. The use of constant ethanol addition in all the exposure treatments would even out possible inhibition of MAO or any other effects in enzyme assays of cell extracts or cell responses due to ethanol. The addition of 0.05% ethanol to the culture medium did not result in any significant change in viability compared to the negative control (containing differentiation medium only). This is very much in line with other research. For

example, in a study, no cytotoxic effect of ethanol at concentrations of 50, 100 and 150 mM (equivalent to 0.29-0.88% v/v ethanol) on an SH-SY5Y cell line was found when exposed for a period of 48 h (Copeland, Leggett, Kanaan, Taylor, & Tizabi, 2005). Similarly, another study also reported that 50 mM ethanol (equivalent to 0.29% v/v ethanol) did not significantly reduce the viability of SH-SY5Y cells when exposed for a period of 72 hours (Sangaunchom & Dharmasaroja, 2020). The concentration of ethanol used in this study can therefore be considered to be non-toxic to cells.

The results of MTT assays showed no cytotoxic effect of nicotine on differentiated SH-SY5Y cells at concentrations as high as 250 µM. This agrees with the findings of similar research where nicotine concentration up to 20 µM did not have any cytotoxic effect when exposed to SH-SY5Y cells for the time period of 1, 3 and 5 days (Ambrose et al., 2007). Similar results were obtained in another study, where nicotine up to 20 µM did not cause any significant decrease in cell viability (Jung et al., 2021). Nicotine did not show any cytotoxicity to a human gingival fibroblast cell line culture when added in concentrations up to 5 mM (Torshabi, Rezaei Esfahrood, Jamshidi, Mansuri Torshizi, & Sotoudeh, 2017). These results, therefore confirm that 0.2 µM nicotine, which is the concentration of major concern in this PhD study, is well below the concentration that can cause toxicity to SH-SY5Y cells.

Similarly, with the results for TPM, there was no decrease in cell viability up to a TPM concentration equivalent to 2 µM nicotine. The TPM concentration equivalent to 10 µM nicotine had a considerable cytotoxic effect that decreased the cell viability by about 20%. However, this result was not statistically significant, while the TPM concentration equivalent to 250 µM nicotine killed all the cells. This is not considered of concern, as the concentration causing cytotoxicity is much higher than 0.2 µM, which is the concentration used in all the experiments in our study. The result obtained here is in fact, very comparable to that of a similar study, where TPM with a nicotine concentration of 0.2 µM used in the main experiments of this research did not have any significant cytotoxic effect even until 5 days of exposure (Ambrose et al., 2007). They also found that TPM with a nicotine

concentration of 10 µM had a cytotoxic effect when exposed for 5 days, and 20 µM nicotine showed cytotoxicity as early as 3 days. The cytotoxicity observed at higher concentrations is very normal and expected as different compounds have-dose dependent cytotoxicity, and cigarette smoke consists of several toxic compounds. Studies on comparative cancer risk rankings, cardiovascular effects, respiratory effects, reproductive and developmental effects, effects on kidney, liver etc. and toxicity of cigarette smoke have been reported (Fowles et al., 2000). These results would therefore justify dose-dependent cytotoxicity of TPM and support the use of TPM for studies if the concentration to be used is well below the concentration which causes overt toxicity.

The cocktail of MAOIs also did not seem to have any visible cytotoxic effect on the SH-SY5Y cell line. A 250-fold MAOI concentration seemed to be decreasing the viability slightly, but the result was not statistically significant. Previous studies have shown the MAOIs (linoleic acid, linolenic acid, catechol, quinol, 4-methylcatechol and 4-ethylcatechol) to have some cytotoxic effect on different cell lines, including SH-SY5Y cells (Li et al., 2006; Oliveira et al., 2010; Iuchi, Ema, Suzuki, Yokoyama, & Hisatomi, 2019; Litwiniuk et al., 2020; Hrubša et al., 2022). However, the concentration at which the cytotoxicity was seen is in the micromolar range and is much higher than the concentrations used in this study. This would again justify the lack of cytotoxicity of the MAOI cocktail at the concentrations used in the treatment exposures.

5.5 Conclusion

This study was able to successfully determine MAO activity in SH-SY5Y cell lysates after different exposure treatments for 1, 3, 5 and 7 days. Based on the results obtained, the candidate MAOIs have significant inhibitory properties and can be considered as major components responsible for MAO inhibition by cigarette smoke. Exposure for 3 days was chosen as the optimal period of exposure for further analysis. This study was able to successfully confirm that none of the components present in the exposure treatments

(nicotine, TPM and MAOI) at the concentrations used for exposure studies had any significant overt cytotoxicity when cells were exposed for the period of 3 days.

Chapter Six: The effect of nicotine, TPM and tobacco smoke MAOIs on mRNA and protein expression levels of MAO.

6.1 Introduction

This chapter provides a detailed analysis of the impact of nicotine, TPM and tobacco MAOIs on mRNA and protein expression levels of MAO. In this PhD project, the impact of exposure treatments on MAO activity was investigated using SH-SY5Y cells (Chapter 5). It was observed that TPM and MAOIs inhibited MAO activity in differentiated SH-SY5Y cells (Section 5.3.3.4). In this chapter, change in *MAOA* and *MAOB* mRNA expression (Section 6.2.2), and change in MAO-A and MAO-B protein expression (Section 6.2.3) is assessed. It was intended to see if the change in enzyme activity seen in SH-SY5Y cells in response to exposure treatments for a period of 3 days is also reflected by a change in mRNA and/or protein levels.

6.2 Materials and Methods

6.2.1 Exposure treatment

SH-SY5Y cells were differentiated, as explained in Section 3.3, and then incubated with different exposure treatments for 3 days as explained in Section 4.2.6. Exposure for 3 days was selected as this time point was concluded to be the optimum time period for assessing the effect of different treatments on gene expression, protein levels etc. (Section 5.5). Briefly, three replicates of SH-SY5Y cells were differentiated for a period of 7 days, and then exposed to the treatments: ethanol, nicotine, TPM and MAOIs for a period of 3 days. The medium containing the treatments was changed on Day 2 of exposure, and the expression of MAO-A and MAO-B proteins and mRNA from SH-SY5Y cells was investigated after the end of the exposure period.

6.2.2 Assessing change in mRNA expression

6.2.2.1 Gene expression assay for determination of primer efficiency

DNA-directed RNA polymerase II subunit F (*POLR2F*) and glyceraldehyde-3-phosphate dehydrogenase (*GAPDH*) were chosen to be used as housekeeping genes based on a similar study (Hoerndli, Toigo, Schild, Götz, & Day, 2004). Predesigned TaqMan Gene Expression Assays (ThermoFisher Scientific) for the reference and target genes were used in the experiments. All assay systems had TaqMan minor grove binder (MGB) probes, including a fluorescein amidites (FAM) reporter on the 5' end and a nonfluorescent quencher at the 3' end. The following PCR primers were used: *MAOA* (Hs00165140_m1), *MAOB* (Hs01106246_m1), *GAPDH* (Hs02786624_g1), *POLR2F* (Hs04398334_m1).

In order to determine the efficiency of the primers, cDNA obtained from untreated SH-SY5Y cells were serially diluted in the range of 3- to 243- fold dilutions for *GAPDH* and 5- to 625- fold dilutions for the other three primer pairs. Each dilution of the sample was amplified using the TaqMan assay system as per the method explained in Section 3.9. Once the threshold cycle (Ct) value was obtained, a standard curve was generated by plotting the mean Ct value of each dilution point against the dilution factor transformed to logarithmic-base-10 value using Microsoft Excel. The best-fit straight line was found using regression analysis, and the slope of the obtained line was used to calculate the efficiency of the primers using the following equation:

$$\text{Efficiency} = 10^{(-1/n)} - 1$$

where n is the slope obtained from the best-fit line of the standard curve (Peters, Helps, Hall, & Day, 2004)

6.2.2.2 *MAO-A* and *MAO-B* gene expression

Using the samples collected for different treatments (Section 6.2.1), the change in mRNA expression was determined using qPCR, as explained in Section 3.9. Briefly, after the end of 3 days of exposure, total RNA was extracted using an RNeasy extraction kit and the RNA concentration and quality were measured. The measurement of RNA concentration and overall quality of the SH-SY5Y mRNA samples exposed to control, nicotine, TPM and MAOIs was performed by Massey Genome Service, Palmerston North. RNA samples were stored at -80˚C until the process of reverse transcription to obtain cDNA was initiated. Equivalent amounts of total RNA in each of the sample were then converted to cDNA using an iScript® cDNA Synthesis kit (Bio-Rad). qPCR was conducted using the LightCycler ® 96 (Roche LifeScience) instrument and using the fluorescent, double-stranded DNA-specific TaqMan predesigned gene expression assays (ThermoFisher). qPCR was performed with three replicates for each cDNA sample, and gene expression of MAOA and MAOB relative to the housekeeping genes GAPDH and POLR2F was determined using the 2−ΔΔCt method.

6.2.3 Assessing change in protein levels

6.2.3.1 Exposure treatment, collection of cell lysate and determination of protein concentration

Differentiated SH-SY5Y cells were incubated with different exposure treatments, as explained in Section 4.2.6, and cell lysates were collected, as described in Section 3.4. Protein concentrations of the lysates were determined as described in Section 3.5. Briefly, differentiated SH-SY5Y cells were incubated with exposure treatment for a period of 3 days after the completion of the differentiation cycle. Once the exposure was completed, the cell culture medium was removed, and 10 mL of cold PBS was added. Cells were detached from the cell culture flask by tapping the flask on the bench. Cells suspended in the PBS were sedimented by centrifugation, and the supernatant was discarded. Cell pellets were homogenised by triturating with an appropriate

amount of cell lysis buffer (200 µL lysis buffer per $1X10^7$ cells). Protein assay was then initiated by pipetting 10 µl each of standard or sample into the wells of a 96-well plate. BCA reagent (200 µl) was added to each well and was incubated at 37˚C for 30 minutes, cooled to room temperature, and absorbance was measured at 562 nm. The concentration of protein in the sample was obtained using the standard curve from a range of BSA concentrations (0, 0.125, 0.25, 0.50, 0.75, 1, 1.5, 2 mg/mL).

6.2.3.2 Assessing change in protein levels

SH-SY5Y cell lysates exposed to different treatments for 3 days were investigated for MAO-A and MAO-B protein expression levels as described in Section 3.8. Briefly, 2.5 mg protein samples were diluted (5:1) using 5x reducing sample buffer. The concentration of 2.5 mg protein was used as this concentration of protein gave the best bands for MAO-A and MAO-B when different concentrations (1, 2.5, 5, 10 mg) of proteins were trialled. The protein samples were denatured by heating at 95°C for 1 min on a dry heating block, and allowed to cool. Electrophoresis was performed, and the proteins from the gel were transferred to the PVDF membrane using a transfer apparatus (Criterion™ Blotter, Bio-rad). The membrane was then blocked using a blocking buffer and washed three times with 1x T-TBS. It was incubated afterwards in primary and secondary antibody solution diluted in 1x T-TBS as per the manufacturer's suggestion, details of which are listed in Table 14. The membrane was washed with 1x T-TBS following the incubation process and then visualised on an iBright CL 1000 Chemiluminescence reader with the aid of the Chemiluminescence substrate mix.

Table 14: Details of A) primary and B) secondary antibodies used in the Western blotting procedure.

A) Primary Antibody

Epitope	Host	Supplier	Dilution
MAO-A	Rabbit	Abcam (Ab126751)	1:2000
MAO-B	Rabbit	Abcam (Ab133270)	1:2000
β-Tubulin	Rabbit	Abcam (Ab6046)	1:500

B) Secondary Antibody

Epitope	Conjugate	Supplier	Dilution
Goat Anti Rabbit IgG	HRP	Abcam (Ab205718)	1:10000

6.2.3.3 Quantification of Western blots:

The images of the Western blots for MAO-A, MAO-B and β-tubulin were quantified using the software Image J as described in Section 3.8.5. The band densities were determined using the software, and the densities for MAO-A and MAO-B were normalised to the density of the β-tubulin band, and then expressed relative to the control.

6.3 Results

6.3.1 qPCR

6.3.1.1 Efficiency of primers

The efficiency of the primers used in the assay is shown in Table 15 and was found to be within the acceptable limit (90-110%) and did not vary much from the 100% mark. This confirmed the suitability of the primers, optimal reagent concentration and reaction conditions of the primer used in the assays and hence, validated the gene expression assay used to calculate the relative gene expression of *MAOA* and *MAOB*. The efficiency was calculated from the standard curve generated by plotting log-base 10 of cDNA dilution and Ct value (Figure 27).

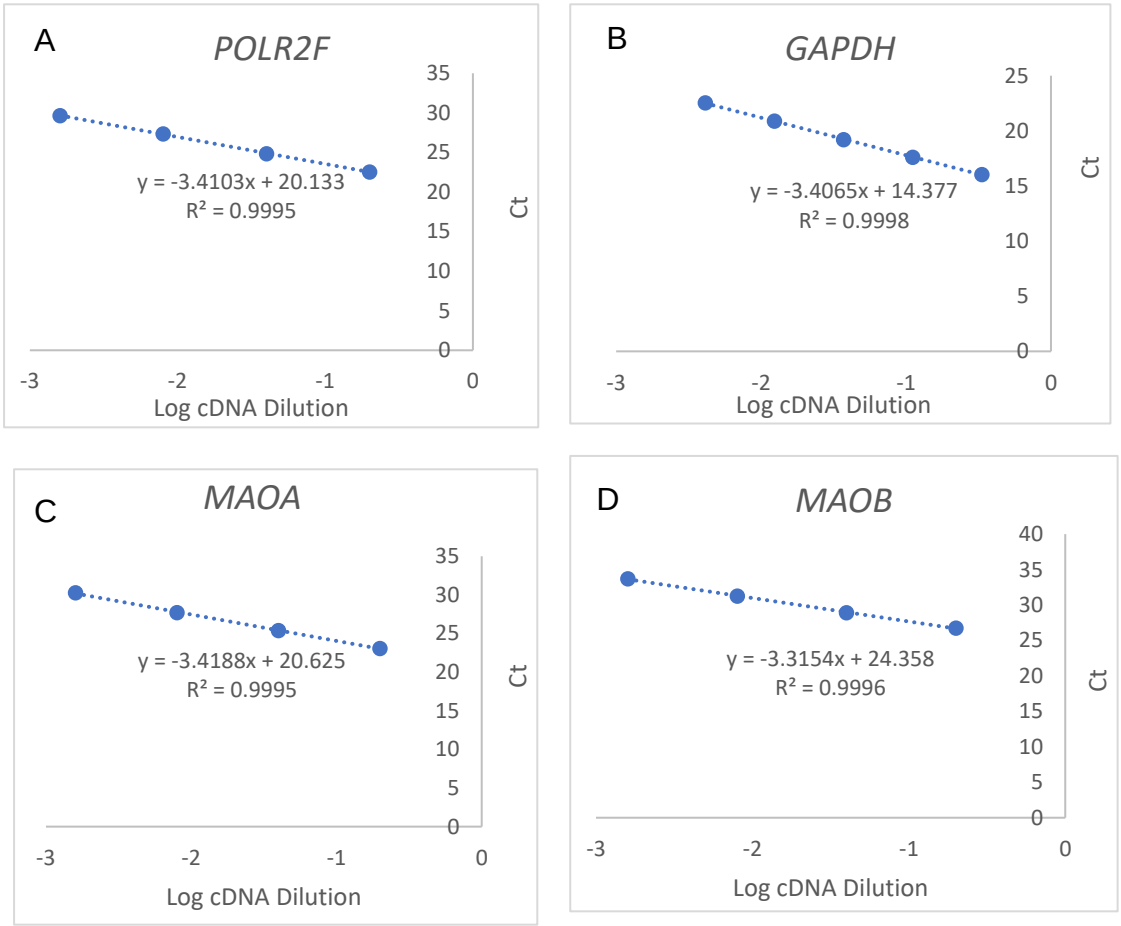

Figure 27: Scatter plot for calculation of primer efficiencies A) POLR2F B) GAPDH C) MAOA D) MAOB.

Table 15: Calculation of average efficiency (3 biological replicates of each primer).

Target Genes	**Average Primer Efficiency (%)**
POLR2F	93.22
GAPDH	95.55
MAOA	95.62
MAOB	98.19

6.3.1.2 Relative Gene Expression of *MAOA* and *MAOB*

As described in the methods section, the relative expression of *MAOA* and *MAOB* genes normalised to the housekeeping gene *GAPDH* was calculated. There was no significant change in the expression of *MAOA* gene in Nicotine, TPM or MAOIs treatment groups with respect to the control as shown in Figure 28 A. There was a slight decrease in *MAOB* gene expression of nicotine, TPM and MAOI exposure treatments compared to the control as shown in Figure 28 B. However, the decreases were not statistically significant (p= nicotine - 0.569, TPM - 0.894, MAOI - 0.99). Average Ct values from 9 samples (3 technical replicates each of 3 independent samples) are shown in Table 16 for all genes used in this experiment for different exposure treatments, and exposure treatments do not seem to change the Ct values.

Table 16: Average Ct values and SEM (3 technical replicates each of 3 independent samples) of all 4 genes in control, nicotine, TPM and MAOI exposure treatments.

	GAPDH	*POLR2F*	*MAOA*	*MAOB*
Control	24.23, 0.53	29.32, 0.40	30.28, 0.68	32.12, 0.50
Nicotine	23.71, 0.13	28.81, 0.19	29.80, 0.77	32.08, 0.17
TPM	23.55, 0.32	28.61, 0.03	29.68, 0.67	31.89, 0.32
MAOI	23.83, 0.43	28.84, 0.20	29.97, 0.63	32.06, 0.47

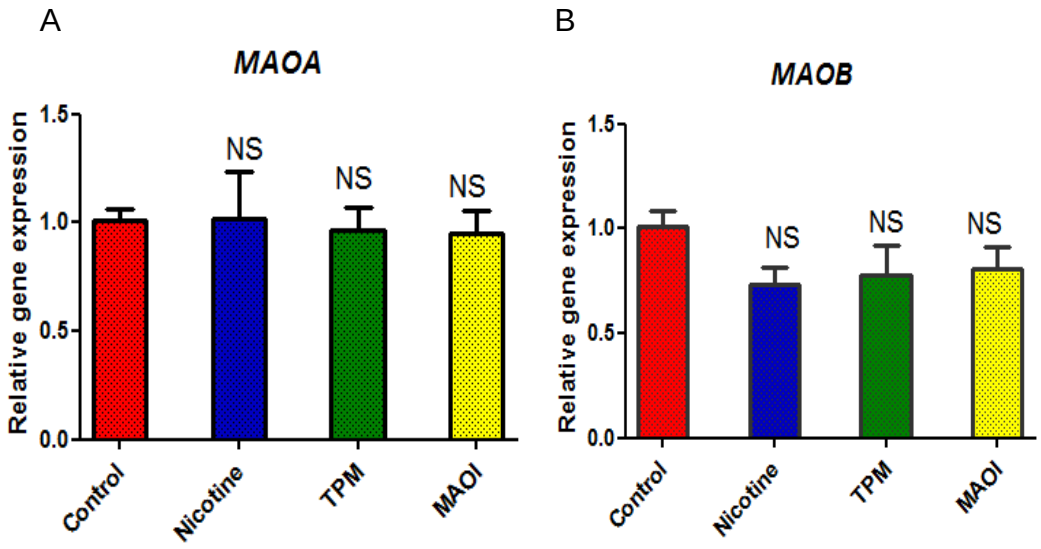

Figure 28: A) MAOA and B) MAOB gene expression in SH-SY5Y cells normalized to the housekeeping gene GAPDH following treatment with control, nicotine, TPM, MAOI for a period of 3 day calculated as mean ± ranges according to the 2-ΔΔCt method. (One-way ANOVA with Bonferroni's multiple comparison post-test; α < 0.05; n ≥ 3 independent samples for each condition)

The relative expression of *MAOA* and *MAOB* genes normalised to the housekeeping gene *POLR2F* was also calculated and is shown in Figure 29. There was no significant change in the expression of the *MAOA* gene from any of the treatments, while a small but statistically insignificant decrease of *MAOB* expression with nicotine treatment (p = 0.634), TPM (p = 0.726) and

MAOI (p = 0.933) exposure treatments relative to the control was observed. The result obtained was very similar compared to *GAPDH* being used for normalisation. This suggests that the *MAOA* and *MAOB* gene expression result is stable when compared with more than one housekeeping gene.

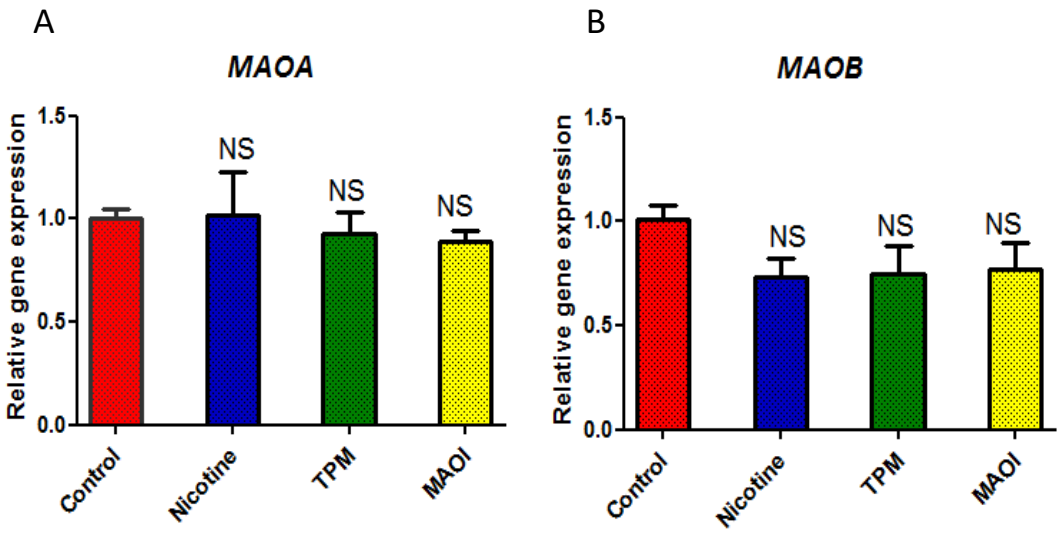

Figure 29: A) MAOA and B) MAOB gene expression in SH-SY5Y cells normalised to the housekeeping gene POLR2F following treatment with control, nicotine, TPM, Tobacco MAOI for a period of 3 day calculated as mean ± ranges according to the 2-ΔΔCt method. (One-way ANOVA with Bonferroni's multiple comparison post-test; α < 0.05; n ≥ 3 independent samples for each condition.

6.3.2 Western blotting

Western blotting was performed on a portion of the protein sample of different exposure treatments collected for the MAO assay to determine if changes in MAO enzyme activity were associated with changes in protein level, as shown in Figures 30A and 31A. The band densities of MAO-A and MAO-B were normalised to the band density of β-tubulin, a house-keeper protein, as shown in Figures 30B and 31B, respectively. There was a very slight decrease in MAO-A protein levels with nicotine, TPM and MAOI exposure treatments. However, none of them were statistically significant. The nicotine exposure treatment had almost identical MAO-B protein levels compared to the control. TPM caused a decrease in MAO-B protein level to about 70% of control. However, the decrease was not statistically significant (p = 0.489). MAOI

exposure treatment caused a decrease in MAO-B protein levels to about 90% of the control. However, this decrease was also statistically insignificant.

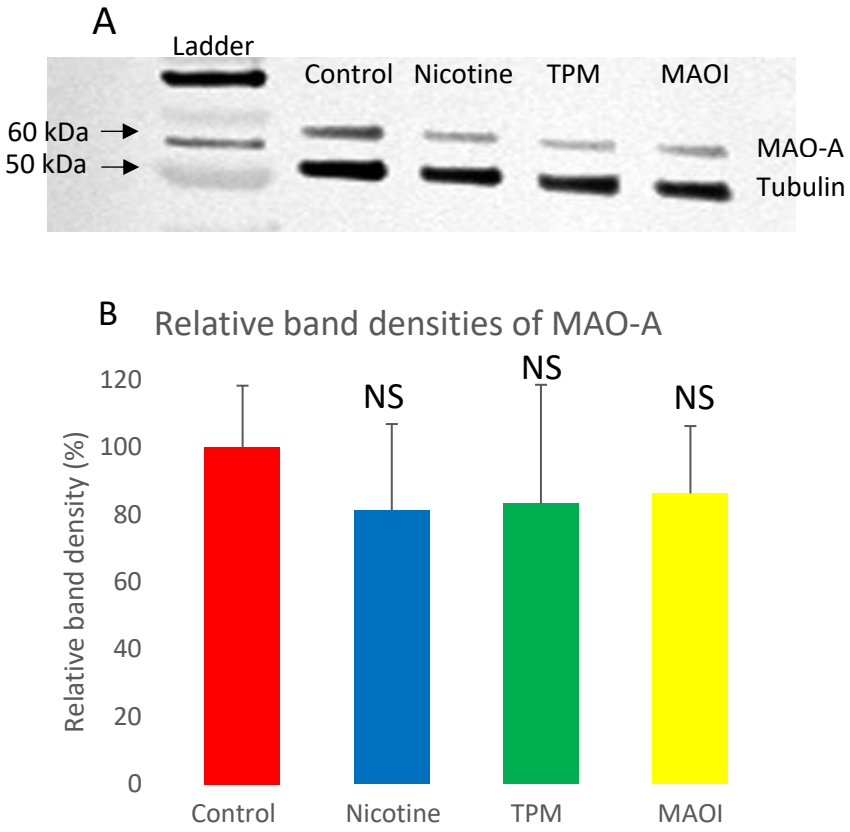

Figure 30: A) Representative Western blot of MAO-A in differentiated SH-SY5Y after exposure treatments. Control, nicotine, TPM and Tobacco MAOI exposure treatment for a period of 3 days. MAO-A specific bands are at 60 kDa, and the β -tubulin loading at 50 kDa. B) Relative band density of MAO-A specific bands (mean ± SEM). No statistically significant differences were observed in protein abundance on Western blots for MAO-A (one-way ANOVA with Bonferroni's post-test; α=0.05; n = 3 blots from 3 different samples).

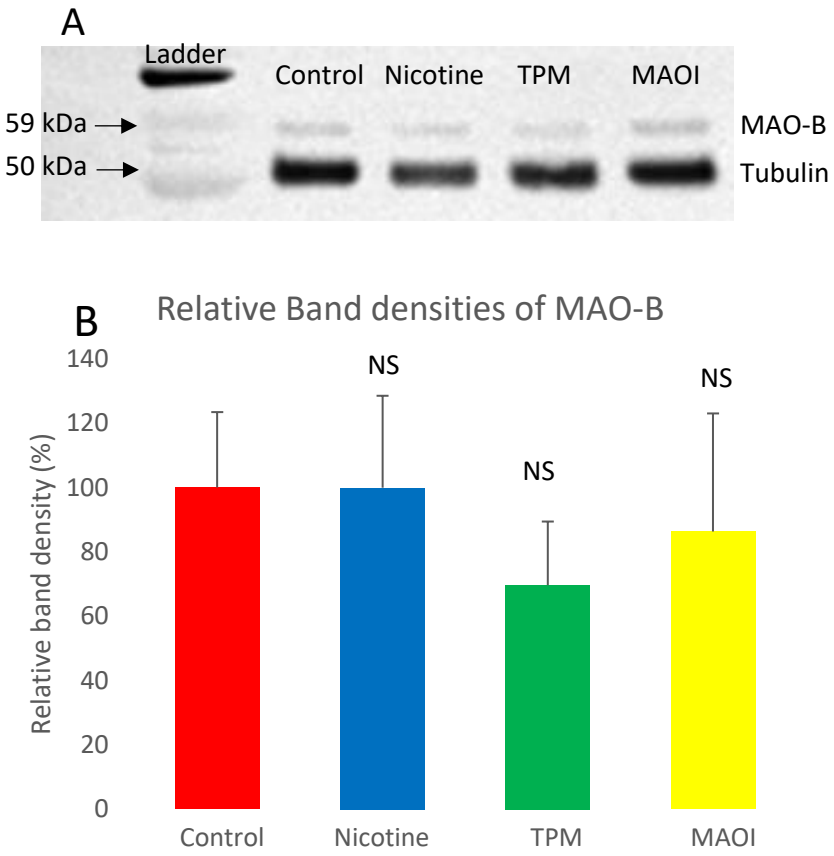

Figure 31: (A) Representative Western blot of MAO-B in differentiated SH-SY5Y cells after exposure treatments. Control, nicotine, TPM and MAOI exposure treatment for 3 days. MAO-B specific bands are at 59 kDa, and the β -tubulin loading at 50 kDa. (B) Relative band density of MAO-B specific bands (mean ± SEM). No statistically significant differences were observed in protein abundance on Western blots for MAO-B (one-way ANOVA with Bonferroni's post-test; α=0.05; n = 3 blots from 3 different samples)

6.4 Discussion

As 3 days of exposure period was concluded to be the optimum time period for exposure based on the results of MAO assays (Section 5.5), gene expression for each treatment was determined for 3 days of exposure only. Cells grown in a flask were divided into two parts; one for the isolation of proteins and the other for the isolation of RNA in order to control the variation between gene expression results and enzyme activity results that might arise from changes in culture condition. Some studies suggested that commonly used housekeeping genes may not be stable depending on the experimental conditions and tissue or cell type (De Kok et al., 2005; Schmittgen & Zakrajsek, 2000). Consideration was, therefore, required for the selection of appropriate housekeeping genes in this study. It was confirmed in a study that at least two housekeeping genes, *GAPDH* and *POLR2F,* were suitable to be used as reference genes in differentiated SH-SY5Y cell culture (Hoerndli, Toigo, Schild, Götz, & Day, 2004). Therefore, these two housekeeping genes were selected to be used as reference genes. The use of multiple housekeeping genes would also help prevent bias in the results and further validate the gene expression.

Since there was a significant decrease in MAO activity in SH-SY5Y cells after exposure treatments, it was expected to observe a change in protein and gene expression levels of MAO-A or MAO-B, which would provide a straightforward interpretation for the change in MAO activity observed. Changes in MAO protein or gene expression may suggest that TPM or MAOI are able to induce their MAO inhibitory effect by changing gene expression. Different studies have shown cigarette smoke and its components to induce changes in protein and gene expression levels (discussed in Section 2.5). Changes in mRNA expression may explain the reason behind long-term MAO inhibition seen in smokers. However, our results showed that different exposure treatments for 3 days did not cause any significant change in the mRNA level of *MAOA* and *MAOB*. This contradicts the result obtained by Lewis (2010), who observed two different types of TPM caused an increase in *MAOA* gene expression by about 23% and 35% when medium was not

refreshed. *MAOA* gene expression level was, however, seen to decrease and return to near original levels when exposed for 5 days without refreshing the medium. Lewis (2010) also observed that two different types of TPM caused an increase to about 380% and 360% of control when 5 days of refreshed regimen (media refreshed at third day) was used. Change in *MAOB* gene expression level was not significant for 1, 3 or 5 days when exposed to TPM without refreshing the medium while refreshing the medium caused a significant increase to about 270% and 260% of control. Our results, as well as observations from Lewis (2010), would suggest that TPM or its components could induce change in gene expression at specific time points. The active components responsible for causing such changes may be metabolised, causing gene expression to return to original levels. Observing changes in gene expression levels at various points would therefore be a good idea to have a better estimate of the cell's response to exposure treatments.

Similarly, Western blotting was carried out to investigate the change in the expression level of MAO-A and MAO-B protein levels after exposure treatments, which showed no significant changes. β-actin, β-tubulin and GAPDH are the most commonly used housekeeping proteins for Western blots (Li & Shen, 2013). The use of β-tubulin for a similar study (Lewis, 2010) encouraged its use as an internal control in this project. MAO-A and MAO-B protein expression levels were measured after exposing SH-SY5Y cells to TPM for a period of 5 days, and a similar result was obtained. However, a direct comparison cannot be made in this case, as 3 days of exposure was used in our study. The protein expression of MAO-A and MAO-B has not been well studied otherwise.

The divergence between gene and protein expression and enzyme activity data is not uncommon, and has been found in other studies (Glanemann et al., 2003; Velki, Meyer-Alert, Seiler, & Hollert, 2017; Xu, Han, & Huang, 2011). It has been suggested that mRNA levels would not necessarily reflect the

level of enzyme activity or level of proteins (Glanemann et al., 2003). Several factors, such as post-translational modification, protein degradation, change in enzyme microenvironment, binding to other molecules, or epigenetic regulation, may be responsible for the disparity in the result seen in this study (Walsh, 2006; Portela & Esteller, 2010)

There is a complex relationship between mRNA levels and enzyme activities, and this would prevent the prediction of enzymatic activity from the gene expression data. A study found the induction pattern of specific genes did not match with the enzyme activity of those genes and argued that the mRNA levels would explain the condition of the cell activity at any specific time while the enzyme activity might represent post-translational levels (Jin et al., 2010). In another study, inconsistent change in gene and protein expression of MAO-A and MAO-B under different conditions (refreshed and continuous medium) and time points were observed (Lewis, 2010). It has also been found that environmental changes can affect the stability of specific transcripts (Nilsson, Belasco, Cohen, & Von Gabain, 1984). The stability of any specific transcript could cause an initial change in the level of mRNA which would then remain unchanged. mRNA can be translated several times to form proteins which convert to active enzymes. This would create an imbalance in which there is an initial change in mRNA level that is lagged by the change in enzyme activity. The result obtained in our study suggests that the enzyme activity is directly inhibited and no signs of an indirect mechanism (such as reduction in the amount of MAO protein or gene expression) contributing to this, which are supported by the studies mentioned earlier in this section.

6.5 Conclusion

The study investigated the effect of exposure treatments on gene and protein expression of MAO-A and MAO-B in differentiated SH-SY5Y cells over a three-day period. No significant change in the mRNA level of *MAOA* and *MAOB* after exposure to the treatments for 3 days was observed. Change in protein expression of MAO-A and MAO-B was also not observed for the same time point. This suggests that a decrease in MAO activity observed earlier (Chapter 5) may have been caused directly as a result of the presence of inhibitors in the exposure treatment, rather than being caused by a change in protein or mRNA levels. However, periodic synthesis or degradation of protein and mRNA could also be possible and they could demonstrate altered expression levels at day 1, 5 or 7. Further investigation to determine the mechanism of MAO inhibition would provide a clearer picture of the impact of TPM and its components on MAO isoenzyme protein and mRNA expression level.

Chapter Seven: Effect of exposure treatments on global gene expression

7.1 Introduction

TPM and MAOIs have been shown to significantly inhibit the MAO activity in differentiated SH-SY5Y cells (Chapter 5). However, no effect was seen in the gene or protein expression of MAO-A and MAO-B (Chapter 6). This chapter details the investigation made to understand the effect of the exposure treatments at the genome-wide level. The differential gene expression results (Section 7.3.3) from this chapter can provide information about the expression of specific genes of interest and provide a general overview of changes in the entire set of genes. The analysis of differential gene expression data to understand the pathways that might be involved in causing reduced MAO activity, as seen in this study, has also been performed (Section 7.3.4). Understanding the functional properties of the genes that are differentially expressed at the different exposure treatments might help establish a link between the exposure treatments and the decreased MAO activity observed in this PhD project.

7.2 Methods

7.2.1 Sample preparation

As discussed and concluded from the results of the MAO assays (Sections 5.4 - 5.5), exposure for 3 days was selected for examining the impact of nicotine, TPM, and MOAIs on gene expression in differentiated SH-SY5Y cells. After exposure for 3 days as outlined in Section 6.2.1, half of the total RNA extracted was stored at -80˚C. This RNA sample was sent to Massey Genome Service (MGS), Palmerston North, for RNAseq analysis. The

concentration and quality of RNA were determined by MGS before RNA sequencing was performed.

7.2.2 Gene expression analysis

A range of software tools were used by Mauro Truglio, Bioinformatician, MGS to perform RNA sequence analysis to identify changes in gene expression, which are listed below:

- Custom Python and R scripts
- FastQC v.0.11.9
- MultiQC v.1.10.1
- BBduk v.38.94
- HISAT2 v.2.2.1
- StringTie v.2.1.7
- GFFcompare v.0.11.2
- DESeq2 v.3.13

Raw data were first checked for any leftover adapters and low-quality reads; reads containing adapters were clipped off, using the software BBduk (Jonkhout et al., 2021; Kechin, Boyarskikh, Kel, & Filipenko, 2017). Then, read quality was assessed for each sample using FastQC, and the results were collected by MultiQC (Andrews, 2010; Ewels, Magnusson, Lundin, & Käller, 2016). The reads that passed the quality filtering were used for downstream analysis.

Differential expression analyses to identify sets of genes differentially expressed between two or more data sets were performed using the HISAT2/String Tie pipeline shown in Figure 32. HISAT2 is a rapid alignment program used for mapping next-generation sequencing reads to the reference human genome (Pertea et al., 2016).

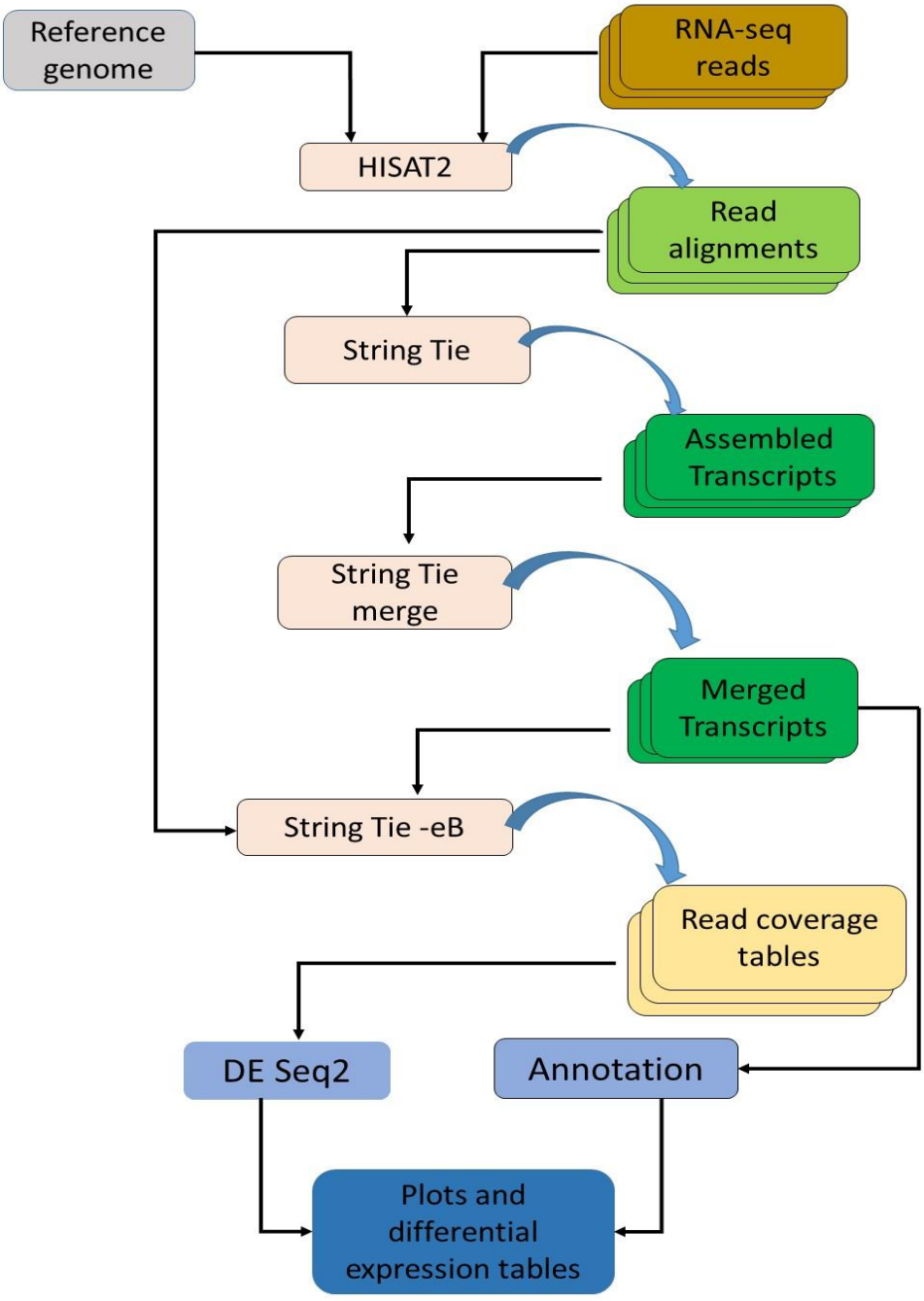

Figure 32: The HISAT2/StringTie pipeline used in RNAseq analysis (Pertea, Kim, Pertea, Leek, & Salzberg, 2016).

All reads were mapped using splice-aware mapper HISAT2 against the HG38 version of the reference human genome obtained from the NCBI website (Kim, Langmead, & Salzberg, 2015).

StringTie was used to assemble the reads into transcripts for each sample. The tool GFFcompare was used to assess the overall quality of the assembled transcripts by comparison to the HG38 reference (Pertea et al., 2016).

Raw count tables were generated by using the HISAT2 alignments and the reference transcriptome. These tables were produced at two different levels: transcript and gene. Since the aim of the study was to determine the differential gene expression after exposure to different treatments, only the gene table was taken into consideration.

An analysis of normalised counts' profiles was performed and plotted as a heatmap for all the treatments, principal component analysis (PCA) plots and PCA plot analysis were performed using the top 50 most varying genes.

DESeq2 was used to generate differential expression calls and statistics for the treatment comparisons based on the observed read counts for each gene. Filters (p-adj < 0.05; log2FoldChange > 2 or < -2) were applied to the results for the entire set of genes. Here,

log2FoldChange: Indicates how much the gene expression seems to have changed between the comparison and control groups. This value is reported on a logarithmic base 2 scale.

p-adj: Adjusted P-value for multiple testing for the gene or transcript.

The functional roles of the differentially expressed genes were then explored using an online tool called Database for Annotation, Visualisation, and Integrated Discovery (DAVID) to better understand the biological functions of the genes with differential expression. DAVID is an online bioinformatics tool that is helpful in systematically determining the functional significance of a list of genes using an integrated biological knowledgebase. Gene enrichment was determined using the gene ontology function and pathway analysis of the Kyoto Encyclopaedia of Genes and Genomes (KEGG) from the list of

differentially expressed genes for each treatment compared to the control. A cellular pathway analysis is helpful to visualise cellular pathways represented by differentially expressed genes and how genes of interest are related to each other, while gene ontology helps identify the biological processes and molecular functions that are perturbed by the treatment based on three domains: cellular component, molecular function and biological process (Huang, Sherman, & Lempicki, 2009a).

For the gene ontology GOTERM_BP_DIRECT, GOTERM_CC_DIRECT AND GOTERM_MF-DIRECT were selected under the function “Gene ontology”, and for pathway analyses, KEGG_PATHWAY under the function “Pathway” charts were selected (Huang, Sherman & Lempicki, 2009b).

The GeneMANIA online tool was also used to analyse differentially expressed gene lists as GeneMANIA is a flexible tool able to generate hypotheses about gene function and extend the list of genes listed as input with functionally similar genes identified using genomics and proteomics databases available (Warde-Farley et al., 2010). The list of differentially expressed genes was provided as input, and a GeneMania chart was obtained. The molecular function setting for gene ontology weighting was used with maximum resultant genes (n=20) and maximum resultant attribute (n=10). The analysis using the DAVID tool was done by Mauro Truglio and I performed the analysis using GeneMANIA tool as suggested by Mauro Truglio.

7.3 Results

7.3.1 Total RNA concentration and quality

Total RNA concentration and RNA quality score (equivalent to RNA Integrity Number or RIN) for the RNA samples were determined at Massey Genome Service and listed in Table 17. RNA concentration as well as RNA quality score was found to be acceptable (RIN ≥ 7.0) in all the samples, with the minimum RNA quality score of the samples being 7.6 and the maximum being

9.6. The quality scores of the 3rd replicate were slightly lower than the other two replicates.

Table 17: Concentration and quality score of the RNA sample of different exposure treatments.

Sample Name	Treatment group	Actual Concentration (ng/µL)	Volume (µL)	Total Amount (ng)	RNA Quality Score
S01	Ethanol Replicate 1	322	11	3542	9.6
S02	Nicotine Replicate 1	126	12	1512	9.5
S03	TPM Replicate 1	226	12	2712	9.6
S04	MAOI Replicate 1	196	12	2352	9.5
S05	Ethanol Replicate 2	318	12	3816	9.6
S06	Nicotine Replicate 2	394	11	4334	9.6
S07	TPM Replicate 2	194	12	2328	9.4
S08	MAOI Replicate 2	129	12	1548	9.4
S09	Ethanol Replicate 3	126	12	1512	7.9
S10	Nicotine Replicate 3	68	17	1156	9
S11	TPM Replicate 3	102	12	1224	8.7
S12	MAOI Replicate 3	128	11	1408	7.6

7.3.2 Data quality

The average mapping rate of 97.33% was found for the samples and the input reads, as well as the mapping rate per sample, are presented in Appendix, Table B.

The sensitivity and precision of the transcripts were found to be high (Table 18). High sensitivity suggests that almost all the StringTie transcripts matched known human HG38 transcripts, i.e., there were very few false negatives. The high precision values indicates that most of the StringTie transcripts were in the list of known transcripts, with very few false positives or de novo transcripts.

Table 18: Table showing the overall quality of Transcriptome assemblies.

	Sensitivity %	**Precision %**
Base level	100	88.3
Exon level	90.8	91.2
Intron level	100	94.4
Intron chain level	100	83.7
Transcript level	99.4	84.5
Locus level	99.2	95.1

Analysis of normalised counts' profile and the heatmap plot, PCA plot and PCA plot analysis for the top 50 most varying genes showed that samples seemed to be clustering more by replicate than by treatment which is unusual. This is usually a sign of stronger unknown effects between replicates, causing more variation between the replicates than between the different treatments.

7.3.3 Differential gene expression with different exposure treatments

The effect of different treatment exposures for 3 days on the gene expression was determined. Table 19 shows the total number of transcripts with differentially expressed genes in nicotine treatment versus control after the application of the two filters (p-adj < 0.05 and log2FoldChange > 2 or < -2). Ten genes showed differential expression with six genes having increased expression and four genes having decreased expression compared to the control. Similarly, Table 20 shows the total number of transcripts with differentially expressed genes for TPM treatment versus control and MAOI treatment versus control, respectively. TPM versus control had 17 genes with differential expression, where four genes were down-regulated, and 13 genes were up-regulated. Table 21 shows the list of 23 genes with differential expression associated with MAOI treatment. The MAOI versus control treatment comparison showed four genes were down-regulated, and 19

genes up-regulated. Tables 19, 20 and 21 also detail the putative functions of the differentially expressed genes from the 3 comparison groups obtained from the NCBI gene database. It was found that many genes with significant differential expression were yet to be annotated and had no putative functions assigned to them.

Table 19: List of genes with significant differential expression after treatment with nicotine compared to the control.

Gene ID	Gene name	Putative Function	log2Fold Change	P value	Apparent change
NOS1	nitric oxide synthase 1	synthesizes nitric oxide (a reactive free radical), acts as a biologic mediator in several processes, including neurotransmission, and antimicrobial and antitumoral activities.	-2.008	5.91E-09	Decrease
GATA4	GATA binding protein 4	encodes a member of the GATA family of zinc-finger transcription factors. thought to regulate genes involved in embryogenesis and myocardial differentiation and function.	-2.140	1.07E-08	
HOOK3	hook microtubule tethering protein 3	mediates binding to organelles.	-2.699	4.87E-06	
RP1-178F10.1	N/A	unknown	-2.484	5.11E-05	
LINC00342	Long intergenic non-protein coding RNA 342	Biomarker of Huntington's disease	2.350	8.80E-06	
DNAH12	dynein axonemal heavy chain 12	ATP binding activity; dynein intermediate chain binding activity; and dynein light intermediate chain binding activity.	2.743	3.40E-05	

ZNF658B	Zinc Finger Protein 658B	Predicted to enable DNA-binding transcription activator activity, RNA polymerase II-specific and RNA polymerase II cis-regulatory region sequence-specific DNA binding activity.	2.568	6.56E-05	Increase
LINGO1	leucine rich repeat and Ig domain containing 1	Predicted to enable epidermal growth factor receptor binding activity. Predicted to act upstream of or within generation of neurons and protein kinase B signalling.	2.060	9.53E-05	
RP11-848G14.2	N/A	unknown	2.183	0.000450	
RP11-10A14.3	N/A	unknown	2.281	0.000614	

Table 20: List of genes with significant differential expression after treatment with TPM compared to the control.

Gene ID	Gene name	Putative function	log2Fold Change	P value	Apparent change
ZSCAN20	zinc finger and SCAN domain containing 20	Predicted to enable DNA-binding transcription factor activity, RNA polymerase II-specific and RNA polymerase II cis-regulatory region sequence-specific DNA binding activity.	-2.759	1.38E-06	Decrease
PRH2	proline rich protein HaeIII subfamily 2	This gene encodes a member of the heterogeneous family of proline-rich salivary glycoproteins.	-6.431	2.52E-06	
RP11-566K11.5	unknown	unknown	-5.315	6.60E-05	
SYNGR4	synaptogyrin 4	encodes an integral membrane protein	-2.900	0.000279	
RP11-220I1.5	unknown	unknown	6.472	8.04E-06	
RP11-104F15.9	unknown	unknown	4.457	1.30E-05	
RP11-328C8.4	unknown	unknown	2.220	6.23E-05	

USP7	ubiquitin specific peptidase 7	The protein encoded by this gene belongs to the peptidase C19 family, which includes ubiquitinyl hydrolases. This protein deubiquitinates target proteins such as p53 (a tumour suppressor protein) and WASH (essential for endosomal protein recycling)	2.006452715	3.60E-09	Increase
RP11-805J14.5	unknown	unknown	2.117	0.000102	
CTD-2012J19.1	unknown	unknown	3.964	0.000183	
TENM4	teneurin Transmembrane Protein 4	The protein encoded by this gene plays a role in establishing proper neuronal connectivity during development.	2.142	0.000254	
TNFRSF10A	TNF receptor superfamily member 10a	The protein encoded by this gene is a member of the TNF-receptor superfamily and has roles in cell death signal and induces cell apoptosis.	2.448	0.000272	
ZNF34	zinc finger protein 34	Predicted to enable DNA-binding transcription factor activity, RNA polymerase II-specific and RNA	2.019	1.17E-07	

		polymerase II cis-regulatory region sequence-specific DNA binding activity.			
ALPK1	Alpha Kinase 1	Putative function	2.378	0.000294	
AC106869.2	unknown	Predicted to enable DNA-binding transcription factor activity, RNA polymerase II-specific and RNA polymerase II cis-regulatory region sequence-specific DNA binding activity.	2.001	0.000445	
AC007036.5	unknown	This gene encodes a member of the heterogeneous family of proline-rich salivary glycoproteins.	2.276	0.000448	
FOXR2	forkhead box R2	unknown	2.314	0.000522	

Table 21: List of genes with significant differential expression after treatment with cocktail of six candidate MAOIs compared to the control.

Gene ID	Gene name	Putative function	log2Fold Change	P value	Apparent change
ZNF727	zinc finger protein 727	predicted to enable DNA-binding transcription factor activity, RNA polymerase II-specific and RNA polymerase II cis-regulatory region sequence-specific DNA binding activity.	-3.881	0.0000548	Decrease
RP11-310E22.4	unknown	unknown	-2.439	0.000448	
CRYM	crystallin mu	encodes a taxon-specific crystallin protein that binds NADPH. The encoded protein binds thyroid hormone for possible regulatory or developmental roles.	-2.903	0.0000572	
SEMA3F	semaphorin 3F	encodes a member of the semaphorin III family of secreted signalling proteins that are involved in axon guidance during neuronal development.	-2.200	0.0000068	
RP11-805J14.5	unknown	unknown	2.517	0.0000098	

BVES	blood vessel epicardial substance	encodes a member of the POP family of proteins containing three putative transmembrane domains; may play an important role in development of cardiac and skeletal muscle	2.328	0.0000184	Increase
LL22NC03-2H8.4	unknown	unknown	2.212	0.0000224	
ZNF658B	Zinc Finger Protein 658B	Predicted to enable DNA-binding transcription factor activity, RNA polymerase II-specific and RNA polymerase II cis-regulatory region sequence-specific DNA binding activity.	3.828	2.09E-07	
CTD-2012J19.1	unknown	unknown	4.241	0.0000853	
ZNF322P1	Zinc Finger Protein 322 Pseudogene 1,	unknown	4.041	0.0000977	
AC093627.9	unknown	unknown	2.251	0.000106	
SPECC1L-ADORA2A	unknown	unknown	3.257	0.00012	
SARDH	sarcosine dehydrogenase	encodes an enzyme localised to the mitochondrial matrix which catalyses the oxidative demethylation of sarcosine	2.159	0.000144	

DNMBP	dynamin binding protein	encodes a protein belonging to the guanine nucleotide exchange factor family, and which regulates the configuration of cell junctions, links dynamin to actin regulatory proteins.	2.198	0.000147	
DNAH12	dynein axonemal heavy chain 12	Predicted to enable several functions, including ATP binding activity; dynein intermediate chain binding activity; and dynein light intermediate chain binding activity	2.236	0.000233	
DPP8	dipeptidyl peptidase 8	encodes a member of the peptidase S9B family, a small family of dipeptidyl peptidases that are able to cleave peptide substrates at a prolyl bond; this protein may play a role in T-cell activation and immune function.	2.048	1.23E-11	
AGO3	argonaute RISC catalytic component 3	encodes a member of the Argonaute family of proteins which play a role in RNA interference. The encoded protein may play a role in short-interfering-RNA-mediated gene silencing.	2.269	0.000461	

RP11-411B10.4	unknown	unknown	2.927	0.000489	
RP1-100J12.1	unknown	unknown	2.754	0.000512	
CR848007.2	unknown	unknown	3.674	0.000624	
RP11-432B6.3	unknown	unknown	2.656	0.000846	
CTC-260E6.2	unknown	unknown	2.045	0.00101	
COX6CP13	unknown	unknown	3.255	0.00106	

The genes with differential expression in the three comparison groups are presented in a 3-way Venn diagram in Figure 33. Gene ID: *DNAH12* (Dynein Axonemal Heavy chain 12) and *ZNF658B* (Zinc Finger Protein 658 B) are common for nicotine and MAOI treatments, while gene ID: *CTD-2012J19.1* and *RP11-80514.5* for TPM and MAOI treatments. The common genes identified in TPM versus Control and MAOI versus Control comparisons are yet to be annotated and do not have any functions assigned to them. There were no genes that were differentially expressed for Nicotine versus Control and TPM versus Control or for all three comparison groups.

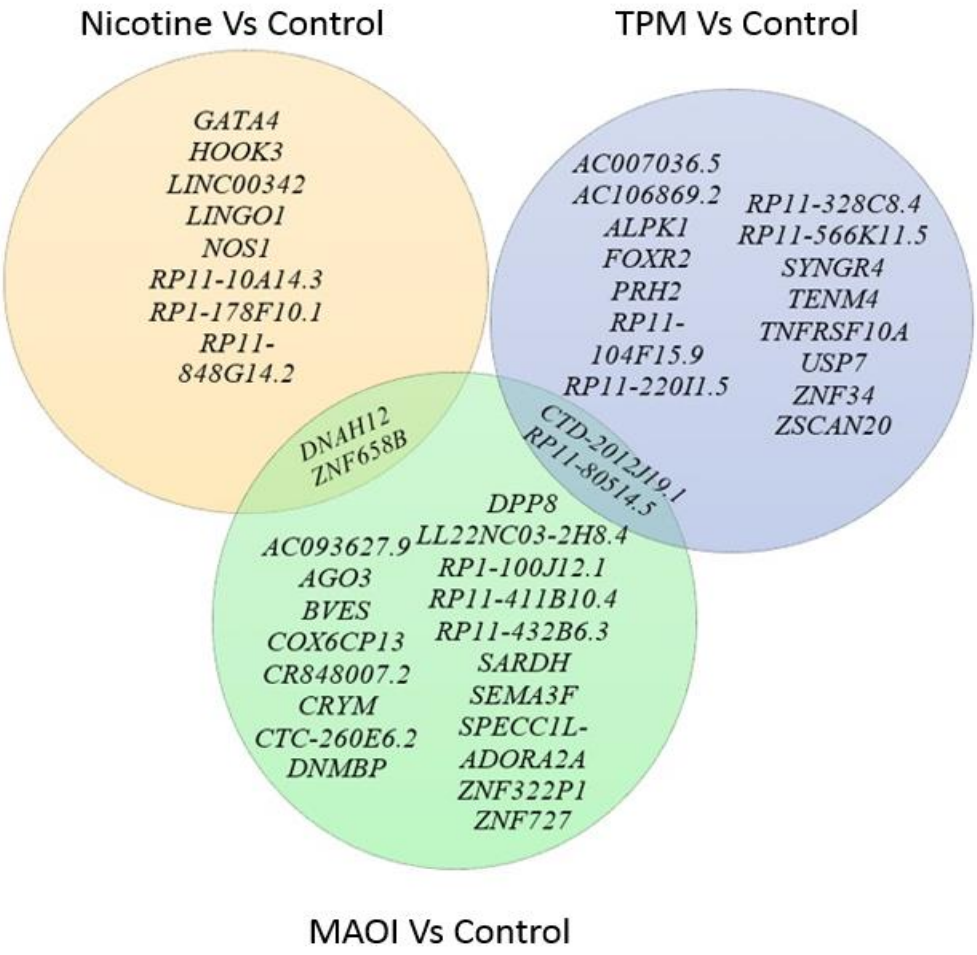

Figure 33: A 3-way Venn diagram showing differentially expressed genes in different comparison groups.

Box plots of some representative genes with significant changes in different exposure treatment groups compared to control are shown in Figure A-C, Appendix.

A comparison of the fold change in expression of *MAOA* and *MAOB* genes obtained using RNAseq and qPCR, is presented in Figure 34. There was no statistically significant change ($p<0.05$) in *MAOA* and *MAOB* gene expression level results in both of these methods, as expected, since the same RNA sample was used for both methods.

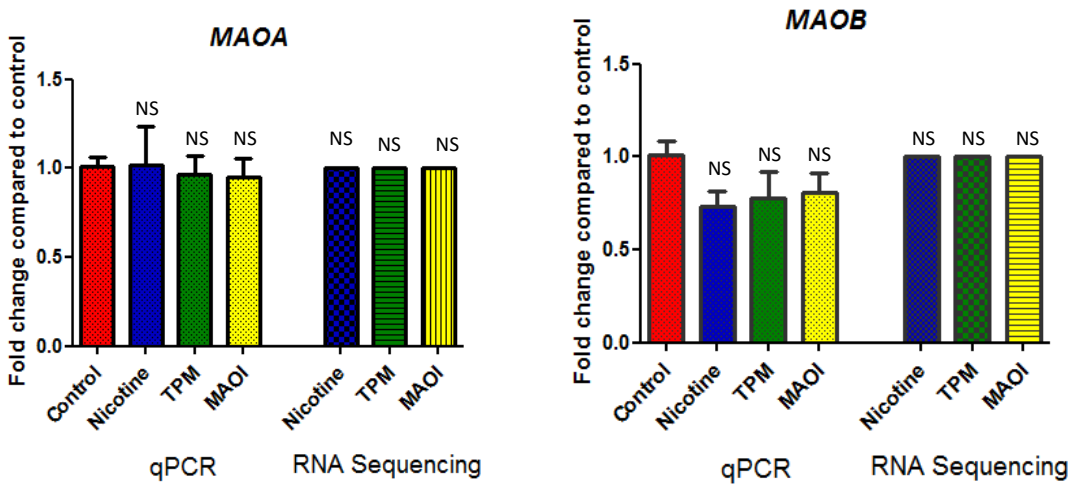

Figure 34: Comparison of result of fold change in MAO expression when SH-SY5Y cells were exposed to Nicotine, TPM and MAOI obtained from qPCR and RNAseq.

7.3.4 Gene ontology and pathway analysis using DAVID

Functional annotation was performed on the list of differentially expressed genes in each of the three comparison groups using DAVID software. Functional annotations obtained for the list of genes from the Nicotine versus Control treatments are listed in Table 22. Pathway analysis revealed the differentially expressed genes from the Nicotine versus Control comparison group were particularly enriched in pathways for amyotrophic lateral sclerosis ($p=0.045$), neurodegeneration-multiple diseases ($p=0.058$) and microtubule ($p=0.062$) as an enriched cellular component. No other gene ontology function

or KEGG pathways were found to be significant for the list of genes in any of the remaining two treatments compared to the control.

Table 22: Summary of GO categories and pathway analysis. These categories were identified by the DAVID tool as affected (in the p-value range of <0.10-0.01) when the list of differentially expressed genes from the nicotine treatment group compared to the control was used as input.

Category	Term	P-value
KEGG PATHWAY	Amyotrophic lateral Sclerosis	0.045
KEGG PATHWAY	Pathways of Neurodegeneration - multiple diseases	0.058
GOTERM_CC_DIRECT	Microtubule	0.062

The GeneMANIA online tool was used to get more information about functionally related gene datasets, which included co-expression, co-localisation, genetic interactions, pathways, physical interactions, predicted networks, and shared protein domains in humans. Figure 35 consists of 5 of 10 differentially expressed genes in the Nicotine versus Control group and 20 further genes in the derived gene network generated by GeneMANIA. Similarly, Figure 36 consists of 9 of 17 differentially expressed genes in the TPM versus Control group and 20 further genes in the derived gene network from GeneMania. Figure 37 consists of 10 of 23 differentially expressed genes in the MAOI versus Control, and 20 further genes in the derived gene network from GeneMania. The detailed study of these genes were beyond the scope of this study. However, the genes identified from GeneMANIA tool can be used as a starting point for future research to get new insights on the effects of the exposure treatment on expression of different genes and potential role those genes can play in the underlying biological processes.

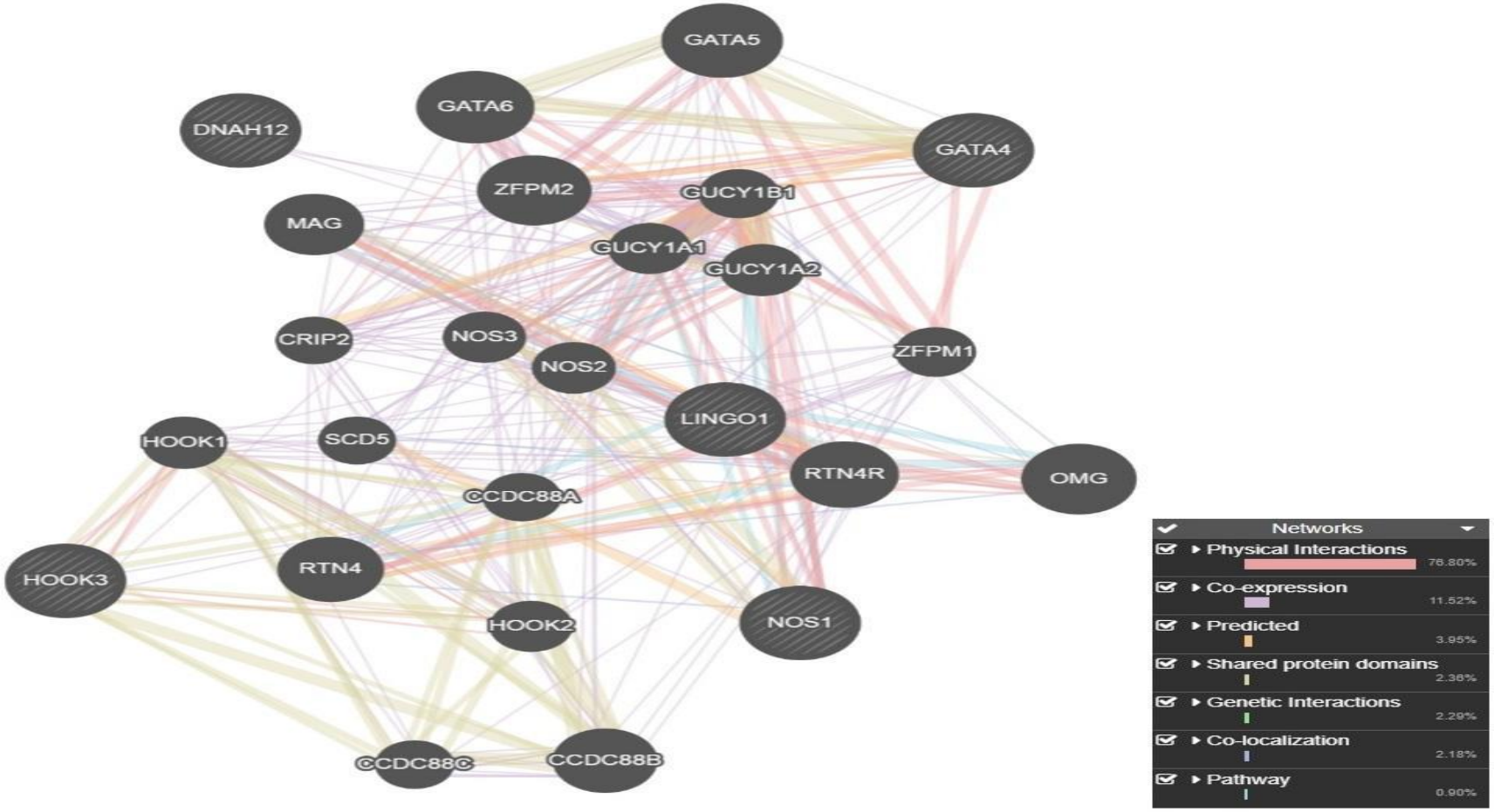

Figure 35: GeneMANIA network built for differentially expressed genes in Nicotine versus Control. The striped circles are the genes submitted to the system; the solid-grey circles are genes that work as intermediates between them. The links are coloured according to the legend on the right; each link represents a publication about that connection.

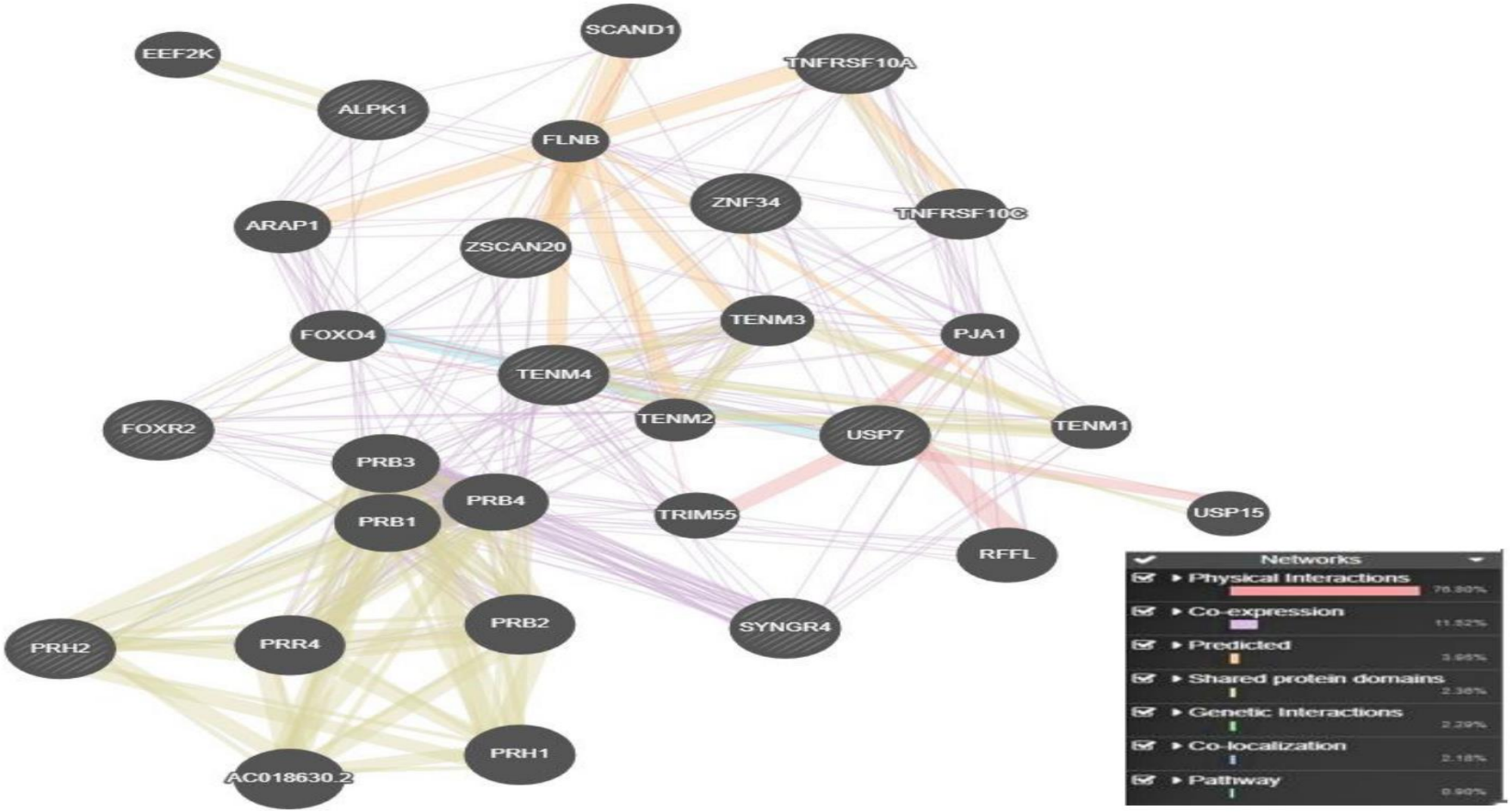

Figure 36: GeneMANIA network built for differentially expressed genes in TPM versus Control. The striped circles are the genes submitted to the system; the solid-grey circles are genes that work as intermediates between them. The links are coloured according to the legend on the right; each link represents a publication about that connection.

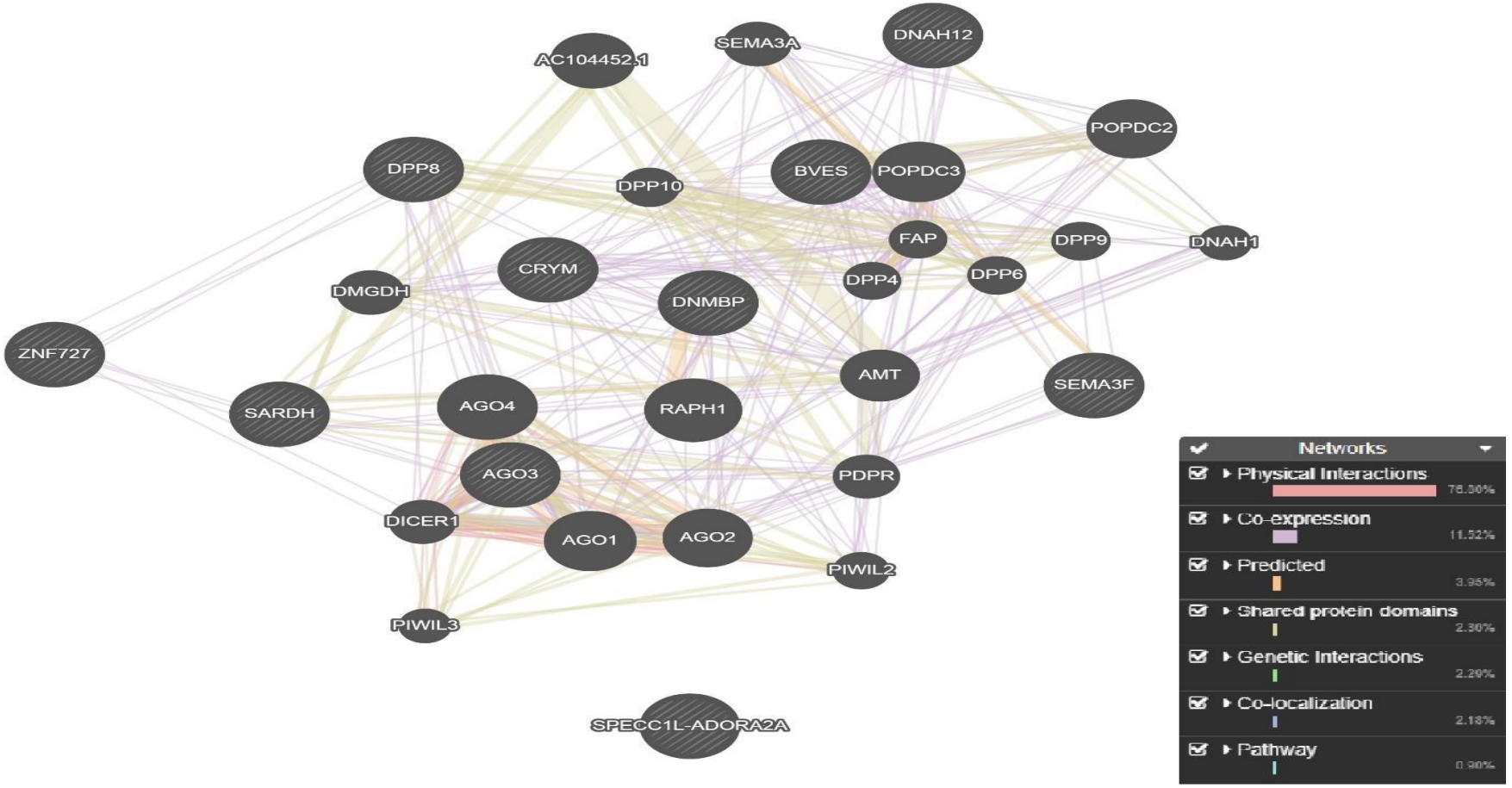

Figure 37: GeneMANIA network built for differentially expressed genes in MAOI versus Control. The striped circles are the genes submitted to the system; the solid-grey circles are genes that work as intermediates between them. The links are coloured according to the legend on the right; each link represents a publication about that connection.

7.4 Discussion

RNAseq is a powerful technology that uses high-throughput sequencing methods to provide a picture of the transcriptome in biological samples after exposure to different experimental conditions (Mackenzie, 2018). RNAseq was performed in order to get further information on the effect of different treatments on the differential expression of genes and understand the biological meaning behind the observed effects. As mentioned in the method section of this chapter, RNAseq was performed only on the samples obtained from SH-SY5Y exposed to different treatment groups for 3 days, as this time period was chosen as the optimum time period of exposure.

Results from RNAseq analysis and qPCR showed that there was no notable change in gene expression of *MAOA* and *MAOB* genes post-exposure to nicotine, TPM or MAOI treatments when compared with the control. The RNAseq analysis was helpful in providing important information about the effects of the different treatments on differential gene expression. Nicotine treatment has been shown to cause downregulation of genes such as *NOS1, GATA4* in this study. These genes have been found in previous studies to be related to nicotine exposure (Schilling et al., 1994; Malinovschi et al., 2006; Jiang et al., 2017). It has been found in a study that smokers have a reduced level of exhaled nitric oxide, but the mechanism of this reduction is not clear (Malinovschi et al., 2006). Nitric oxide synthase 1 synthesises nitric oxide from L-arginine (Schilling et al., 1994). The reduction of *NOS1* mRNA levels induced by nicotine exposure, as seen in our study, can be thought of as one of the possible mechanisms for the reduction in nitric oxide synthase enzyme, which in turn causes a reduced level of exhaled nitric oxide in smokers. Similarly, nicotine treatment also caused significant downregulation of the *GATA4* gene, which encodes a member of the GATA family of zinc-finger transcription factors involved in the regulation of different genes having roles in myocardial differentiation and embryogenesis (Jiang et al., 2017).

A study performed to observe the change in gene expression induced by 1 mM nicotine exposed to SH-SY5Y cells for 24 hours showed 163 genes with altered expression (Dunckley & Lukas, 2006). None of the genes with altered expression in our study matched with that of Dunckley and Lucas' study. A reason for the discrepancy and much lower number of differential gene expressions observed in our study could be the lower concentration of nicotine (0.2 µM) used in this study, together with the variation between replicates.

In the current study, TPM exposure was shown to cause change in expression of genes such as *USP7, ZNF34, ALPK1, TNEM4, FOXR2,* which have been found to have a role in the pathophysiology of different diseases and conditions. Research performed by Zeng et al. (2022) agrees with our result, where cigarette smoke was observed to cause increased gene expression of *USP7*. They used a mouse model to show USP7/p300-dependent pathway was responsible for inhibited cell activity resulting in cell arrest and depletion of endothelial progenitor cells that might lead to COPD. Son et al. (2022) observed that *ZNF34* was among the top 10 genes out of the 140 genes associated with asthma exacerbation in smokers but not in non-smokers. This suggests that smoking can have an effect on *ZNF34* expression of smokers, which might have a role in asthma exacerbation. TPM has also been shown to increase gene expression of *TENM4*, a candidate gene for schizophrenia and a novel cancer stem cell molecule. (Ruiu et al., 2021; Yi et al., 2021). *FOXR2* is another notable gene having increased expression with TPM treatment. This gene has been demonstrated to have high expression in several types of cancer, such as breast, liver and lung cancer and tumour samples of patients. It is well-known that smoking causes several types of cancer, and increased expression of *FOXR2* by TPM may have an important role in the promotion of cancer cell proliferation.

Similarly, MAOI exposure was shown to cause differential gene expression of genes including *BVES*, *SARDH, DNMBP,* which have previously been studied and links found to smoking, addiction and other functions/pathways related to

smoking. We observed that MAOI treatment caused a significant increase in the expression of the *BVES* gene. The *BVES* gene is included in the list of genes that are likely to encode for cell adhesion molecules (CAM). The variation of CAM gene expression is believed to cause effects on different circuits that are specific to addiction and drug reward (Vallender et al., 2017). MAOIs present in cigarette smoke may impart some of the addictiveness of smoking by increasing the expression of *BVES*. Overall, research suggests that smoking poses a significantly increased risk of Alzheimer's disease, but some research has linked cigarette smoking with decreased risk of Alzheimer's disease (Brenner et al., 1993; Durazzo, Mattsson, Weiner, & Initiative, 2014; Riggs, 1996). mRNA of the *DNMBP* has been found to be lower in Alzheimer's brains and increasing the expression of *DNMBP* may help in preserving long-term memory formation (Casoli et al., 2012). The upregulation of *DNMBP* post-exposure to MAOI in our study may possibly be involved in this partly protective feature of cigarette smoking on Alzheimer's Disease. However, enough research on this has not been done and is required to better understand the reason behind the decreased risk observed in some research.

SARDH is another interesting gene, which was found to be upregulated after MAOI exposure in our study. This gene encodes an enzyme sarcosine dehydrogenase, which is responsible for catalysing the oxidative demethylation of sarcosine (NCBI gene database). Sarcosine dehydrogenase, which is found in the soluble portion or the matrix space of mitochondria, is covalently bound to flavin adenine dinucleotide (FAD) along with succinic dehydrogenase, which is a mitochondrial inner membrane enzyme and MAO, which is located in the outer membrane (Dombrowski & Lambooy, 1981). The increased gene expression of *SARDH* may influence the regulation of MAO inhibition due to TPM or MAOI, as both SARDH and MAO have covalent bonding to FAD in common. Further study is required to establish such a relationship and understand the effect it might have on the regulation of MAO inhibition. Increased gene expression of *DPP8* was observed with MAOI treatment. This gene has been found to have increased expression in the NA

of rhesus macaques following long-term cocaine self-administration (Vallender et al., 2017) and a potential target of substances of abuse.

Another gene, *Sema3F*, had decreased expression following MAOI treatment. *Sema3F*, along with other genes related to the semaphorin pathway, has been found to have altered expression in mice exposed to morphine or heroin or in post-mortem brains of patients with chronic alcohol or cocaine use, suggesting its role in addiction (Yuferov et al., 2018).

The pathway enrichment analysis using DAVID revealed differentially expressed genes in the nicotine treatment group compared to control were enriched for amyotrophic lateral sclerosis (ALS) pathway genes. ALS is a neurodegenerative disorder marked by the degeneration of motor neurons (Lin et al., 2020). Cigarette smoking has been found to be associated with ~ 70 % increased risk of ALS in a case study (Wang et al., 2011). *DNAH12* and *NOS1* were found to be related genes, and these genes could be potential targets when studying ALS.

Significant gene ontology functions and pathways could not be generated from the list of differentially expressed genes in the treatment groups compared to the control despite finding quite a few genes with several fold increase/decrease in expression. As samples were seen to be clustering more by replicates than by treatment groups during the analysis of normalised count profiles, this could have prevented the production of a significant gene ontology and pathway analysis result. Variations in sample preparation and culture conditions could be the reason behind this. Efforts were made to have identical cell culture conditions. However, experiments for the first two replicates were performed at one time, while the third replicate was performed later due to space constraints in the incubator. Also, during RNA extraction, cell culture flasks remained at room temperature for some time as the process of RNA extraction was carried out for other samples. These factors, apart

from natural variation in biological samples, could have played a role in replicate-to-replicate variation. Another factor could be several genes with differential expression not yet being annotated or biological functions assigned. However, we were able to discover the differential expression of several genes involved in a wide range of functions and pathways as a result of exposure to nicotine, TPM and MAOI. No appropriate link for several of the differentially expressed genes with smoking or monoamine oxidase inhibition could be found in literature searches. This implies that these treatments have complex biological effects on SH-SY5Y cells, which requires further research. The GeneMANIA result also provides information on several other genes functionally related to differentially expressed genes, which suggests new hypotheses to test in this research. An example of a functionally related gene in the MAOI-versus-control group is dipeptidyl peptidase (*DPP4).* A study found increased gene expression of *DPP4*, *MAOB* and *MAOA* in rat striatum treated with DPP4 inhibitors (Zubkov et al., 2018). DPP4 inhibitors are widely used in the treatment of diabetes (Kumari and Deshmukh, 2022). They also reported DPP4 inhibition improved neuronal degeneration and motor functions and are potential therapeutic targets for PD.

7.5 Conclusion

The study uncovered a few important and novel genes with differential expression as a result of exposure treatments. TPM caused altered expression of genes including *USP7, ZNF34, ALPK1, TNEM4* and *FOXR2*. These genes have been found to have a role in the pathophysiology of different diseases and conditions closely linked to smoking in earlier studies. For example, *FOXR2,* having increased expression with TPM exposure, has been found to have high expression in different types of cancer. Similarly, MAOI exposure was shown to cause differential expression of genes, including *BVES, SARDH, DNMBP*, and *DPP8*. These genes have been closely linked to smoking, addiction, and pathways related to addiction as well as drug reward. Notably, the increased gene expression of *SARDH* due to MAOI exposure may have a role in the regulation of MAO inhibition as both

SARDH and MAO have covalent bonding in common. It was not possible to provide information on gene ontology or pathways that could be involved with differentially expressed genes after exposure treatments. More research is required to verify and substantiate the findings of this study, which can be a topic for future research.

Chapter Eight: Overall Summary and Future Directions

8.1 Summary of the PhD study:

The overall aim of this PhD project was to evaluate the effect of TPM and six candidate MAOIs, recently identified by the Tobacco Research Group, Wellington, on MAO activity and protein and gene expression of MAO using SH-SY5Y cells as the model system to examine this. During the project, differentiation of SH-SY5Y cells was achieved using RA. The expression of neuronal properties and nicotinic acetylcholine receptors, which are the binding sites for nicotine, make SH-SY5Y cells a suitable phenotype for this specific PhD study. Smoking has been shown to inhibit both isoforms of MAO. MAO inhibition is thought to play a role in smoking addiction by preventing the breakdown of neurotransmitters and therefore prolonging as well as enhancing the dopamine reward generated by nicotine (Hogg, 2016). However, studies have failed to completely ascertain cigarette smoke components with MAO inhibitory properties comparable to the MAO inhibitory properties exhibited by cigarette smoke. This is where this PhD project is important and holds significance.

Data generated during this project showed that the six candidate MAOIs could inhibit MAO activity in differentiated SH-SY5Y cells in a comparable fashion to TPM (Chapter 5). The novel candidate MAOIs can therefore be claimed to be among the major components behind the MAO-inhibitory properties of cigarette smoke. Differentiated SH-SY5Y cells were exposed to treatments for different time periods (Chapter 4) to compare the MAO inhibitory effect of nicotine, TPM and MAOIs. TPM and MOAIs both inhibited MAO when incubated for a period of 1 or 3 days. The MAO inhibition seen with MAOI treatment was similar to that when cells were treated with TPM. No significant MAO inhibition was seen in differentiated SH-SY5Y cells exposed to nicotine.

Also, nicotine as well as TPM and the cocktail of MAOIs, failed to impart statistically significant MAO inhibition on the SH-SY5Y cells when treated for 5 or 7 days. Large inter-sample variation was observed in the MAO activity results, which could be a reason for the statistically insignificant MAO inhibitory effect by TPM and MAOIs on days 5 and 7. Another possible reason could be the compensatory mechanism of cells to make more MAO proteins in order to counter the MAO inhibition by TPM and MAOI (Lewis, 2010). It was observed that exposure to MAOIs and TPM for a period of 3 days elicited maximum MAO inhibition in differentiated SH-SY5Y cells. Therefore, exposure treatment for 3 days was chosen to study of the effect of exposure treatment on MAO gene and protein expression (Chapter 6), and global gene expression (Chapter 7).

It was also observed from the toxicity studies (Chapter 5) that the exposure treatments did not have any effect on SH-SY5Y cell viability. This would confirm that exposure treatments were devoid of overt toxicity (Chapter 5).

In order to determine the mechanisms of MAO inhibition, MAO isoenzyme gene and protein expression were determined using qPCR and Western blots, respectively. There was no change in MAO-A or MAO-B protein and gene expression in SH-SY5Y cells treated with different exposure treatments for 3 days. Also, no significant change in MAO protein expression was seen when SH-SY5Y cells were treated with TPM for 3 days. This suggests that either the synthesis and degradation of mRNA and protein could be periodic, which may depend on upstream DNA motifs and transcription factors or the MAO inhibition seen (Chapter 5) was due to the presence of direct inhibitors rather than due to any indirect mechanism. Further experiments to determine MAO isoenzyme protein and gene expression at different time points will help in understanding if there is periodic gene or protein change induced by exposure treatments. This would enhance our understanding of how the exposure treatments impact the gene and protein expression of the MAO isoenzyme.

RNAseq analysis was also able to provide information about several genes such as *USP7, ZNF34, ALPK1, TNEM4, FOXR2, BVES, SARDH, DNMBP, and DPP8,* which were differentially expressed after exposure treatments (Chapter 7). These genes have been previously studied and found closely related to nicotine, TPM or MAOIs, as well as different diseases and conditions associated with cigarette smoking and addiction. Not much information could be revealed regarding gene ontology or pathway analysis from the list of differentially expressed genes in the exposure treatments. This could be due to the presence of large variations between samples, as mentioned earlier. The presence of several genes in the list, which are yet to be annotated and biological functions assigned, suggests the lack of research in this field and provides a promising direction for future research.

8.2 Limitations

This PhD project has been successful in observing the MAO inhibitory activity of the candidate MAOIs identified by the Tobacco Research Group, Wellington, in SH-SY5Y cells. The candidate MAOIs can be claimed as key elements behind the MAO inhibitory property of cigarette smoke. Also, the project has shed light on some important genes that possibly have roles with addiction and pathophysiology of different diseases associated with smoking. However, there are limitations in this study. Firstly, it was seen that results from replicates in different experiments had large variations. This could possibly be attributed to a relatively small number of replicates employed in these experiments. In the RNAseq experiment particularly, the replicates displayed large variation. This might have prevented determining further genes with differential expression as a result of exposure treatments and prevented determining altered pathway expression when tools like DAVID and GeneMANIA were used. Secondly, MAO-A and MAO-B activity was determined from total MAO activity using clorgyline to inhibit MAO-A. It was observed that total MAO activity was comprised mostly of MAO-B activity. However, confirmation of results was not done by using a selective MAO-B inhibitor. Thirdly, it was observed that MAOIs and TPM decreased total MAO

activity. This could be due to the direct inhibition of enzymes by the inhibitors. However, there could also be other indirect mechanisms, such as alteration of receptor expression or modulation of other enzymes like catechol-o-methyltransferase, which were not studied in this PhD project (Tatsumi, Groshan, Blakley, & Richelson, 1997; Youdim, Edmondson, & Tipton, 2006). Fourthly, 3 days was chosen as the optimum time period of exposure to determine the effects of exposure treatment on gene and protein expression. This prevented observing the trend of MAO-A and MAO-B protein and gene expression level change from day 1 to day 7. So, a comprehensive understanding of the impact and time course of exposure treatments on protein and gene expression could not be achieved.

8.3 Future experiments

The limitations and gaps in the finding of this PhD project can be addressed, and knowledge be extended by following up with additional experiments in future, which are discussed below:

8.3.1 Examine the MAO inhibition from TPM and MAOIs exposure observed in this study using other cell culture models and animal studies

The MAO inhibitory properties shown by TPM and the cocktail of MAOIs in this study can be investigated in other cell culture models. As discussed earlier (Section 6.4), different species and different tissues or cell types may have different levels and isoforms of MAO. MAO activity has been studied previously in different cell models, including Bcl-2, U118MG, MH1C1, PC12, HEK293 etc (Goldstein et al., 2016; Inaba-Hasegawa, Shamoto-Nagai, Maruyama, & Naoi, 2017; Santillo, Liu, Ferguson, Vohra, & Wiesenfeld, 2014). The use of different cell culture models may help understand the level and nature of MAO inhibition and their interaction in different cell types. This will provide an idea of whether the MAO inhibition from the exposure treatments observed in our study using the SH-SY5Y cell system is

comparable with the result obtained in other cell systems, and determine the extent to which the findings in this study are generalisable. One consideration that should be adapted is the use of a greater number of biological replicates to increase the statistical power of the experiments performed and amplify the robustness and accuracy of the study.

Most studies relating to MAO functionality are performed in neural cells. However, MAO proteins and mRNA are abundant in most tissues of the human body, such as the stomach, liver, kidney and heart (Ramonet et al., 2003). The inhibition of MAO-A and MAO-B has been shown to cause significant changes in cytokine and chemokine expression in a number of cell cultures and disease models, such as periodontal disease, Parkinson's disease, depression, smoke-induced lung injury. Cytokines and chemokines, which are expressed by local as well as recruited immune cells, regulate acute and chronic inflammation (Ostadkarampour & Putnins, 2021). The study of MAO inhibition with candidate MAOIs and TPM in these cell culture and disease models can have wider implications in understanding the possible therapeutic potential of these candidate MAOIs in these diseases and conditions. Such studies may also help develop candidate MAOIs as therapeutic agents to treat different diseases and conditions involving monoamine oxidase.

Apart from different cell culture types, MAO activity assays performed in SH-SY5Y cells in this study can be expanded to animal models. The use of self-administration animal models have been shown to better predict human drug abuse as the reinforcing ability of the drug can be manifested well in animal models compared to cell culture systems (Panlilio & Goldberg, 2007). Expanding the result obtained in animal self-administration can help understand the ability of our candidate MAOIs to inhibit MAO and observe its effect on addiction. It can also be helpful towards the development of improved therapeutic smoking cessation alternatives to currently available ones.

8.3.2 Determine MAO protein and gene expression levels at different time points

In this study, MAO-A and MOA-B protein and gene expression levels were determined only for 3 days of exposure as it was concluded to be the optimum time period for exposure based on the results of MAO assays (Section 5.5). Determination of MAO-A and MAO-B protein and gene levels at different time points (Day 1, 5 and 7) could help understand if periodic changes in protein and gene levels are present. The increase observed on day 3 might be due to a compensatory mechanism of the cells to counteract the inhibition of MAO enzyme, causing a trend of increase in *MAO-A* gene expression level until day 3. There could be a metabolism of these active compounds causing a decrease in the level observed on Day 7. A future study including several time points to measure protein and gene expression levels can help understand the trend of MAO protein and gene expression level changes and provide comprehensive information on the impact of TPM and candidate MAOIs on MAO isoenzyme gene and protein expression.

8.3.3 Elucidate the Mechanisms of MAO inhibition by treating cell lysates with MAOIs, studying epigenetic changes, and structure-activity relationship of candidate MAOIs

It was observed in this study that TPM and MAOIs inhibited MAO activity in differentiated SH-SY5Y cells. Incubating differentiated SH-SY5Y cell lysates directly with TPM and a cocktail of MAOIs at concentrations used in this PhD study and then determining MAO activity can help confirm if the MAOIs can directly inhibit MAO activity. Further research on the epigenetic effects of TPM and MAOI can also be performed. It was seen that MAO was unable to significantly change the expression levels of MAO-A and MAO-B gene and protein levels. However, it is possible that MAO-A or MAO-B gene and protein levels could have changed at a specific time point not monitored in this study, (also discussed in Section 5.4). It has also been concluded from research that

the increase in MAO synthesis seen in smokers is a result of a compensatory mechanism against the decrease in MAO activity (Launay et al., 2009). They also found a reduction in methylation of the *MAOB* promoter as a result of smoking, which resulted in more active transcription of the gene and a greater MAO-B protein concentration. It is also possible that MAOIs may increase nucleic acid demethylase activity resulting in the generation of aldehydes (Lewis, Miller, & Lea, 2007). The aldehydes, may in turn act on methylene tetrahydrofolate to form β-carbolines from 5-HT, which inhibits MAO activity even more (Grimsby, Chen, Wang, Lan, & Shih, 1991; Vikenes, Farstad, & Nordrehaug, 1999). Epigenetic alteration can be assessed by the study of three major factors: methylation of addiction-related genes, study of posttranslational modification of histones and change in non-coding RNA sequences. These changes can regulate gene transcription, and activation of several enzymes (Zong, Liu, Li, Ouyang, & Chen, 2019).

Similarly, the effect of exposure treatments on the function and the expression level of transporters such as monoamine transporters, dopamine transporters, as well as the level of dopamine in brain regions associated with addiction and reinforcement, such as NA, VTA can be evaluated. The exposure treatment, especially TPM and MAOIs, may synergistically act with nicotine to reinforce addiction by maintaining increased dopamine concentrations in these regions. This has been observed in a study involving the treatment of rats with D-amphetamine, nicotine or a combination of nicotine and MAO-B inhibitors (Villégier, Blanc, Glowinski, & Tassin, 2003). Also, structural studies of candidate MAOIs can be performed to understand how these inhibitors may interact with MAO to determine the location of binding and how these may affect the enzyme's potency, activity or expression levels. This information can have important implications in the design and use of these MAOIs for smoking cessation as well as the treatment of diseases and conditions related to MAO, such as Parkinson's disease and depression.

8.3.4 Study the effect of candidate MAOIs when exposed to cell culture system in combination with nicotine

Different compounds can have synergistic or antagonistic effects when used together. MAO inhibitory activity of different combinations of candidate MAOIs and nicotine, such as PUFAs (linoleic acid, linolenic acid) and nicotine, catechols (quinol, hydroquinone, 4-methylcatechol, 4-ethylcatechol) and nicotine, PUFAs, catechols and nicotine can be performed to understand the effect of candidate MAOIs when used in combination with nicotine. It has been suggested in a previous study (Guillem et al., 2005) that MAO inhibitory activity of MAOIs in cigarette smoke may combine with nicotine to add to the reinforcing properties of tobacco. They performed a behavioural study using a rodent model and found that co-administration of two MAOIs, tranylcypromine hydrochloride and phenelzine sulphate, with nicotine greatly increased the intensity and persistence of addiction to nicotine. Hogg (2016) has also suggested that additive or synergistic effects of MAOIs of different tobacco smoke components may be responsible for MAO inhibition in smokers. Other known MAOIs, such as harman and norharman can also be used to understand if they can show any synergistic effect.

8.3.5 Confirmation of result obtained in MAO-A and MAO-B activity from total MAO activity using a selective MAO-B inhibitor

The MAO-B activity was determined in this project using clorgyline to inhibit all of the MAO-A activity. Clorgyline is a selective MAO-A inhibitor that has been shown to inhibit essentially all the MAO-A present. The result obtained here can be compared or confirmed using a selective MAO-B inhibitor to determine MAO-A activity from the total MAO activity. Similarly, the selectivity of these inhibitors for MAO-A or MAO-B can be determined, and a comparison of the change in levels of MAO-A and MAO-B activity induced by MAOI exposure treatment on SH-SY5Y cells can be performed.

8.3.6 Expand on the result of RNAseq

The result obtained from the RNAseq study in this PhD project could be used as starting point to further analyse and understand the effect of MAOIs and TPM on gene expression in SH-SY5Y cells. The expression levels of important genes having prominent roles in different diseases and conditions can be confirmed using qPCR. Similarly, analysis and further investigation of other derived genes in the gene networks obtained from GeneMANIA analysis for their roles in different processes can be helpful in expanding the knowledge of use in treating tobacco addiction.

8.4 Conclusion

To conclude, this PhD project aimed to investigate the effect of nicotine, TPM and the new candidate MAOIs on MAO activity, MAO gene and MAO protein expression using human neuroblastoma SH-SY5Y cells. The results from this PhD study demonstrated that the candidate MAOIs exhibited MAO inhibitory potential, which was at a similar level to that of TPM. The study of MAO inhibitory activity of the candidate MAOIs in cultured cells for this PhD project, is to my knowledge, the first of its kind. Maximum inhibition was seen when cells were exposed to MAOIs or TPM for 3 days. Therefore, 3 days was chosen as the optimum period of exposure to study the effect of exposure treatment on MAO protein, MAO genes and global gene expression. However, no significant change in the expression level of MAO proteins and MAO genes were observed when differentiated SH-SY5Y cells were exposed to treatments for 3 days. RNAseq analysis uncovered several differentially expressed genes when exposed to nicotine, TPM and MAOIs. Many of these genes were closely related to different diseases and conditions previously linked with smoking and addiction. This suggests a promising direction for future research.

References

Abell, C. W., & Kwan, S.-W. (2000). Molecular characterization of monoamine oxidases A and B.

Adan, A., Kiraz, Y., & Baran, Y. (2016). Cell proliferation and cytotoxicity assays. *Current pharmaceutical biotechnology, 17*(14), 1213-1221.

Adem, A., Mattsson, M. E., Nordberg, A., & Påhlman, S. (1987). Muscarinic receptors in human SH-SY5Y neuroblastoma cell line: regulation by phorbol ester and retinoic acid-induced differentiation. *Developmental brain research, 33*(2), 235-242.

Alberts, B., Johnson, A., Lewis, J., Raff, M., Roberts, K., & Walter, P. (2002). From DNA to RNA. In *Molecular Biology of the Cell. 4th edition*. Garland Science.

Alkondon, M., Pereira, E. F., Almeida, L. E., Randall, W. R., & Albuquerque, E. X. (2000). Nicotine at concentrations found in cigarette smokers activates and desensitizes nicotinic acetylcholine receptors in CA1 interneurons of rat hippocampus. *Neuropharmacology*, *39*(13), 2726-2739.

Alpert, H. R., Connolly, G. N., & Biener, L. (2013). A prospective cohort study challenging the effectiveness of population-based medical intervention for smoking cessation. *Tobacco control, 22*(1), 32-37.

Ambrose, V., Miller, J. H., Dickson, S. J., Hampton, S., Truman, P., Lea, R. A., & Fowles, J. (2007). Tobacco particulate matter is more potent than nicotine at upregulating nicotinic receptors on SH-SY5Y cells. *Nicotine & tobacco research, 9*(8), 793-799.

Anbarasi, K., Vani, G., Balakrishna, K., & Devi, C. S. (2006). Effect of bacoside A on brain antioxidant status in cigarette smoke exposed rats. *Life Sciences, 78*(12), 1378-1384.

Andrews, S. (2010). FastQC: a quality control tool for high throughput sequence data. In: Babraham Bioinformatics, Babraham Institute, Cambridge, United Kingdom.

Arango, M., Quintero-Ronderos, P., Castiblanco, J., & Montoya-Ortíz, G. (2013). Cell culture and cell analysis. *Autoimmunity: from bench to bedside*, 741-754.

Armani, C., Landini, L., & Leone, A. (2010). Interactive effect of cigarette smoking and gene variants for predisposing to cardiovascular disease. *Current pharmaceutical design*, *16*(23), 2531-2538.

Assefa, A. T. (2020). *Statistical methods for testing differential gene expression in bulk and single-cell RNA sequencing data.* Faculty of Sciences, Ghent University, Belgium,

Baker, R. (1974). Temperature distribution inside a burning cigarette. *Nature, 247*(5440), 405-406.

Baker, R. R. (2006). Smoke generation inside a burning cigarette: modifying combustion to develop cigarettes that may be less hazardous to health. *Progress in Energy and Combustion Science, 32*(4), 373-385.

Balfour, D. J. K. (2008). The psychobiology of nicotine dependence. *European Respiratory Review*, *17*(110), 172-181.

Banerjee, A., Haswell, L. E., Baxter, A., Parmar, A., Azzopardi, D., Corke, S., . . . Gaca, M. D. (2017). Differential gene expression using RNA sequencing profiling in a reconstituted airway epithelium exposed to conventional cigarette smoke or electronic cigarette aerosols. *Applied in vitro toxicology, 3*(1), 84-98.

Barik, J., & Wonnacott, S. (2009). Molecular and cellular mechanisms of action of nicotine in the CNS. In *Nicotine Psychopharmacology* (pp. 173-207): Springer.

Batra, V., Patkar, A. A., Berrettini, W. H., Weinstein, S. P., & Leone, F. T. (2003). The genetic determinants of smoking. *Chest, 123*(5), 1730-1739.

Bench, C., Price, G., Lammertsma, A., Cremer, J., Luthra, S., Turton, D., . . . Da Prada, M. (1991). Measurement of human cerebral monoamine oxidase type B (MAO-B) activity with positron emission tomography (PET): a dose ranging study with the reversible inhibitor Ro 19-6327. *European journal of clinical pharmacology, 40*(2), 169-173.

Benowitz, N. L. (1996). Pharmacology of nicotine: addiction and therapeutics. *Annual review of pharmacology and toxicology, 36*(1), 597-613.

Benowitz, N. L. (2009). Pharmacology of nicotine: addiction, smoking-induced disease, and therapeutics. *Annual review of pharmacology and toxicology, 49*, 57-71.

Berlin, I., & M. Anthenelli, R. (2001). Monoamine oxidases and tobacco smoking. *International Journal of Neuropsychopharmacology*, *4*(1), 33-42.

Berry, M., Juorio, A., & Paterson, I. (1994). The functional role of monoamine oxidases A and B in the mammalian central nervous system. *Progress in neurobiology, 42*(3), 375-391.

Borland, R., Partos, T. R., Yong, H. H., Cummings, K. M., & Hyland, A. (2012). How much unsuccessful quitting activity is going on among adult smokers? Data from the International Tobacco Control Four Country cohort survey. *Addiction, 107*(3), 673-682.

Boulton, A., Yu, P., & Tipton, K. (1988). Biogenic amine adducts, monoamine oxidase inhibitors, and smoking. *The Lancet, 331*(8577), 114-115.

Boyle, J. O., Gümüş, Z. H., Kacker, A., Choksi, V. L., Bocker, J. M., Zhou, X. K., ... & Dannenberg, A. J. (2010). Effects of cigarette smoke on the human oral mucosal transcriptome. *Cancer prevention research*, *3*(3), 266-278.

Brennan, K. A., Crowther, A., Putt, F., Roper, V., Waterhouse, U., & Truman, P. (2015). Tobacco particulate matter self-administration in rats: differential effects of tobacco type. *Addiction biology*, *20*(2), 227-235.

Brenner, D., Kukull, W. A., Van Belle, G., Bowen, J., McCormick, W., Teri, L., & Larson, E. (1993). Relationship between cigarette smoking and Alzheimer's disease in a population-based case-control study. *Neurology, 43*(2), 293-293.

Brunzell, D. H., Russell, D. S., & Picciotto, M. R. (2003). In vivo nicotine treatment regulates mesocorticolimbic CREB and ERK signaling in C57Bl/6J mice. *Journal of neurochemistry, 84*(6), 1431-1441.

Büttner, P., Mosig, S., & Funke, H. (2007). Gene expression profiles of T lymphocytes are sensitive to the influence of heavy smoking: A pilot study. *Immunogenetics*, *59*, 37-43.

Carr, L. A., & Basham, J. K. (1991). Effects of tobacco smoke constituents on MPTP-induced toxicity and monoamine oxidase activity in the mouse brain. *Life Sciences, 48*(12), 1173-1177.

Casoli, T., Di Stefano, G., Fattoretti, P., Giorgetti, B., Balietti, M., Lattanzio, F., . . . Platano, D. (2012). Dynamin binding protein gene expression and memory performance in aged rats. *Neurobiology of aging, 33*(3), 618. e615-618. e619.

Castagnoli, K., Steyn, S.J., Magnin, G., Van Der Schyf, C. J., Fourie, I., Khalil, A., et al. (2002) Studies on the interactions of tobacco leaf and tobacco smoke constituents and monoamine oxidase. Neurotoxicity Res*earch, 4*(2), 151-160.

Centers for Disease Control and Prevention (US); National Center for Chronic Disease Prevention and Health Promotion (US); Office on Smoking and Health (US). How Tobacco Smoke Causes Disease: The Biology and Behavioral Basis for Smoking-Attribu5Disease: A Report of the Surgeon General. Atlanta (GA): Centers for Disease Control and Prevention (US); 2010. 3, Chemistry and Toxicology of Cigarette Smoke and Biomarkers of Exposure and Harm. Available from: https://www.ncbi.nlm.nih.gov/books/NBK53014/2010.

Chaiton, M., Diemert, L., Cohen, J. E., Bondy, S. J., Selby, P., Philipneri, A., & Schwartz, R. (2016). Estimating the number of quit attempts it takes to quit smoking successfully in a longitudinal cohort of smokers. *BMJ open, 6*(6), e011045.

Charlesworth, J. C., Curran, J. E., Johnson, M. P., Göring, H. H., Dyer, T. D., Diego, V. P., ... & Blangero, J. (2010). Transcriptomic epidemiology of smoking: the effect of smoking on gene expression in lymphocytes. *BMC medical genomics*, *3*(1), 1-11.

Chen, K. (2004). Organization of MAO A and MAO B promoters and regulation of gene expression. *Neurotoxicology, 25*(1-2), 31-36.

Chen, K., Wu, H. F., & Shih, J. C. (1993). The deduced amino acid sequences of human platelet and frontal cortex monoamine oxidase B are identical. *Journal of neurochemistry, 61*(1), 187-190.

Chen, P. H., Tu, H. P., Wang, S. J., Ko, A. M. S., Lee, C. P., Chiang, T. A., . . . Ko, C. H. (2012). Monoamine oxidase A variants are associated with heavy betel quid use. *Addiction biology, 17*(4), 786-797.

Cheung, Y.-T., Lau, W. K.-W., Yu, M.-S., Lai, C. S.-W., Yeung, S.-C., So, K.-F., & Chang, R. C.-C. (2009). Effects of all-trans-retinoic acid on human SH-SY5Y neuroblastoma as in vitro model in neurotoxicity research. *Neurotoxicology, 30*(1), 127-135.

Coder, D. M. (2001). Assessment of cell viability. *Current protocols in cytometry, 15*(1), 9.2. 1-9.2. 14.

Cook, M. (2013). Māori smoking, alcohol and drugs—tūpeka, waipiro me te tarukino—Māori use of tobacco. *Te Ara—the Encyclopedia of New Zealand*.Copeland, R. L., Leggett, Y. A., Kanaan, Y. M., Taylor, R. E., & Tizabi, Y. (2005). Neuroprotective effects of nicotine against salsolinol-induced cytotoxicity: implications for Parkinson's disease. *Neurotoxicity research, 8*(3), 289-293.

Creasey, N. (1956). Factors which interfere in the manometric assay of monoamine oxidase. *Biochemical Journal, 64*(1), 178-183.

D'Anna, C., Cigna, D., Costanzo, G., Bruno, A., Ferraro, M., Di Vincenzo, S., . . . Pace, E. (2015). Cigarette smoke alters the proteomic profile of lung fibroblasts. *Molecular BioSystems, 11*(6), 1644-1652.

Dani, J. A., & Balfour, D. J. (2011). Historical and current perspective on tobacco use and nicotine addiction. *Trends in Neuroscience, 34*(7), 383-392. 10.1016/j.tins.2011.05.001

Das, B. C., Thapa, P., Karki, R., Das, S., Mahapatra, S., Liu, T.-C., . . . Van Veldhuizen, P. (2014). Retinoic acid signaling pathways in development and diseases. *Bioorganic & medicinal chemistry, 22*(2), 673-683.

Day, J. J., & Carelli, R. M. (2007). The nucleus accumbens and Pavlovian reward learning. *The Neuroscientist, 13*(2), 148-159.

De Colibus, L., Li, M., Binda, C., Lustig, A., Edmondson, D. E., & Mattevi, A. (2005). Three-dimensional structure of human monoamine oxidase A (MAO A): relation to the structures of rat MAO A and human MAO B. *Proceedings of the National Academy of Sciences, 102*(36), 12684-12689.

De Kok, J. B., Roelofs, R. W., Giesendorf, B. A., Pennings, J. L., Waas, E. T., Feuth, T., ... & Span, P. N. (2005). Normalization of gene expression measurements in tumor tissues: comparison of 13 endogenous control genes. *Laboratory investigation*, *85*(1), 154-159.

De Oliveira, D., Pitanga, B., Grangeiro, M. S., Lima, R., Costa, M. d. F. D., Costa, S. L., . . . El-Bachá, R. d. S. (2010). Catechol cytotoxicity in vitro: Induction of glioblastoma cell death by apoptosis. *Human & experimental toxicology, 29*(3), 199-212.

Dombrowski, J. J., & Lambooy, J. P. (1981). Sarcosine dehydrogenase and the vital economy of hepatic mitochondria utilizing riboflavin homologs. *International Journal of Biochemistry, 13*(2), 171-178.

Dowlati, Y., de Jesus, D. R., Selby, P., Fan, I., & Meyer, J. H. (2019). Depressed mood induction in early cigarette withdrawal is unaffected by acute monoamine precursor supplementation. *Neuropsychiatric disease and treatment, 15*, 311.

Drevets, W. C., Gautier, C., Price, J. C., Kupfer, D. J., Kinahan, P. E., Grace, A. A., . . . Mathis, C. A. (2001). Amphetamine-induced dopamine release in human ventral striatum correlates with euphoria. *Biological psychiatry, 49*(2), 81-96.

Dunckley, T., & Lukas, R. J. (2003). Nicotine modulates the expression of a diverse set of genes in the neuronal SH-SY5Y cell line. *Journal of Biological Chemistry*, *278*(18), 15633-15640.

Dunckley, T., & Lukas, R. J. (2006). Nicotinic modulation of gene expression in SH-SY5Y neuroblastoma cells. *Brain research, 1116*(1), 39-49.

Durazzo, T. C., Mattsson, N., Weiner, M. W., & Initiative, A. s. D. N. (2014). Smoking and increased Alzheimer's disease risk: a review of potential mechanisms. *Alzheimer's & Dementia, 10*, S122-S145.

Edmondson, D., Mattevi, A., Binda, C., Li, M., & Hubalek, F. (2004). Structure and mechanism of monoamine oxidase. *Current medicinal chemistry, 11*(15), 1983-1993.

Edwards, R., Ball, J., Hoek, J., Wilson, N., & Waa, A. (2021). Key findings on smoking and e-cigarette use prevalence and trends in the 2020/21 NZ Health Survey. *Public Health Expert [blog]*

Ekblom, J., Zhu, Q.-S., Chen, K., & Shih, J. (1996). Monoamine oxidase gene transcription in human cell lines: treatment with psychoactive drugs and ethanol. *Journal of Neural Transmission, 103*(6), 681-692.

Essman, W. B. (1977). Serotonin and monoamine oxidase in mouse skin: effects of cigarette smoke exposure. *Journal of medicine, 8*(2), 95-101.

Etter, J.-F., & Stapleton, J. A. (2006). Nicotine replacement therapy for long-term smoking cessation: a meta-analysis. *Tobacco control, 15*(4), 280-285.

Ewels, P., Magnusson, M., Lundin, S., & Käller, M. (2016). MultiQC: summarize analysis results for multiple tools and samples in a single report. *Bioinformatics, 32*(19), 3047-3048.

Fang, I.-J., & Trewyn, B. G. (2012). Application of mesoporous silica nanoparticles in intracellular delivery of molecules and proteins. *Methods in enzymology, 508*, 41-59.

Finberg, J. P. (2014). Update on the pharmacology of selective inhibitors of MAO-A and MAO-B: focus on modulation of CNS monoamine neurotransmitter release. *Pharmacology & therapeutics*, *143*(2), 133-152.

Fowler, J. S., Logan, J., Wang, G.-J., & Volkow, N. D. (2003). Monoamine oxidase and cigarette smoking. *Neurotoxicology, 24*(1), 75-82.

Fowler, J. S., Volkow, N., Wang, G.-J., Pappas, N., Logan, J., MacGregor, R., . . . Wolf, A. (1996a). Inhibition of monoamine oxidase B in the brains of smokers. *Nature, 379*(6567), 733-736.

Fowler, J. S., Volkow, N. D., Logan, J., Pappas, N., King, P., MacGregor, R., . . . Gatley, S. J. (1998). An acute dose of nicotine does not inhibit MAO B in baboon brain in vivo. *Life Sciences, 63*(2), PL19-PL23.

Fowler, J. S., Volkow, N. D., Wang, G.-J., Pappas, N., Logan, J., Shea, C., . . . Zezulkova, I. (1996b). Brain monoamine oxidase A inhibition in cigarette smokers. *Proceedings of the National Academy of Sciences, 93*(24), 14065-14069.

Fowles, J., Bates, M., & Noiton, D. (2000). The chemical constituents in cigarettes and cigarette smoke: priorities for harm reduction. *A report to the New Zealand Ministry of Health*, 1-65.

Gaweska, H., & Fitzpatrick, P. F. (2011). Structures and mechanism of the monoamine oxidase family. *Biomolecular concepts, 2*(5), 365-377.

Geha, R. M., Chen, K., Wouters, J., Ooms, F., & Shih, J. C. (2002). Analysis of conserved active site residues in monoamine oxidase A and B and their three-dimensional molecular modeling. *Journal of Biological Chemistry, 277*(19), 17209-17216.

Geha, R. M., Rebrin, I., Chen, K., & Shih, J. C. (2001). Substrate and inhibitor specificities for human monoamine oxidase A and B are influenced by a single amino acid. *Journal of Biological Chemistry, 276*(13), 9877-9882.

Geiss, O., & Kotzias, D. (2007). Tobacco, cigarettes and cigarette smoke. *Journal of EUR-scientific & technical research series, 73*, 21.

Gene expression assays user Guide, T. single-tube assays, 2019 (Pub. No. 4333458 R)

George, T. P., & Weinberger, A. H. (2008). Monoamine oxidase inhibition for tobacco pharmacotherapy. *Clinical Pharmacology & Therapeutics, 83*(4), 619-621.

Glanemann, C., Loos, A., Gorret, N., Willis, L. B., O'brien, X. M., Lessard, P. A., & Sinskey, A. J. (2003). Disparity between changes in mRNA abundance and enzyme activity in Corynebacterium glutamicum: implications for DNA microarray analysis. *Applied microbiology and biotechnology*, *61*, 61-68.

Goldstein, D. S., Jinsmaa, Y., Sullivan, P., Holmes, C., Kopin, I. J., & Sharabi, Y. (2016). Comparison of monoamine oxidase inhibitors in decreasing production of the autotoxic dopamine metabolite 3, 4-dihydroxyphenylacetaldehyde in PC12 cells. *Journal of Pharmacology and Experimental Therapeutics*, *356*(2), 483-492.

Gordon, J., & Amini, S. (2021). General overview of neuronal cell culture. *Neuronal Cell Culture: Methods and Protocols*, 1-8.

Grimsby, J., Chen, K., Wang, L.-J., Lan, N. C., & Shih, J. C. (1991). Human monoamine oxidase A and B genes exhibit identical exon-intron organization. *Proceedings of the National Academy of Sciences, 88*(9), 3637-3641.

Gu, Q. (2017). Neural Cell Lines (Lineage). In *Neural Cell Biology* (pp. 169-186): CRC Press.

Gugatschka, M., Darnhofer, B., Grossmann, T., Schittmayer, M., Hortobagyi, D., Kirsch, A., ... & Karbiener, M. (2019). Proteomic Analysis of Vocal Fold Fibroblasts Exposed to Cigarette Smoke Extract: Exploring the Pathophysiology of Reinke's Edema*[S]. *Molecular & Cellular Proteomics*, *18*(8), 1511-1525.

Guillem, K., Vouillac, C., Azar, M. R., Parsons, L. H., Koob, G. F., Cador, M., & Stinus, L. (2005). Monoamine oxidase inhibition dramatically increases the motivation to self-administer nicotine in rats. *Journal of Neuroscience, 25*(38), 8593-8600.

Hackett, N. R., Butler, M. W., Shaykhiev, R., Salit, J., Omberg, L., Rodriguez-Flores, J. L., . . . Didon, L. (2012). RNA-Seq quantification of the human small airway epithelium transcriptome. *BMC genomics, 13*(1), 1-31.

Harada, M., & Nagatsu, T. (1973). A sensitive fluorometric assay for monoamine oxidase activity. *Analytical biochemistry, 56*(1), 283-288.

Harris, A. C., Muelken, P., Alcheva, A., Stepanov, I., & LeSage, M. G. (2022). Cigarette smoke extract, but not electronic cigarette aerosol extract, inhibits monoamine oxidase in vitro and produces greater acute aversive/anhedonic effects than nicotine alone on intracranial self-stimulation in rats. *Frontiers in Neuroscience*, *16*, 868088.

Hartmann-Boyce, J., Chepkin, S. C., Ye, W., Bullen, C., & Lancaster, T. (2018). Nicotine replacement therapy versus control for smoking cessation. *Cochrane database of systematic reviews*(5)

Harvey, B. G., Heguy, A., Leopold, P. L., Carolan, B. J., Ferris, B., & Crystal, R. G. (2007). Modification of gene expression of the small airway epithelium in response to cigarette smoking. *Journal of molecular medicine*, *85*, 39-53

Haswell, L. E., Corke, S., Verrastro, I., Baxter, A., Banerjee, A., Adamson, J., . . . Minet, E. (2018). In vitro RNA-seq-based toxicogenomics assessment shows reduced biological effect of tobacco heating products when compared to cigarette smoke. *Scientific reports, 8*(1), 1-18.

Hauptmann, N., & Shih, J. C. (2001). 2-Naphthylamine, a compound found in cigarette smoke, decreases both monoamine oxidase A and B catalytic activity. *Life Sciences, 68*(11), 1231-1241.

Herman, M. A., & Roberto, M. (2015). The addicted brain: understanding the neurophysiological mechanisms of addictive disorders. *Frontiers in integrative neuroscience, 9*, 18.

Herraiz, T., & Chaparro, C. (2005). Human monoamine oxidase is inhibited by tobacco smoke: β-carboline alkaloids act as potent and reversible inhibitors. *Biochemical and biophysical research communications, 326*(2), 378-386.

Hoerndli, F. J., Toigo, M., Schild, A., Götz, J., & Day, P. J. (2004). Reference genes identified in SH-SY5Y cells using custom-made gene arrays with validation by quantitative polymerase chain reaction. *Analytical biochemistry*, *335*(1), 30-41.

Hogg, R. C. (2016). Contribution of monoamine oxidase inhibition to tobacco dependence: a review of the evidence. *Nicotine & tobacco research, 18*(5), 509-523.

Hong, S. W., Teesdale-Spittle, P., Page, R., & Truman, P. (2022). A review of monoamine oxidase (MAO) inhibitors in tobacco or tobacco smoke. *NeuroToxicology*.

Hrubša, M., Alva, R., Parvin, M. S., Macáková, K., Karlíčková, J., Fadraersada, J., . . . Mladěnka, P. (2022). Comparison of Antiplatelet Effects of Phenol Derivatives in Humans. *Biomolecules, 12*(1), 117.

Hosur, V., Leppanen, S., Abutaha, A., & Loring, R. H. (2009). Gene regulation of α4β2 nicotinic receptors: microarray analysis of nicotine-induced receptor up-regulation and anti-inflammatory effects. *Journal of neurochemistry*, *111*(3), 848-858.

Huan, T., Joehanes, R., Schurmann, C., Schramm, K., Pilling, L. C., Peters, M. J., ... & Levy, D. (2016). A whole-blood transcriptome meta-analysis identifies gene expression signatures of cigarette smoking. *Human molecular genetics*, *25*(21), 4611-4623.

Huang, D. W., Sherman, B. T., & Lempicki, R. A. (2009a). Systematic and integrative analysis of large gene lists using DAVID bioinformatics resources. *Nature protocols, 4*(1), 44-57.

Huang, D. W., Sherman, B. T., & Lempicki, R. A. (2009b). Bioinformatics enrichment tools: paths toward the comprehensive functional analysis of large gene lists. *Nucleic acids research, 37*(1), 1-13.

Hughes, J. R., Keely, J., & Naud, S. (2004). Shape of the relapse curve and long-term abstinence among untreated smokers. *Addiction, 99*(1), 29-38.

Ikemoto, S. (2007). Dopamine reward circuitry: two projection systems from the ventral midbrain to the nucleus accumbens–olfactory tubercle complex. *Brain research reviews, 56*(1), 27-78.

Inaba-Hasegawa, K., Shamoto-Nagai, M., Maruyama, W., & Naoi, M. (2017). Type B and A monoamine oxidase and their inhibitors regulate the gene expression of Bcl-2 and neurotrophic factors in human glioblastoma U118MG cells: different signal pathways for neuroprotection by selegiline and rasagiline. *Journal of Neural Transmission*, *124*(9), 1055-1066.

Iuchi, K., Ema, M., Suzuki, M., Yokoyama, C., & Hisatomi, H. (2019). Oxidized unsaturated fatty acids induce apoptotic cell death in cultured cells. *Molecular Medicine Reports, 19*(4), 2767-2773.

Jack Henningfield, M. J. H., Christine Ann Rose, David T. Sweanor. (2019). Smoking.

Jahn, K., Wieltsch, C., Blumer, N., Mehlich, M., Pathak, H., Khan, A., . . . Frieling, H. (2017). A cell culture model for investigation of synapse influenceability: epigenetics, expression and function of gene targets important for synapse formation and preservation in SH-SY5Y neuroblastoma cells differentiated by retinoic acid. *Journal of Neural Transmission, 124*(11), 1341-1367.

Jamal, A., King, B. A., Neff, L. J., Whitmill, J., Babb, S. D., & Graffunder, C. M. (2016). Current cigarette smoking among adults—United States, 2005–2015. *Morbidity and mortality weekly report*, *65*(44), 1205-1211.

Jha, P., MacLennan, M., Chaloupka, F. J., Yurekli, A., Ramasundarahettige, C., Palipudi, K., ... & Gupta, P. C. (2015). Global hazards of tobacco and the benefits of smoking cessation and tobacco taxes. Disease Control Priorities. The World Bank, 3, 175-194.

Jiang, H., Jiang, Q., Liu, W., & Feng, J. (2006). Parkin suppresses the expression of monoamine oxidases. *Journal of Biological Chemistry, 281*(13), 8591-8599.

Jiang, X. Y., Feng, Y. L., Ye, L. T., Li, X. H., Feng, J., Zhang, M. Z., ... & Yu, X. Y. (2017). Inhibition of Gata4 and Tbx5 by nicotine-mediated DNA methylation in myocardial differentiation. *Stem cell reports*, *8*(2), 290-304.

Jin, Y., Zhang, X., Shu, L., Chen, L., Sun, L., Qian, H., ... & Fu, Z. (2010). Oxidative stress response and gene expression with atrazine exposure in adult female zebrafish (Danio rerio). *Chemosphere*, *78*(7), 846-852.

John, L., Sharma, G., Chaudhuri, S. P., & Pillai, B. (2005). Cigarette smoke extract induces changes in growth and gene expression of Saccharomyces cerevisiae. *Biochemical and biophysical research communications, 338*(3), 1578-1586.

Johnstone, R., Quan, P., & Carruthers, W. (1962). Composition of cigarette smoke: some low-boiling components. *Nature, 195*(4848), 1267-1269.

Jonkhout, N., Cruciani, S., Santos Vieira, H. G., Tran, J., Liu, H., Liu, G., . . . Vauti, F. (2021). Subcellular relocalization and nuclear redistribution of the RNA methyltransferases TRMT1 and TRMT1L upon neuronal activation. *RNA biology, 18*(11), 1905-1919.

Jordan, H., Hidajat, M., Payne, N., Adams, J., White, M., & Ben-Shlomo, Y. (2017). What are older smokers' attitudes to quitting and how are they managed in primary care? An analysis of the cross-sectional English Smoking Toolkit Study. *BMJ open, 7*(11), e018150.

Jung, Y. J., Choi, H., & Oh, E. (2021). Effects of particulate matter and nicotine for the MPP+-induced SH-SY5Y cells: Implication for Parkinson's disease. *Neuroscience letters, 765*, 136265.

Kaya, B., Sağlık, B. N., Levent, S., Özkay, Y., & Kaplancıklı, Z. A. (2016). Synthesis of some novel 2-substituted benzothiazole derivatives containing benzylamine moiety as monoamine oxidase inhibitory agents. *Journal of enzyme inhibition and medicinal chemistry, 31*(6), 1654-1661.

Kechin, A., Boyarskikh, U., Kel, A., & Filipenko, M. (2017). cutPrimers: a new tool for accurate cutting of primers from reads of targeted next generation sequencing. *Journal of Computational Biology, 24*(11), 1138-1143.

Kelsen, S. G., Duan, X., Ji, R., Perez, O., Liu, C., & Merali, S. (2008). Cigarette smoke induces an unfolded protein response in the human lung: a proteomic approach. *American journal of respiratory cell and molecular biology, 38*(5), 541-550.

Khalil, A. A., Davies, B., & Castagnoli Jr, N. (2006). Isolation and characterization of a monoamine oxidase B selective inhibitor from tobacco smoke. *Bioorganic & medicinal chemistry, 14*(10), 3392-3398.

Khalil, A. A., Steyn, S., & Castagnoli, N. (2000). Isolation and characterization of a monoamine oxidase inhibitor from tobacco leaves. *Chemical research in toxicology, 13*(1), 31-35.

Kim, D., Langmead, B., & Salzberg, S. L. (2015). HISAT: a fast spliced aligner with low memory requirements. *Nature methods, 12*(4), 357-360.

Kim, Y.-H., An, Y.-J., Jo, S., Lee, S.-H., Lee, S. J., Choi, S.-J., & Lee, K. (2018). Comparison of volatile organic compounds between cigarette smoke condensate (CSC) and extract (CSE) samples. *Environmental Health and Toxicology, 33*(3)

Kitamura, Y., Mise, N., Mori, Y., Suzuki, Y., Ohashi, T., Tada-Oikawa, S., ... & Ichihara, S. (2020). Proteomic identification of the proteins related to cigarette smoke-induced cardiac hypertrophy in spontaneously hypertensive rats. *Scientific reports, 10(1), 18825.*

Klus, H., Boenke-Nimphius, B., & Müller, L. (2016). Cigarette mainstream smoke: The evolution of methods and devices for generation, exposure and collection. *Beiträge Zur Tabakforschung International/contributions to Tobacco Research, 27*(4), 137-274.

Kokelj, S., Östling, J., Georgi, B., Olsson, H. K., & Olin, A. C. (2020). Late Breaking Abstract-Proteomic changes in respiratory tract lining fluid associated with smoking.

Kopa, P. N., & Pawliczak, R. (2018). Effect of smoking on gene expression profile–overall mechanism, impact on respiratory system function, and reference to electronic cigarettes. *Toxicology mechanisms and methods*, *28*(6), 397-409.

Korecka, J. A., van Kesteren, R. E., Blaas, E., Spitzer, S. O., Kamstra, J. H., Smit, A. B., ... & Bossers, K. (2013). Phenotypic characterization of retinoic acid differentiated SH-SY5Y cells by transcriptional profiling. *PloS one*, *8*(5), e63862.

Kovalevich, J., & Langford, D. (2013). Considerations for the use of SH-SY5Y neuroblastoma cells in neurobiology. In *Neuronal Cell Culture* (pp. 9-21): Springer.

Krajl, M. (1965). A rapid microfluorimetric determination of monoamine oxidase. *Biochemical pharmacology, 14*(11), 1684-1685.

Kubota, K., Yamaguchi, T., Abe, Y., Fujiwara, T., Hatazawa, J., & Matsuzawa, T. (1983). Effects of smoking on regional cerebral blood flow in neurologically normal subjects. *Stroke, 14*(5), 720-724.

Kuete, V., Karaosmanoğlu, O., & Sivas, H. (2017). Anticancer Activities of African Medicinal Spices and Vegetables. In V. Kuete (Ed.), *Medicinal*

Spices and Vegetables from Africa (pp. 271-297): Academic Press. https://doi.org/10.1016/B978-0-12-809286-6.00010-8

Kukurba, K. R., & Montgomery, S. B. (2015). RNA sequencing and analysis. *Cold Spring Harbor Protocols, 2015*(11), pdb. top084970.

Kumar, P., Nagarajan, A., & Uchil, P. D. (2018). Analysis of cell viability by the MTT assay. *Cold spring harbor protocols*, *2018*(6), pdb-prot095505.

Kumari, S., & Deshmukh, R. (2022). Dipeptidyl peptidase 4 (DPP4) inhibitors stride up the management of Parkinson's disease. *European Journal of Pharmacology*, 175426.

Launay, J.-M., Del Pino, M., Chironi, G., Callebert, J., Peoc'h, K., Mégnien, J.-L., . . . Rendu, F. (2009). Smoking induces long-lasting effects through a monoamine-oxidase epigenetic regulation. *PloS one, 4*(11), e7959.

Lewis, A., Miller, J., & Lea, R. (2007). Monoamine oxidase and tobacco dependence. *Neurotoxicology, 28*(1), 182-195.

Lewis, A. J. (2010). Tobacco smoke extract modulates activity and expression of monoamine oxidase and μ opioid receptor in cultured human neuroblastoma cells (Doctoral dissertation, Open Access Te Herenga Waka-Victoria University of Wellington).

Li, R., & Shen, Y. (2013). An old method facing a new challenge: re-visiting housekeeping proteins as internal reference control for neuroscience research. *Life sciences*, *92*(13), 747-751.

Li, X., Zhuang, Z., Liu, J., Huang, H., Wei, Q., & Yang, X. (2006). Proteomic analysis to identify the cellular responses induced by hydroquinone in human embryonic lung fibroblasts. *Toxicology Mechanisms and Methods, 16*(1), 1-6.

Li, X., Wang, W., Xi, Y., Gao, M., Tran, M., Aziz, K. E., ... & Chen, J. (2016). FOXR2 interacts with MYC to promote its transcriptional activities and tumorigenesis. *Cell reports*, *16*(2), 487-497.

Lin, J., Huang, P., Chen, W., Ye, C., Su, H., & Yao, X. (2020). Key molecules and pathways underlying sporadic amyotrophic lateral sclerosis: integrated analysis on gene expression profiles of motor neurons. *Frontiers in Genetics, 11*, 578143.

Litwiniuk, A., Domańska, A., Chmielowska, M., Martyńska, L., Bik, W., & Kalisz, M. (2020). The effects of alpha-linolenic acid on the secretory activity of astrocytes and β amyloid-associated neurodegeneration in differentiated SH-SY5Y cells: Alpha-linolenic acid protects the SH-SY5Y cells against β amyloid toxicity. *Oxidative medicine and cellular longevity, 2020*

Livak,K. J., & Schmittgen, T.D. (2001). Analysis of relative gene expression data using real-time quantitative PCR and the $2^{-\Delta\Delta CT}$ method. *methods*, *25*(4), 402-408.

Lopes, F. M., Schröder, R., da Frota Júnior, M. L. C., Zanotto-Filho, A., Müller, C. B., Pires, A. S., . . . Kapczinski, F. (2010). Comparison between proliferative and neuron-like SH-SY5Y cells as an in vitro model for Parkinson disease studies. *Brain research, 1337*, 85-94.

Mackenzie, R. J. (2018). RNA-seq: Basics, Applications and Protocol. *Retrieved from Technology Networks: https://www. technologynetworks. com/genomics/articles/rna-seqbasics-applications-and-protocol-299461*

Mahmood, T., & Yang, P. C. (2012). Western blot: technique, theory, and trouble shooting. *North American journal of medical sciences*, *4*(9), 429.

Malinovschi, A., Janson, C., Holmkvist, T., Norbäck, D., Meriläinen, P., & Högman, M. (2006). Effect of smoking on exhaled nitric oxide and flow-independent nitric oxide exchange parameters. *European Respiratory Journal, 28*(2), 339-345.

Masroor, M., Shireen, E., & Naeem, S. (2019). Evaluation of inhibitory potential of PUFAs from fish oil against monoamine oxidase-b: a molecular docking study. *International Journal of Biology and Biotechnology, 16*(4), 901-909.

Massey, J. B., & Churchich, J. E. (1977). Kynuramine, a fluorescent substrate and probe of plasma amine oxidase. *Journal of Biological Chemistry, 252*(22), 8081-8084.

Méndez-Álvarez, E., Soto-Otero, R., Sánchez-Sellero, I., & López-Rivadulla Lamas, M. (1998). *In vitro inhibition of catalase activity by cigarette smoke: relevance for oxidative stress.* Paper presented at the Journal of Applied Toxicology: An International Forum Devoted to Research and Methods Emphasizing Direct Clinical, Industrial and Environmental Applications.

Ministry of Health, (2021). Annual Update of Key Results 2020/21: New Zealand Health Survey. Retrieved 05-10-2022 from https://www.health.govt.nz/publication/annual-update-key-results-2020-21-new-zealand-health-survey#:~:text=Most%20New%20Zealanders%20are%20in,good%20health%20in%202020%2F21

Mishra, A., Chaturvedi, P., Datta, S., Sinukumar, S., Joshi, P., & Garg, A. (2015). Harmful effects of nicotine. *Indian journal of medical and paediatric oncology: official journal of Indian Society of Medical & Paediatric Oncology, 36*(1), 24.

Moraes, F. P., & de Azevedo, W. F. (2012). Targeting imidazoline site on monoamine oxidase B through molecular docking simulations. *Journal of molecular modeling, 18*(8), 3877-3886.

Morinan, A., & Garratt, H. M. (1985). An improved fluorimetric assay for brain monoamine oxidase. *Journal of pharmacological methods, 13*(3), 213-223.

Murthy, V.H. (2017). Facing addiction in the United States: the surgeon general's report of alcohol, drugs, and health. *Jama*, *317*(2), 133-134.

Myers Smith, K., Phillips-Waller, A., Pesola, F., McRobbie, H., Przulj, D., Orzol, M., & Hajek, P. (2022). E-cigarettes versus nicotine replacement treatment as harm reduction interventions for smokers who find quitting difficult: randomized controlled trial. *Addiction*, *117*(1), 224-233.

Nagatsu, T., Nakano, T., Kato, T., & Higashida, H. (1981). Expression of A and B types of monoamine oxidase in neuroblastoma hybrid cells. *Neurochemistry international, 3*(2), 137-142.

Nakano, T., Kawai, S., & Nagatsu, T. (1984). A simple assay for monoamine oxidase using glutathione peroxidase and glutathione reductase. *The Japanese Journal of Pharmacology, 35*(2), 163-167.

Naoi, M., Maruyama, W., & Shamoto-Nagai, M. (2018). Type A and B monoamine oxidases distinctly modulate signal transduction pathway

and gene expression to regulate brain function and survival of neurons. *Journal of Neural Transmission, 125*(11), 1635-1650.
National Center for Biotechnology Information (2022). PubChem Compound Summary for CID 5280450, Linoleic acid. Retrieved October 24, 2022 from https://pubchem.ncbi.nlm.nih.gov/compound/Linoleic-acid.
National Center for Biotechnology Information (2022). PubChem Compound Summary for CID 5280934, Linolenic acid. Retrieved October 24, 2022 from https://pubchem.ncbi.nlm.nih.gov/compound/Linolenic-acid.
National Center for Biotechnology Information (2022). PubChem Compound Summary for CID 785, Hydroquinone. Retrieved October 24, 2022 from https://pubchem.ncbi.nlm.nih.gov/compound/Hydroquinone.
National Center for Biotechnology Information (2022). PubChem Compound Summary for CID 289, Catechol. Retrieved October 24, 2022 from https://pubchem.ncbi.nlm.nih.gov/compound/Catechol.
National Center for Biotechnology Information (2022). PubChem Compound Summary for CID 9958, 4-Methylcatechol. Retrieved October 24, 2022 from https://pubchem.ncbi.nlm.nih.gov/compound/4-Methylcatechol.
National Center for Biotechnology Information (2022). PubChem Compound Summary for CID 70761, 4-Ethylcatechol. Retrieved October 24, 2022 from https://pubchem.ncbi.nlm.nih.gov/compound/4-Ethylcatechol.
Nestler, E. J. (2001). Molecular neurobiology of addiction. *American Journal on Addictions*, *10*(3), 201-217.
Nestler, E. J. (2005). Is there a common molecular pathway for addiction? *Nature neuroscience, 8*(11), 1445-1449.
Ng, I. C., Pawijit, P., Tan, J., & Yu, H. (2019). Anatomy and physiology for biomaterials research and development.
Nilsson, G., Belasco, J. G., Cohen, S., & Von Gabain, A. (1984). Growth-rate dependent regulation of mRNA stability in Escherichia coli. *Nature*, *312*(5989), 75-77.
Nisell, M., Nomikos, G. G., Chergui, K., Grillner, P., & Svensson, T. H. (1997). Chronic nicotine enhances basal and nicotine-induced Fos immunoreactivity preferentially in the medial prefrontal cortex of the rat. *Neuropsychopharmacology*, *17*(3), 151-161.
Nutt, D. J. (1996). Addiction: brain mechanisms and their treatment implications. *The Lancet, 347*(8993), 31-36.
Nuutinen, S., Barik, J., Jones, I. W., & Wonnacott, S. (2007). Differential effects of acute and chronic nicotine on Elk-1 in rat hippocampus. *Neuroreport, 18*(2), 121-126.
Oreland, L., Fowler, C. J., & Schalling, D. (1981). Low platelet monoamine oxidase activity in cigarette smokers. *Life Sciences, 29*(24), 2511-2518.
Ostadkarampour, M., & Putnins, E. E. (2021). Monoamine oxidase inhibitors: a review of their anti-inflammatory therapeutic potential and mechanisms of action. *Frontiers in Pharmacology*, *12*, 676239.
Pagliusi, S. R., Tessari, M., DeVevey, S., Chiamulera, C., & Pich, E. M. (1996). The reinforcing properties of nicotine are associated with a specific patterning of c-fos expression in the rat brain. *European Journal of Neuroscience*, *8*(11), 2247-2256.
Pankow, J. F., Kim, K., Luo, W., & McWhirter, K. J. (2018). Gas/particle partitioning constants of nicotine, selected toxicants, and flavor

chemicals in solutions of 50/50 propylene glycol/glycerol as used in electronic cigarettes. *Chemical research in toxicology, 31*(9), 985-990.
Panlilio, L. V., & Goldberg, S. R. (2007). Self-administration of drugs in animals and humans as a model and an investigative tool. *Addiction*, *102*(12), 1863-1870.
Park, J.-M., Chang, K.-H., Park, K.-H., Choi, S.-J., Lee, K., Lee, J.-Y., . . . Lee, M.-Y. (2016). Differential effects between cigarette total particulate matter and cigarette smoke extract on blood and blood vessel. *Toxicological Research, 32*(4), 353-358.
Paulo, J. A., & Gygi, S. P. (2017). Nicotine-induced protein expression profiling reveals mutually altered proteins across four human cell lines. *Proteomics, 17(1-2), 1600319.*
Pertea, M., Kim, D., Pertea, G. M., Leek, J. T., & Salzberg, S. L. (2016). Transcript-level expression analysis of RNA-seq experiments with HISAT, StringTie and Ballgown. *Nature protocols, 11*(9), 1650-1667.
Peters, I. R., Helps, C. R., Hall, E. J., & Day, M. J. (2004). Real-time RT-PCR: considerations for efficient and sensitive assay design. *Journal of immunological methods*, *286*(1-2), 203-217.
Pich, E. M., Pagliusi, S. R., Tessari, M., Talabot-Ayer, D., van Huijsduijnen, R. H., & Chiamulera, C. (1997). Common neural substrates for the addictive properties of nicotine and cocaine. *Science*, *275*(5296), 83-86.
Polyak, K., & Meyerson, M. (2003). Gene Expression: MRNA Transcript Analysis. In *Holland-Frei Cancer Medicine. 6th edition*: BC Decker.
Portela, A., & Esteller, M. (2010). Epigenetic modifications and human disease. *Nature biotechnology*, *28*(10), 1057-1068.
Presgraves, S. P., Ahmed, T., Borwege, S., & Joyce, J. N. (2003). Terminally differentiated SH-SY5Y cells provide a model system for studying neuroprotective effects of dopamine agonists. *Neurotoxicity research, 5*(8), 579-598.
Ramonet, D., Rodriguez, M., Saura, J., Lizcano, J. M., Romera, M., Unzeta, M., ... & Mahy, N. (2003). Localization of monoamine oxidase A and B and semicarbazide-sensitive amine oxidase in human peripheral tissues. *Inflammopharmacology*, *11*(2), 111-117.
Rehm, H., Wiedenmann, B., & Betz, H. (1986). Molecular characterization of synaptophysin, a major calcium-binding protein of the synaptic vesicle membrane. *The EMBO journal, 5*(3), 535-541.
Riederer, P., Konradi, C., Schay, V., Kienzl, E., Birkmayer, G., Danielczyk, W., ... & Youdim, M. B. (1987). Localization of MAO-A and MAO-B in human brain: a step in understanding the therapeutic action of L-deprenyl. *Advances in Neurology*, *45*, 111-118.
Real-Time PCR (qPCR) | AAT Bioquest. (n.d.). Retrieved October 26, 2022, from https://www.aatbio.com/catalog/real-time-pcr-qpcr
Ren, Y., Jiang, H., Ma, D., Nakaso, K., & Feng, J. (2011). Parkin degrades estrogen-related receptors to limit the expression of monoamine oxidases. *Human molecular genetics, 20*(6), 1074-1083.
Richards, J. G., Saura, J., Ulrich, J., & Da Prada, M. (1992). Molecular neuroanatomy of monoamine oxidases in human brainstem. *Psychopharmacology (Berl), 106 Suppl*, S21-23.

Riggs, J. E. (1996). The “protective” influence of cigarette smoking on Alzheimer's and Parkinson's diseases: quagmire or opportunity for neuroepidemiology? *Neurologic clinics, 14*(2), 353-358.
Rigotti, N. A. (2012). Strategies to help a smoker who is struggling to quit. *Jama, 308*(15), 1573-1580.
Riss, T., Niles, A., Moravec, R., Karassina, N., & Vidugiriene, J. (2019). Cytotoxicity assays: in vitro methods to measure dead cells. *Assay Guidance Manual [Internet]*
Riss, T. L., Moravec, R. A., Niles, A. L., Duellman, S., Benink, H. A., Worzella, T. J., & Minor, L. (2016). Cell viability assays. *Assay Guidance Manual [Internet]*
Rodgman, A., & Perfetti, T. A. (2008). *The chemical components of tobacco and tobacco smoke*: CRC press.
Rose, J. E. (2006). Nicotine and nonnicotine factors in cigarette addiction. Psychopharmacology, 184, 274-285.
Ruiu, R., Barutello, G., Arigoni, M., Riccardo, F., Conti, L., Peppino, G., ... & Quaglino, E. (2021). Identification of TENM4 as a Novel Cancer Stem Cell-Associated Molecule and Potential Target in Triple Negative Breast Cancer. *Cancers*, *13*(4), 894.
Russo, M., Cocco, S., Secondo, A., Adornetto, A., Bassi, A., Nunziata, A., . . . Seru, R. (2011). Cigarette smoke condensate causes a decrease of the gene expression of Cu–Zn superoxide dismutase, Mn superoxide dismutase, glutathione peroxidase, catalase, and free radical-induced cell injury in SH-SY5Y human neuroblastoma cells. *Neurotoxicity research, 19*(1), 49-54.
Sakuma, H., Kusama, M., Munakata, S., Ohsumi, T., & Sugawara, S. (1983). The distribution of cigarette smoke components between mainstream and sidestream smoke: I. Acidic components. *Contributions to Tobacco & Nicotine Research*, *12*(2), 63-71
Sampedro-Piquero, P., de Guevara-Miranda, D. L., Pavón, F. J., Serrano, A., Suárez, J., de Fonseca, F. R., . . . Castilla-Ortega, E. (2019). Neuroplastic and cognitive impairment in substance use disorders: a therapeutic potential of cognitive stimulation. *Neuroscience & Biobehavioral Reviews, 106*, 23-48.
Sampedro-Piquero, P., Santín, L. J., & Castilla-Ortega, E. (2019). Aberrant brain neuroplasticity and function in drug addiction: a focus on learning-related brain regions. *Behavioral Neuroscience*, 1-24.
Sangaunchom, P., & Dharmasaroja, P. (2020). Caffeine potentiates ethanol-induced neurotoxicity through mTOR/p70S6K/4E-BP1 inhibition in SH-SY5Y cells. *International Journal of Toxicology, 39*(2), 131-140.
Santillo, M. F., Liu, Y., Ferguson, M., Vohra, S. N., & Wiesenfeld, P. L. (2014). Inhibition of monoamine oxidase (MAO) by β-carbolines and their interactions in live neuronal (PC12) and liver (HuH-7 and MH1C1) cells. *Toxicology in Vitro*, *28*(3), 403-410.
Schilling, J., Holzer, P., Guggenbach, M., Gyurech, D., Marathia, K., & Geroulanos, S. (1994). Reduced endogenous nitric oxide in the exhaled air of smokers and hypertensives. *European Respiratory Journal, 7*(3), 467-471.
Schmittgen, T. D., & Zakrajsek, B. A. (2000). Effect of experimental treatment on housekeeping gene expression: validation by real-time, quantitative

RT-PCR. *Journal of biochemical and biophysical methods*, *46*(1-2), 69-81.
Ściskalska, M., Zalewska, M., Grzelak, A., & Milnerowicz, H. (2014). The influence of the occupational exposure to heavy metals and tobacco smoke on the selected oxidative stress markers in smelters. *Biological trace element research, 159*(1), 59-68.
Shahi, G. S., Das, N. P., & Moochhala, S. M. (1991). 1-Methyl-4-phenyl-1, 2, 3, 6-tetrahydropyridine-induced neurotoxicity: partial protection against striato-nigral dopamine depletion in C57BL/6J mice by cigarette smoke exposure and by β-naphthoflavone-pretreatment. *Neuroscience letters, 127*(2), 247-250.
Sheehan, T. J., Hamnett, H. J., Beasley, R., & Fitzmaurice, P. S. (2019). Chemical and physical variations of cannabis smoke from a variety of cannabis samples in New Zealand. *Forensic sciences research, 4*(2), 168-178.
Shipley, M. M., Mangold, C. A., & Szpara, M. L. (2016). Differentiation of the SH-SY5Y human neuroblastoma cell line. *JoVE (Journal of Visualized Experiments)*, (108), e53193.
Siddhartha, P. (2019). *Quantifying Māori spend on tobacco, alcohol and gambling.*
Smith, C., & Hansch, C. (2000). The relative toxicity of compounds in mainstream cigarette smoke condensate. *Food and Chemical Toxicology, 38*(7), 637-646.
Smith, C. J., & Osborn, A. M. (2009). Advantages and limitations of quantitative PCR (Q-PCR)-based approaches in microbial ecology. *FEMS microbiology ecology, 67*(1), 6-20.
Smith, T. T., Rupprecht, L. E., Cwalina, S. N., Onimus, M. J., Murphy, S. E., Donny, E. C., & Sved, A. F. (2016). Effects of monoamine oxidase inhibition on the reinforcing properties of low-dose nicotine. *Neuropsychopharmacology*, *41*(9), 2335-2343.
Smokefree, Health Promotion Agency. (2020). History of Tobacco Control. Retrieved 05-10-2022 from https://www.smokefree.org.nz/history-of-tobacco-control#:~:text=Toxic%20Substances%20Act%20was%20amended,legislation%20to%20ban%20tobacco%20advertising.
Snyder, S. H., & Hendley, E. D. (1968). A simple and sensitive fluorescence assay for monoamine oxidase and diamine oxidase. *Journal of Pharmacology and Experimental Therapeutics, 163*(2), 386-392.
Sokolova, E., Matteoni, C., & Nistri, A. (2005). Desensitization of neuronal nicotinic receptors of human neuroblastoma SH-SY5Y cells during short or long exposure to nicotine. *British journal of pharmacology, 146*(8), 1087-1095.
Soleimani, F., Dobaradaran, S., De-la-Torre, G. E., Schmidt, T. C., & Saeedi, R. (2021). Content of toxic components of cigarette, cigarette smoke vs cigarette butts: A comprehensive systematic review. *Science of the Total Environment*, 152667.
Son, J.-H., Park, J.-S., Lee, J.-U., Kim, M. K., Min, S.-A., Park, C.-S., & Chang, H. S. (2022). A genome-wide association study on frequent exacerbation of asthma depending on smoking status. *Respiratory Medicine*, 106877.

Stratton, K., Shetty, P., Wallace, R., & Bondurant, S. (2001). Clearing the smoke: the science base for tobacco harm reduction—executive summary. *Tobacco control, 10*(2), 189-195.

Suarez-Torres, J. D., Alzate, J. P., & Orjuela-Ramirez, M. E. (2020). The NTP Report on Carcinogens: A valuable resource for public health, a challenge for regulatory science. *Journal of Applied Toxicology, 40*(1), 169-175.

Supino, R. (1995). MTT assays. In *In vitro toxicity testing protocols* (pp. 137-149): Springer.

Tatsumi, M., Groshan, K., Blakely, R. D., & Richelson, E. (1997). Pharmacological profile of antidepressants and related compounds at human monoamine transporters. *European journal of pharmacology*, *340*(2-3), 249-258.

Tenne, M., Finberg, J., Youdim, M., & Ulitzur, S. (1985). A new rapid and sensitive bioluminescence assay for monoamine oxidase activity. *Journal of neurochemistry, 44*(5), 1378-1384.

Teo, Z. L., Savas, P., & Loi, S. (2016). Gene expression analysis: current methods. In *Molecular pathology in cancer research* (pp. 107-136): Springer.

Tipton, K., & Dawson, A. (1968). The distribution of monoamine oxidase and α-glycerophosphate dehydrogenase in pig brain. *Biochemical Journal, 108*(1), 95-99.

Tipton, K. F., Davey, G., & Motherway, M. (2000). Monoamine oxidase assays. *Current protocols in pharmacology, 9*(1), 3.6. 1-3.6. 42.

Tobacco (2022) World Health Organization. World Health Organization. Available at: https://www.who.int/news-room/fact-sheets/detail/tobacco#:~:text=Tobacco%20kills%20more%20than%208,%2D%20and%20middle%2Dincome%20countries. (Accessed: April 21, 2023).

Torshabi, M., Rezaei Esfahrood, Z., Jamshidi, M., Mansuri Torshizi, A., & Sotoudeh, S. (2017). Efficacy of vitamins E and C for reversing the cytotoxic effects of nicotine and cotinine. *European Journal of Oral Sciences, 125*(6), 426-437.

NAGATSU, T., & YAGI, K. (1966). A simple assay of monoamine oxidase and D-amino acid oxidase by measuring ammonia. *The Journal of Biochemistry*, *60*(2), 219-221.

Trainor, S. (2008). Tobacco control in New Zealand: a history. *Wellington: The Cancer Control Council of New Zealand*.

Truman, P., Grounds, P., & Brennan, K. A. (2017). Monoamine oxidase inhibitory activity in tobacco particulate matter: Are harman and norharman the only physiologically relevant inhibitors? *Neurotoxicology, 59*, 22-26.

Truman, P., Stanfill, S., Heydari, A., Silver, E., & Fowles, J. (2019). Monoamine oxidase inhibitory activity of flavoured e-cigarette liquids. *Neurotoxicology, 75*, 123-128.

Turetz, M. L., O'Connor, T. P., Tilley, A. E., Strulovici-Barel, Y., Salit, J., Dang, D., ... & Crystal, R. G. (2009). Trachea epithelium as a "canary" for cigarette smoking-induced biologic phenotype of the small airway epithelium. *Clinical and translational science*, *2*(4), 260-272.

U.S. Department of Health and Human Services. (2014). *The Health consequences of smoking—50 years of progress: A report of the Surgeon General*. Retrieved from https://www.hhs.gov/sites/default/files/consequences-smoking-exec-summary.pdf

United States. Surgeon General's Advisory Committee on Smoking. (1964). Smoking and Health: Report of the Advisory Committee to the Surgeon General of the Public Health Service (No. 1103). US Department of Health, Education, and Welfare, Public Health Service.

Valavanidis, A., Vlachogianni, T., & Fiotakis, K. (2009). Tobacco smoke: involvement of reactive oxygen species and stable free radicals in mechanisms of oxidative damage, carcinogenesis and synergistic effects with other respirable particles. *International journal of environmental research and public health, 6*(2), 445-462.

Valjent, E., Corbillé, A. G., Bertran-Gonzalez, J., Hervé, D., & Girault, J. A. (2006). Inhibition of ERK pathway or protein synthesis during reexposure to drugs of abuse erases previously learned place preference. *Proceedings of the National Academy of Sciences*, *103*(8), 2932-2937.

Vallender, E. J., Goswami, D. B., Shinday, N. M., Westmoreland, S. V., Yao, W. D., & Rowlett, J. K. (2017). Transcriptomic profiling of the ventral tegmental area and nucleus accumbens in rhesus macaques following long-term cocaine self-administration. *Drug and alcohol dependence*, *175*, 9-23.

Van Amsterdam, J. G., Talhout, R., Vleeming, W., & Opperhuizen, A. (2006). Contribution of monoamine oxidase (MAO) inhibition to tobacco and alcohol addiction.

Van den Berge, K., Hembach, K. M., Soneson, C., Tiberi, S., Clement, L., Love, M. I., ... & Robinson, M. D. (2019). RNA sequencing data: hitchhiker's guide to expression analysis. *Annual Review of Biomedical Data Science*, *2*, 139-173.

Van der Toorn, M., Koshibu, K., Schlage, W. K., Majeed, S., Pospisil, P., Hoeng, J., & Peitsch, M. C. (2019). Comparison of monoamine oxidase inhibition by cigarettes and modified risk tobacco products. *Toxicology Reports, 6*, 1206-1215.

Van Kempen, G. M., van Brussel, J. L., & Pennings, E. J. (1985). Assay of platelet monoamine oxidase in whole blood. *Clinica chimica acta, 153*(3), 197-202.

Velki, M., Meyer-Alert, H., Seiler, T. B., & Hollert, H. (2017). Enzymatic activity and gene expression changes in zebrafish embryos and larvae exposed to pesticides diazinon and diuron. *Aquatic Toxicology*, *193*, 187-200.

Vikenes, K., Farstad, M., & Nordrehaug, J. E. (1999). Serotonin is associated with coronary artery disease and cardiac events. *Circulation, 100*(5), 483-489.

Villégier, A.-S., Blanc, G., Glowinski, J., & Tassin, J.-P. (2003). Transient behavioral sensitization to nicotine becomes long-lasting with monoamine oxidases inhibitors. *Pharmacology Biochemistry and Behavior, 76*(2), 267-274.

Wadgave, U., & Nagesh, L. (2016). Nicotine replacement therapy: an overview. *International journal of health sciences, 10*(3), 425.
Walsh, C. (2006). *Posttranslational modification of proteins: expanding nature's inventory*. Roberts and Company Publishers.
Wang, H., O'Reilly, É. J., Weisskopf, M. G., Logroscino, G., McCullough, M. L., Thun, M. J., ... & Ascherio, A. (2011). Smoking and risk of amyotrophic lateral sclerosis: a pooled analysis of 5 prospective cohorts. *Archives of neurology*, *68*(2), 207-213.
Wang, Y., Zhao, J., Cao, C., Yan, Y., Chen, J., Feng, F., . . . Zhao, J. (2018). The role of E2F1-topoIIβ signaling in regulation of cell cycle exit and neuronal differentiation of human SH-SY5Y cells. *Differentiation, 104*, 1-12.
Wang, Z., Gerstein, M., & Snyder, M. (2009). RNA-Seq: a revolutionary tool for transcriptomics. *Nature reviews genetics, 10*(1), 57-63.
Warde-Farley, D., Donaldson, S. L., Comes, O., Zuberi, K., Badrawi, R., Chao, P., . . . Lopes, C. T. (2010). The GeneMANIA prediction server: biological network integration for gene prioritization and predicting gene function. *Nucleic acids research, 38*(suppl_2), W214-W220.
Weissbach, H., Smith, T. E., Daly, J. W., Witkop, B., & Udenfriend, S. (1960). A rapid spectrophotometric assay of monoamine oxidase based on the rate of disappearance of kynuramine. *Journal of Biological Chemistry, 235*(4), 1160-1163.
West, R. (2009). The Multiple Facets of Cigarette Addiction and What They Mean for Encouraging and Helping Smokers to Stop. *Journal of Chronic Obstructive Pulmonary Diseases, 6*(4), 7. 10.1080/15412550903049181
Western Blotting: Protein Quantification. Advansta Inc. (n.d.). Retrieved October 26, 2022, from https://advansta.com/wikis/preparing-samples-for-western-blot-analysis-protein-quantification/
Westfall, T. C., & Brasted, M. (1972). The mechanism of action of nicotine on adrenergic neurons in the perfused guinea-pig heart. *Journal of Pharmacology and Experimental Therapeutics, 182*(3), 409-418.
Westlund, K. N., Denney, R. M., Kochersperger, L. M., Rose, R. M., & Abell, C. W. (1985). Distinct monoamine oxidase A and B populations in primate brain. Science, 230(4722), 181-183.
Westlund, K. N., Denney, R. M., Rose, R. M., & Abell, C. W. (1988). Localization of distinct monoamine oxidase A and monoamine oxidase B cell populations in human brainstem. Neuroscience, 25(2), 439-456.
Winikoff, S. E., Zeh, H. J., DeMarco, R., & Lotze, M. T. (2011). Cytolytic assays. *Measuring Immunity: Basic Science and Clinical Practice; Elsevier Academic Press: Cambridge, MA, USA*, 343.
Wright, W. R., Parzych, K., Crawford, D., Mein, C., Mitchell, J. A., & Paul-Clark, M. J. (2012). Inflammatory transcriptome profiling of human monocytes exposed acutely to cigarette smoke. *PLoS One*, *7*(2), e30120.
Wu, J. B., Chen, K., Ou, X. M., & Shih, J. C. (2009). Retinoic acid activates monoamine oxidase B promoter in human neuronal cells. *Journal of Biological Chemistry*, *284*(25), 16723-16735.

Xicoy, H., Wieringa, B., & Martens, G. J. M. (2017). The SH-SY5Y cell line in Parkinson's disease research: a systematic review. *Molecular Neurodegeneration, 12*(1), 10. 10.1186/s13024-017-0149-0

Xie, H.-r., Hu, L.-s., & Li, G.-y. (2010). SH-SY5Y human neuroblastoma cell line: in vitrocell model of dopaminergic neurons in Parkinson's disease. *Chinese medical journal, 123*(8), 1086-1092.

Xu, L., Han, L., & Huang, B. (2011). Antioxidant enzyme activities and gene expression patterns in leaves of Kentucky bluegrass in response to drought and post-drought recovery. *Journal of the American Society for Horticultural Science*, *136*(4), 247-255.

Yan, L.-J. (2014). Protein redox modification as a cellular defense mechanism against tissue ischemic injury. *Oxidative medicine and cellular longevity, 2014*

Yan, Z., Caldwell, G. W., Zhao, B., & Reitz, A. B. (2004). A high-throughput monoamine oxidase inhibition assay using liquid chromatography with tandem mass spectrometry. *Rapid communications in mass spectrometry, 18*(8), 834-840.

Yang, M., Kohler, M., Heyder, T., Forsslund, H., Garberg, H. K., Karimi, R., ... & Wheelock, Å. M. (2018). Long-term smoking alters abundance of over half of the proteome in bronchoalveolar lavage cell in smokers with normal spirometry, with effects on molecular pathways associated with COPD. Respiratory research, 19(1), 1-11.

Yeh, C.-C., Barr, R. G., Powell, C. A., Mesia-Vela, S., Wang, Y., Hamade, N. K., . . . Santella, R. M. (2008). No effect of cigarette smoking dose on oxidized plasma proteins. *Environmental research, 106*(2), 219-225.

Yi, X., Li, M., He, G., Du, H., Li, X., Cao, D., ... & Zhou, D. (2021). Genetic and functional analysis reveals TENM4 contributes to schizophrenia. *Iscience*, *24*(9), 103063.

Youdim, M. B., Edmondson, D., & Tipton, K. F. (2006). The therapeutic potential of monoamine oxidase inhibitors. *Nature reviews neuroscience*, *7*(4), 295-309.

Yu, P., Bailey, B., & Durden, D. (1986). High-performance liquid chromatography of aldehydes and acids formed in monoamine oxidase-catalyzed reactions. *Analytical biochemistry, 152*(1), 160-166.

Yu, P., & Boulton, A. (1987). Irreversible inhibition of monoamine oxidase by some components of cigarette smoke. *Life Sciences, 41*(6), 675-682.

Yuferov, V., Zhang, Y., Liang, Y., Zhao, C., Randesi, M., & Kreek, M. J. (2018). Oxycodone self-administration induces alterations in expression of integrin, semaphorin and ephrin genes in the mouse striatum. *Frontiers in psychiatry, 9*, 257.

Zeng, M., Zhang, X., Xing, W., Wang, Q., Liang, G., & He, Z. (2022). Cigarette smoke extract mediates cell premature senescence in chronic obstructive pulmonary disease patients by up-regulating USP7 to activate p300-p53/p21 pathway. *Toxicology Letters, 359*, 31-45.

Zhang, W., Xiao, S., & Ahn, D. U. (2013). Protein oxidation: basic principles and implications for meat quality. *Critical reviews in food science and nutrition, 53*(11), 1191-1201.

Zhang, Y. (2018). Cell toxicity mechanism and biomarker. *Clinical and translational medicine, 7*(1), 1-6.

Zhou, M., & Panchuk-Voloshina, N. (1997). A one-step fluorometric method for the continuous measurement of monoamine oxidase activity. *Analytical biochemistry, 253*(2), 169-174.

Zhou, B. P., Wu, B., Kwan, S. W., & Abell, C. W. (1998). Characterization of a highly conserved FAD-binding site in human monoamine oxidase B. *Journal of Biological Chemistry*, *273*(24), 14862-14868.

Zong, D., Liu, X., Li, J., Ouyang, R., & Chen, P. (2019). The role of cigarette smoke-induced epigenetic alterations in inflammation. *Epigenetics & Chromatin, 12*(1), 1-25.

Zubkov, E. A., Zorkina, Y. A., Orshanskaya, E. V., Khlebnikova, N. N., Krupina, N. A., & Chekhonin, V. P. (2018). Changes in gene expression profiles in adult rat brain structures after neonatal action of dipeptidyl peptidase-IV inhibitors. *Neuropsychobiology*, *76*(2), 89-99

Appendix

Table A. Summary of reported chemicals in cigarette smoke (Fowles et al. 2000)

S.N	**Chemical**	**IARC classification**	**Cancer potency $(mg/kg/d)^{-1}$**	**Non-cancer REL and target organ ($V\ g/m^3$)**
1	1,3-Butadiene	2A	3.4	8 (repro/dev)
2	1-Aminonaphthalene			
3	1-Methylpyrrolidine			
4	2-,3- and 4-Methylpyridines			
5	2,5-Dimethylpyrazine			
6	2-Aminonaphthalene	1	1.8	
7	3-Aminobiphenyl			
8	3-Ethenylpyridine			
9	4-Aminobiphenyl	1	21	
10	4-N-nitrosomethylamino) -1-(3-pyridyl)-1-butanone (NNK)	2B		
11	Acetaldehyde	2B	0.01	
12	Acetone			
13	Acrolein	3		
14	Acrylonitrile	2A	1	
15	Ammonia			
16	Arsenic	1	12	
17	Benz(a)anthracene	2A	0.39	
18	Benzene	1	0.1	
19	Benzo (a) pyrene	2A	3.9	

20	Benzo (b) fluoranthene	2B	0.39	
21	Benzo (j) fluoranthene	2B	0.39	
22	Benzo (k) fluoranthene	2B	0.39	
23	Beryllium	1	8.4	
24	Bicyclohexyl			
25	Butyraldehyde			
26	Cadmium	1	15	0.01 (kidney/resp)
27	Carbon Monoxide			
28	Catechol	2B		
29	Chlorinated dioxins and furans	1	1.30E+05	
30	Chromium (hex)	1	51	0.0008 (resp)
31	Chrysene	3	0.039	
32	Crotonaldehyde	3		
33	Cyclohexane			
34	Cyclopentane			
0	Dibenz (a,h) acridine	2B	0.39	
36	Dibenz (a,j) acridine	2B	0.39	
37	Dibenz (a,h) anthracene	2A	4.1	
38	7H-Dibenzo (c,g) carbazole	2B	3.9	
39	Dibenzo (a,i) pyrene	2B	39	
40	Dibenzo (a,l) pyrene	2B	39	
41	Dimethylamine			
42	1,1-Dimethylhydrazine	2B		
43	3-Ethenylpyridene			
44	Ethylamine			

45	Ethylbenzene			
46	Formaldehyde	2A	0.021	
47	Furfural			
48	Hydrazine	2B	17	
49	Hydrogen cyanide			
50	Hydrogen sulphide			
51	Hydroquinone			
52	Indeno (1,2,3-c,d) pyrene	2B	0.39	
53	Isoprene	2B		
54	Lead	2B	0.042	
55	m + p cresol			4(card)
56	Mercury			0.3(nerv)
57	Methyl acrylate			
58	Methyl chloride			
59	5-Methylchrysene	2B	3.9	
60	Methyl ethyl ketone			1000(repro)
61	Methylamine			
62	Methylpyrazines			
63	Nickel	1	0.91	0.05 (resp/immune)
64	Nicotine			
65	Nitric oxide			
66	Nitrogen dioxide			20 (resp)
67	2-Nitropropane	2B		
68	N-nitrosoanabasine (NAB)	3		
69	N-nitrosoanabatine (NAT)	3		
70	N-nitroso-n-butylamine (NBA)	2B	11	

71	N-nitrosodimethanolamine (NMDA)	2B	2.8	
72	N-nitrosoethylamine (NDEA)	2A	36	
73	N-nitrosodimethylamine (NDMA)	2A	16	
74	N-nitrosodimethylmethylamine	2B	22	
75	N-nitrosomorpholine	2B	6.7	
76	N-nitrosonornicotine (NNN)	2B	1.4	
77	N-nitrosopyrrolidine (NP)	2B	21	
78	o-Cresol			4 (card)
79	Phenol			600 (aliment/card/kidney/nerv)
80	Polonium-210			
81	Propionaldehyde			
82	Pyridine			
83	Pyrrole			
84	Pyrrolidine			
85	Quinoline			
86	Resorcinol			
87	Selenium			0.08 (resp)
88	Styrene	2B		1000 (nerv)
89	Toulene			400 (dev/nerv/aliment)
90	2-Toluidine			
91	Trimethylamine			
92	Urethane	2B	1	
93	Vinyl acetate	2B		200 (resp)
94	Vinyl chloride	1	0.27	
95	Xylenes			200 (nerv/resp)

1: known human carcinogens;

2A: probable human carcinogens;

2B: possible human carcinogens;

3: unclassifiable as a human carcinogen;

resp = respiratory system; repro/dev = reproductive or developmental processes; aliment = alimentary system (GI tract, liver); immune = immune system; card = cardiovascular system; nerv = nervous system; end = endocrine system

Table B: Mapping rates for RNAseq reads against Homo sapiens transcript reference sequences across all samples.

Sample	Input reads	Mapping rate (%)
S01	29,509,645	97.56
S02	28,465,868	97.40
S03	28,863,170	97.58
S04	32,493,351	95.11
S05	28,767,471	97.62
S06	38,584,819	97.50
S07	34,246,839	97.45
S08	27,365,919	97.73
S09	30,457,044	97.43
S10	32,762,161	97.42
S11	27,538,473	97.63
S12	26,444,760	97.55
Total	365,499,520	97.33 (mean)

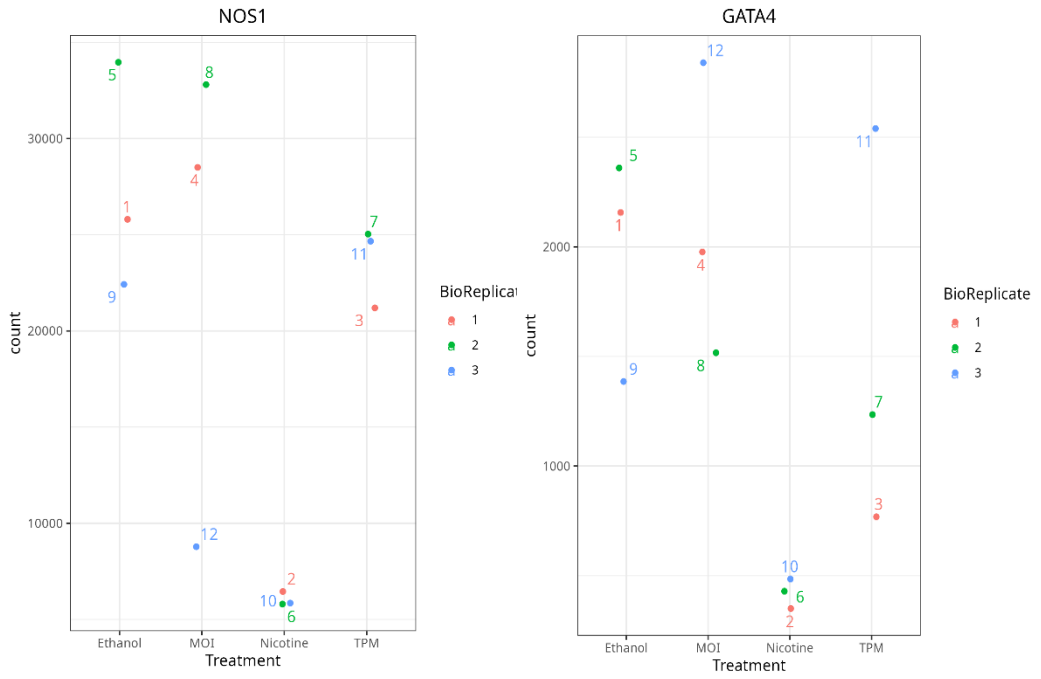

Figure A: Box plots of some representative genes with significant changes in nicotine treatment group compared to control.

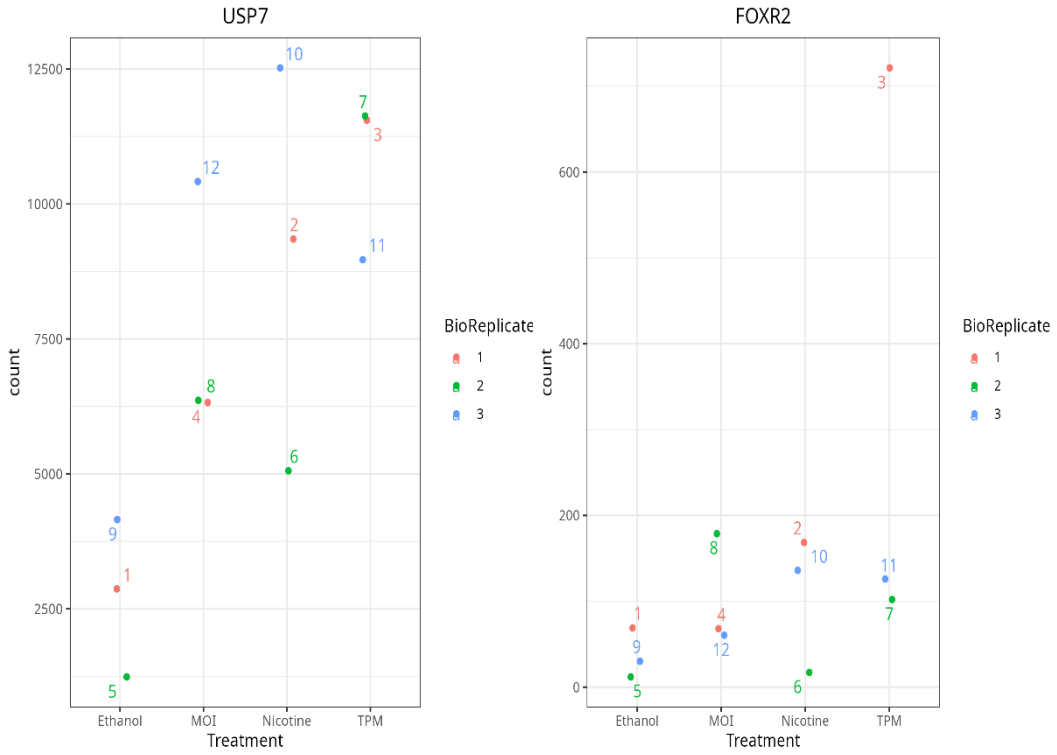

Figure B: Box plots of some representative genes with significant changes in TPM treatment group compared to control.

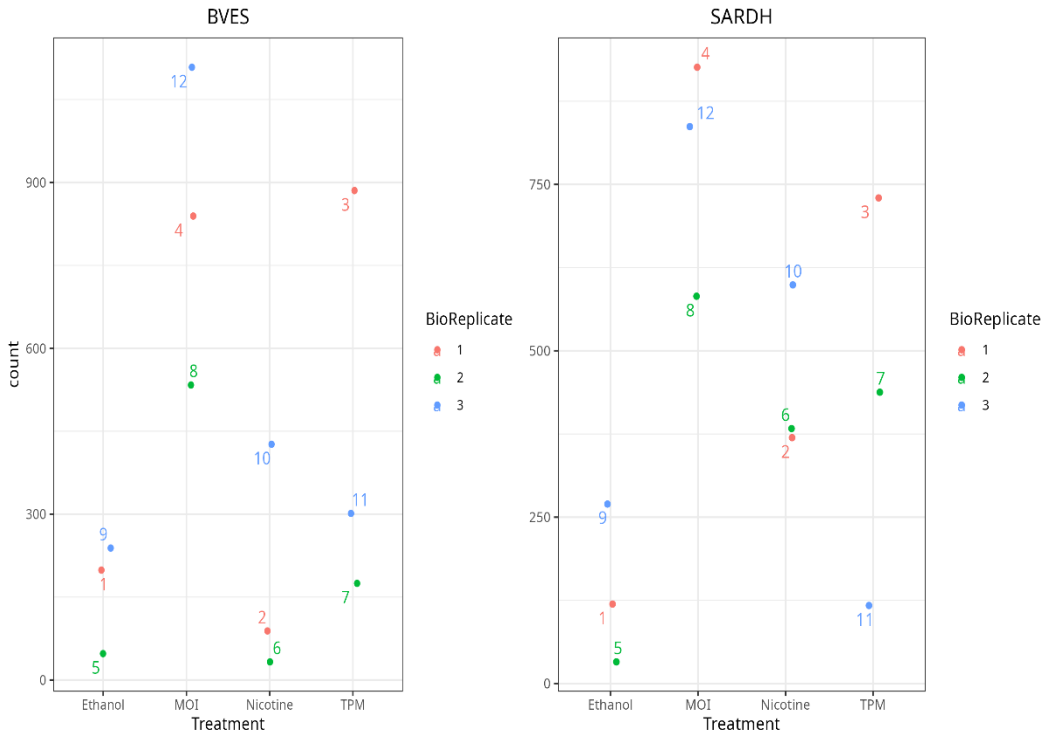

Figure C: Box plots of some representative genes with significant changes in MAOI treatment group compared to control.

ELSEVIER LICENSE

This Agreement between Mr. Prakshit Niraula ("You") and Elsevier ("Elsevier") consists of your license details and the terms and conditions provided by Elsevier and Copyright Clearance Center.

License Number	5534261502065
License date	Apr 22, 2023
Licensed Content Publisher	Elsevier
Licensed Content Publication	Archives of Biochemistry and Biophysics
Licensed Content Title	Structural insights into the mechanism of amine oxidation by monoamine oxidases A and B
Licensed Content Author	Dale E. Edmondson,Claudia Binda,Andrea Mattevi
Licensed Content Date	Aug 15, 2007
Licensed Content Volume	464
Licensed Content Issue	2
Licensed Content Pages	8
Start Page	269
End Page	276
Type of Use	reuse in a thesis/dissertation
Portion	figures/tables/illustrations
Number of figures/tables/illustrations	2
Format	both print and electronic
Are you the author of this Elsevier article?	No
Will you be translating?	No
Title	Investigating the Impact of Tobacco Particulate Matter and selected components on Monoamine Oxidase Activity, Protein Expression, and Gene Expression in Brain SH-SY5Y Cells.
Institution name	Massey University
Expected presentation date	May 2023
Order reference number	1
Portions	Figures 1, 3
Requestor Location	Mr. Prakshit Niraula 62A Morgans Road, Glenwood, Timaru

	Timaru, Canterbury 7910 New Zealand Attn: Mr. Prakshit Niraula
Publisher Tax ID	GB 494 6272 12
Total	0.00 USD